From Pollutant to Fuel

A proof of principle for electricity production using

nitrogen from sewage as a fuel

M.M. Zwart

TU Delft Delft University of Technology

Challenge the future

From Pollutant to Fuel

A proof of principle for electricity production using nitrogen from sewage as a fuel

by

Maartje Marij Zwart

for the degree of:

Master of Science in Civil Engineering

Date of submission: 29 September 2014

Date of defense: 9 October 2014

Committee:

Prof. dr.ir. J.B. van Lier	Delft University of Technology Sanitary Engineering Section
Assoc. Prof. dr.ir. H. Spanjers	Delft University of Technology Sanitary Engineering Section
Ir.G. Smith	Pentair Process Technologies
Dr. Ir. D. van de Bor	Delft University of Technologies Process and Energy Section
Prof.dr.ir. P.V. Aravind	Delft University of Technologies Energy Technology Section

Sanitary Engineering Section, Department of Water Management

Faculty of Civil Engineering and Geosciences

Delft University of Technology, Delft

TU Delft Delft University of Technology

Acknowledgment

This thesis would have been completely different without the help of many people.

First of all I would like to thank HenRi Spanjers for his dedicated and very involved supervision during the entire process of my thesis research. I also would like to thank Geo Smith, for sharing his practical knowledge and impressive insights in process technology. Without the help of Dennis van de Bor, my research would have stranded somewhere in the middle. I would like to thank Dennis for being exactly what I needed: an enthusiastic expert who wanted to try to make this work. Furthermore, I would like to thank Jules van Lier and P. Aravind for their input, critical thinking and insights.

Next to my graduation committee, one of the most important contributors to this thesis research was Zhongbo Zhou. Even though Zhongbo looked terrified when I told him that I planned to operate the anaerobic tank (later to be named 'Tankie') that he had been working on (and suffering with) for months, during his time in Delft he was always on my side in the laboratory. He did not only teach me how to deal with all Tankie's operational issues, he also took all the time necessary to keep Tankie on track, time and time again. When he finished his work in Delft and returned to China, I missed him as a laboratory-mate but particularly as a friend. I would like to thank him for that.

Next to Zhongbo, I would like all other people that supported me in and around the lab during my thesis. Especially Raluca, Ramiro, David and Marisa outside the lab and Albert, Weilai and Suellen in the lab, thank you for all the nice dinners, lunches and coffees and for accepting my constant complaining about Tankie. This also counts for my housemates and the afstudeer-koffie group.

More practically, I would like to acknowledge Patrick and Tonny for facilitating my work in the lab, even though I always seemed to have 'just óne more question'. I would like to thank Daniel T. Eyde from St. Cloud Mining for supplying me with the zeolites, all the way from the USA. Furthermore, I want to thank Eva Promes for her help with everything related to fuel cells.

I would like to thank Raphael Ihringer, for allowing me to use his solid oxide fuel cell set-up in Switzerland. Raphael did not only invite me to come to Switzerland, but also spend two full days instructing and helping me, together with Pierre and Issam. Thank you for your help and enthusiasm.

Last but not least, I want to thank Mam, Pap, Maaike, Erik en de Tomaatjes for being the perfect basis that they are.

Marij Zwart

Delft, September 2014

Executive Summary

The necessary removal of organically bound nitrogen and ammonium from sewage conventionally requires energy for aeration and reduces the potential biogas production in the following anaerobic stage due to the required carbon source for de-nitrification. It has recently been demonstrated that fuel cells can generate electricity, using ammonia as a fuel. The objective of this thesis research is to connect the necessity to remove organically bound-nitrogen and ammonium from sewage with the potential of reduced nitrogen, as incorporated in the compound ammonia, as a valuable and sustainable fuel for a fuel cell. The organically bound nitrogen present in sewage was converted into ammonium ions through anaerobic digestion in an Anaerobic Membrane BioReactor (AnMBR). These ammonium ions were separated from the AnMBR effluent using Ion Exchange (IE). Through a fractionized collection of the IE brine, the ammonium ions were concentrated and a distillation tower was used to further concentrate and convert the ammonium ions into a concentrated ammonia solution. This solution proved sufficiently rich in ammonia to be fed directly to a Solid Oxide Fuel Cell (SOFC), generating electricity. Thus, the described combination of technologies removed ammonium and organically bound nitrogen from the wastewater, producing an effluent with an extremely low ammonium concentration (<4 mg TN/L whereas 10 mg TN/L is allowable according to the discharge regulations) and electricity. The distillation tower proved to be the weakest link in the series of technologies considering the nitrogen recovery. However, the low nitrogen recovery can be attributed to the use of a non-optimal distillation tower design. A distillation tower is a frequently applied conventional technology, and therefore it is reasonable to assume the possibility of optimizing the nitrogen recovery and the energy demand. Assuming an optimized distillation tower and an integrated heat recovery design in between the SOFC and the distillation tower, it is theoretically possible to achieve a net electricity production while also meeting the nitrogen discharge regulations.

List of Abbreviations

AnMBR: Anaerobic membrane bioreactor

AnWT: Anaerobic wastewater Treatment

BV: Bed Volume

CF: Concentration Factor

COD: Chemical Oxygen Demand

CSTR: Completely Stirred Rank Reactors

EMF: Electromotive Force

HETP: Height Equivalent to a Theoretical Plate

HRT: Hydraulic Retention Time

IE: Ion Exchange

MF: Microfiltration

NF: Nanofiltration

OCV: Open-Circuit Voltage

PCC: Peak Concentration Collection

RO: Reverse Osmosis

SAC: Strong Acid Cation exchange

SOFC: Solid Oxide Fuel Cell

SS: Suspended Solids

TMP: Transmembrane Pressure

UASB: Upflow Anaerobic Sludge Bed

UF: Ultra Filtration

VFA: Volatile Fatty Acids

WAC: Weak Acid Cation exchange

Glossary

AnMBR effluent: The effluent from the Anaerobic Membrane Bio-Reactor (AnMBR). Since the AnMBR and the ion exchange set up are placed in series, the effluent of the AnMBR is the influent for the ion exchange installation.

Bed Volume (BV): The dry weight of ion exchanger material, thus the volume of natural zeolites that is present in the column as supplied by the supplier.

Brine: The effluent regeneration solution. The salt solution that passed the ion exchange column, and thus is enriched with ammonium. The brine of the ion exchange is the influent of the distillation tower.

Concentration Factor (CF): The concentration factor is calculated by dividing the obtained ammonium concentration by the initial ammonium concentration. For example, if an influent ammonium solution of 100 mg NH_4-N/L is concentrated to a solution of 200 mg NH_4-N/L, this can be indicated with a concentration factor of 2.

Ion exchange capacity: The ion exchange capacity refers to the maximum mass of ammonium (mg) that can be absorbed per gram of zeolite. A distinction can be made between the theoretical ion exchange capacity (supplied by the supplier) and the operational ion exchange capacity (as measured under actual operations).

Ion Exchange effluent: The water that has been treated using ion exchange, thus the water that has passed the ion exchange column.

Peak Concentration Collection (PCC): The concept of a fractionized collection of the ion exchange brine, collecting only that part of the regeneration effluent that holds most of the regenerated ammonium, in order produce a concentrated ammonium solution.

Regeneration solution: The salt solution that is used for regeneration of the ion exchange bed.

Regime: A combination of tested operational ion exchange parameters. A regime refers to a tested combination of the salt concentration in the used regeneration solution and the regeneration flow.

Selectivity: The selectivity is a measure of the preference of the ion exchanger for a particular ion above other ions in the solution. The selectivity has no unit. The selectivity for ammonium can be shown through the comparison between the ion exchange capacity with only ammonium ions present, and the ion exchange capacity in the presence of competing ions. The ion exchanger with the smallest difference between those two exchange capacities, has the strongest selectivity for ammonium.

CONTENTS

1 INTRODUCTION

Nitrogen is essential for living organisms. When a surplus occurs, however, nitrogen can contribute to accelerated eutrophication, oxygen depletion and fish toxicity in lakes and rivers (Jha and Hayashi, 2009). Consequentially, nitrogen in wastewater is regarded as a pollutant that has to be removed from wastewater before it can be discharged into the environment. Sewage is the most abundant type of wastewater and it contains organically bound nitrogen-compounds and ammonium (NH_4^+), principally originating from urine and feces (Hedstrom, 2001).

The traditional method for nitrogen removal from wastewater is based on biological treatments (Malonvanyy, 2013, Jha and Hayashi, 2009, Verkerk, 2003). In recent years, autotrophic nitrification and anoxic denitrification have become a dominant approach of nitrogen removal (Chen et al, 2014). This approach is cost-intensive, time-consuming and opposes the upcoming concept of wastewater treatment as an energy producing process (Chen et al, 2014). Nitrification and denitrification reduce the potential of a wastewater treatment plant to serve as an energy producer in two ways. First, energy is required for aeration during nitrification. Second, denitrification reduces the potential biogas production in the subsequent biological treatment step of anaerobic digestion. This is because denitrification demands a carbon source for nitrogen removal. Consequently, the fraction of the chemically bound energy content of sewage that can be converted in the energy carrier biogas is reduced.

According to Richard Buckminster Fuller (1971) 'pollution is nothing but the resources that we are not harvesting. We allow them to disperse only because we are ignorant to their value'. This quote is very applicable to wastewater in general, and particularly to nitrogen in wastewater. This becomes even more clear if the pollution problem is conceived from a completely different part of research, i.e. the application of fuel cells.

Fuel cells are devices that electro-chemically convert the chemical energy of gaseous or liquid compounds into electrical energy through a chemical reaction with oxygen or another oxidizing agent (Kreuer, 2003). Proponents believe that fuel cells could provide a solution to the significant global challenges for human and environmental health and welfare, by efficiently and simultaneously minimizing the impact of energy conversion processes, together with the opportunity to reduce the dependency of fossil fuels (Kreuer, 2003, Christensen et al, 2006). Hydrogen is currently the common choice of fuel, but due to its low energy density and safety concerns related to its high flammability, the exploration of alternative fuels seems to be crucial for the commercialization and feasible up-scaling of fuel cell technology (Ma et al, 2006, Dekker and Rietveld, 2006).

In recent research, ammonia (NH_3) has been identified as a sustainable fuel, for especially the Solid Oxide Fuel Cell (SOFC) (Zamfirescu and Dincer, 2008, Staniforth and Ormerod, 2008, Dekker and Rietveld, 2005, Fournier et al, 2006, Wojcik et al, 2003). Organically bound nitrogen and ammonium can be converted into ammonia. Advantages of ammonia above hydrogen as a fuel for fuel cells are the higher volumetric energy density, and the facts that ammonia is carbon free and that ammonia can be easily liquefied, which is useful for transport and storage. Furthermore, ammonia is less flammable compared to other potential fuels, leaks are easily observable because of the smell and the by-products of its cell reaction are merely nitrogen gas and water (Fuerte et al, 2009, Wojcik et al, 2003).

The objective of the research presented in this thesis is to connect the necessity to remove organically bound-nitrogen and ammonium from sewage with the potential of ammonia, as a valuable and sustainable fuel for a fuel cell. It has been tried to combine and implement a series of technologies which together remove nitrogen from sewage, while utilizing the

potential of ammonia as a sustainable energy source, instead of consuming energy for nitrogen removal. In other words, it has been pursued to prevent nitrogen pollution by producing electricity.

To produce electricity with the nitrogen from sewage as a fuel, this nitrogen has to be fed to a fuel cell as an ammonia rich gas. To create an ammonia rich gas out of the ammonium and organically bound nitrogen from sewage, the organically bound nitrogen first has to be converted into ammonium ions. Afterwards, this ammonium ions have to be isolated from the rest of the sewage, concentrated and converted into ammonia.

Anaerobic digestion is an anaerobic wastewater treatment (AnWT) step aiming to remove the organic material by producing the sustainable fuel biogas. Conventionally, the anaerobic step is combined with nitrification/denitrification step to remove the nitrogen. AnWT has drawn considerable attention for sewage treatment, due to the energy that can be recovered from biogas and the reduced energy demands due to the absence of aeration for organic matter oxidation (Ozgun et al, 2013). Furthermore, the relatively plain reactor systems make a decentralized application at any scale theoretically possible (van Lier, 2008a). As luck would have it, during the anaerobic digestion process in which organic material is converted into biogas and carbon dioxide, organically bound nitrogen is converted into the most reduced from of nitrogen: ammonium. And ammonium can be easily converted into the potential fuel ammonia.

The application of membranes in wastewater treatment has increased in recent years due to membrane costs reduction and more strict environmental regulations (Salazar-Pelaez et al, 2011). Anaerobic Membrane BioReactor (AnMBR) technology has been recognized as a plausible alternative for the conventional anaerobic treatment processes, with a superior effluent quality as the main advantage (Ozgun et al, 2013b). This technology, which combines the anaerobic digestion process with Ultra-Filtration (UF), proved to be a feasible and cost-effective alternative for producing an ammonium rich and solids free effluent out of wastewater, with a high degree of pathogen removal, while occupying a small footprint (Ozgun et al, 2013).

Especially the production of an ammonium rich, solids free effluent out of sewage makes the AnMBR technology convenient to include in the chain of technologies combined in this thesis research. For being solids-free is one of the main effluent requirements for the subsequent recommended technology in the chain: Ion Exchange (IE). Ion exchange will be used to separate the ammonium from the wastewater and to create a concentrated ammonium solution.

This thesis describes the development of a series of progressive technologies, capable of converting nitrogen present in sewage from a pollutant into a resource for sustainable electricity production. In this thesis, the following research question will be answered:

Can nitrogen from sewage be utilized as a fuel for electricity production, while meeting the discharge quality standards for nitrogen removal?

This research question is subdivided into the following sub-questions:

1. Is it possible to convert the total nitrogen content of sewage into ammonium ions through anaerobic digestion?
2. Can the ammonium ions from the anaerobic digestion effluent be separated and concentrated through ion exchange, while producing an effluent that meets the discharge quality standards for nitrogen removal?
3. Is it possible to produce a gas mixture from the concentrated ammonium solution (resulting from ion exchange) that is sufficiently rich in ammonia to be operable for a solid oxide fuel cell for the generation of electricity?

Since the combined technologies differ widely, this thesis is subdivided in sections. Each section covers per technology first the theoretical background and second the data obtained from actual implementation of the technology in the laboratory. Section I concerns the first treatment step of the chain that sewage is fed to, the Anaerobic Membrane BioReactor (the AnMBR). Section II describes the Ion Exchange (IE) treatment step, followed by an imperative further concentration step accomplished through distillation discussed in section III. Finally section IV elaborates upon the actual power production with a Solid Oxide Fuel Cell (SOFC) with ammonia originating from sewage as the fuel. These four sections are succeeded by a chapter that gives insights in the energy production of the total system, the general discussion, and the conclusion.

Section I: The Anaerobic Membrane BioReactor

2 ANAEROBIC MEMBRANE BIOREACTOR THEORY

Sewage is the most abundant type of low-strength wastewater (Ozgun et al, 2013a). Over the past years, initiatives and studies arose that recognize the potential of sewage treatment plants as net producers of renewable energy (Ozgun et al, 2013, Frijns et al, 2013, Zhang et al, 2013, Liu et al, 2004). By converting the chemically bound energy content of the organic fraction of sewage into the renewable energy carrier, the wastewater treatment plant does not only prevent environmental pollution, but also contributes to the reduction of our carbon dioxide emissions by producing an useful sustainable energy carrier, i.e. biogas.

Considering this win-win situation, the development and selection of appropriate energy recovery technologies that convert the inherent energy in wastewater into a renewable energy source has received much attention (Ozgun, 2013a). Anaerobic wastewater treatment (AnWT) has evolved into a competitive treatment technology, considering energy conservation and the production of renewable energy carriers from waste streams (van Lier, 2008a). In addition to the energy that is recovered in the form of biogas, the application of anaerobic processes distinctly reduces the overall energy demand for sewage treatment plants because no energy is required for aeration (Ozgun et al, 2013b). Furthermore, the relatively plain reactor systems make a decentralized application at any scale theoretically possible (van Lier, 2008a).

Treatment of sewage by different types of anaerobic systems has drawn considerable attention of various researchers (Ozgun et al, 2013b). Key to the success of AnWT was the development of high-rate upflow anaerobic sludge blanket (UASB) reactor systems by Lettinga and his colleagues, which have the capability to retain a high concentration of slow growing biomass by the formation of well settable sludge (Lettinga et al, 1980). The formation of well settable sludge allows for the uncoupling of the solids retention time from the hydraulic retention time, resulting in a sludge age that is much higher than the hydraulic retention time (Ozgun et al, 2013b). The UASB reactor permits with its highly settleable sludge, efficient treatment at high organic loading rates with a significant decrease in reactor size (Lettinga et al, 1980).

During the recent years, the UASB reactor has been extensively studied and applied in both developed and developing countries, where it has been established as a robust and successful wastewater treatment technology (Sato et al, 2006). However, especially when sewage is treated in more temperate climates, the UASB effluent quality remains a challenge and post-treatment is often necessary (Salazar-Pelaez et al, 2011).

2.1 ANAEROBIC MEMBRANE BIOREACTORS

The application of membranes in wastewater treatment has increased in recent years due to membrane costs reduction, more strict environmental regulations and the increased water re-use potential once membranes are applied (Salazar-Pelaez et al, 2011). Anaerobic membrane bioreactor (AnMBR) technology has been recognized as a possible alternative for the conventional anaerobic treatment processes, with a superior effluent quality as the main advantage (Ozgun et al, 2013b). In an AnMBR, biomass can be effectively retained inside the reactor, providing optimal conditions for organic matter degradation without any carry-over of suspended solids (SS) (Ozgun et al, 2013b). Recent research results indicate that the AnMBR technology is feasible, particularly in moderate climate regions, when high effluent quality of treated effluents is required (Ozgun et al, 2013a, Lin et al, 2013, Kocadagistan and Topcu, 2007, An et al, 2009).

Different types of AnMBR configurations are used. In membrane coupled UASB systems, the sludge bed at the bottom of the UASB reactor acts as a biofilter prior to the membrane unit by entrapping most of the particulate matter via adsorption and biodegradation (Ozgun et al, 2013b).Higher fluxes can be obtained with UASB coupled systems in comparison to other

configurations of AnMBRs, like completely stirred rank reactors (CSTRs). However, research on the combination of UASB systems and membranes is still limited.

2.2 PROCESS DESCRIPTION

2.2.1 ANAEROBIC DIGESTION

The fermentation process in which organic material is degraded and biogas is produced, is referred to as anaerobic digestion (Van Lier et al, 2008b). Anaerobic digestion is a natural process occurring in many places where organic material is available and no oxygen is present, like in stomachs of ruminants, marshes, sediments or lakes.

Anaerobic treatment itself is effective in removing biodegradable organic compounds, while producing useful energy in the form of biogas (mainly consisting out of methane and carbon dioxide) and leaving mineralized compounds like NH_4^+, PO_4^{3-} and S^{2-} in solution. Organically bound nitrogen (nitrogen that is present as incorporated in proteins, amino acids or urea) will be converted into ammonium NH_4^+.

A measure for the amount of organic compounds in water is the Chemical Oxygen Demand (COD). The COD expresses the oxygen equivalent of the organic material in wastewater that can be oxidized chemically in mg/L (Metcalf and Eddy, 2003). Although there is no fundamental relationship between the energy contained within the wastewater and the COD (values found in literature range between 17.7 kJ/gCOD to 28.7 kJ/gCOD), the COD remains the best indicator of potential available internal energy of wastewater that can theoretically be converted into biogas through anaerobic digestion (Heidrich et al, 2010). The anaerobic degradation of organic matter is a multi-step process of series and parallel reactions (Van Lier, 2008b). Via these processes, the microbial consortia involved (microorganisms of several different species) jointly convert complex organic matter and ultimately mineralize it into the most reduced form of carbon: methane (Van Lier, 2008b). Just like the present nitrogen is also mineralized into the most reduced form of nitrogen: ammonium. This process of COD degradation proceeds in four successive stages, namely:

1. Hydrolysis, where enzymes excreted by fermentative bacteria (exo-enzymes) convert complex undissolved material into less complex, dissolved compounds which can pass through the cell walls and membranes of the fermentative bacteria
2. Acidogenesis, where the dissolved compounds present in cells of fermentative bacteria are converted into a number of simple compounds which are then excreted. The compounds produced this phase include volatile fatty acids (VFAs), alcohols, lactic acid, carbon dioxide, ammonium, hydrogen sulphide and water as well as new cell material
3. Acetogenesis, where digestion products are converted into acetate, hydrogen and carbon dioxide, as well as new cell material
4. Methanogenesis, where acetate, hydrogen plus carbonate, formate or methanol are converted into methane, carbon dioxide and new cell material.

These processes plus the bacterial groups involved are indicated in figure 2.1.

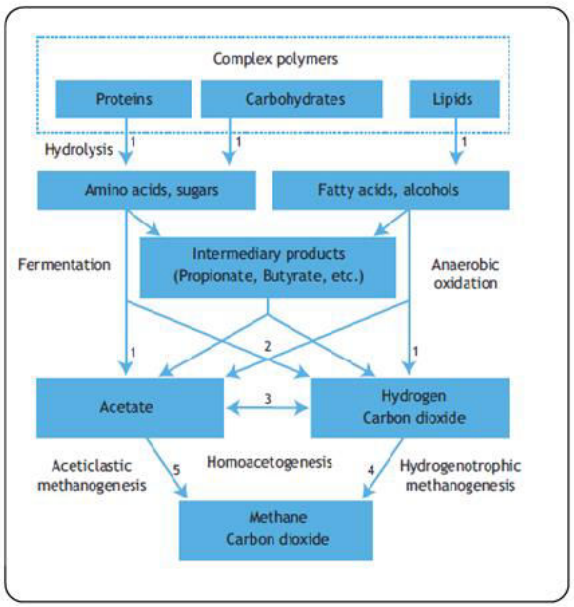

Figure 2.1 Reactive scheme for the anaerobic digestion of polymeric materials. Numbers indicate bacterial groups involved: 1. Hydrolytic and fermentative bacteria, 2. Acetogenic bacteria, 3. Homo-acetogenic bacteria, 4. Hydrogenotrophic methanogens, 5. Aceticlastic methanogens (Gujer and Zehnder, 1983 via Van Lier et al, 2008b)

Figure 2.1 suggests an unidirectional degradation of organic matter to the end production methane and carbon dioxide. In practice, other back-reactions may occur, like the formation of higher VFA or alcohols out of acetate and propionate. Under stable reactor performance under mesophilic conditions (temperatures between 20 °C and 40°C), acetate is the major precursor of methane (about 70% of the COD flux) (Van Lier et al, 2008b). Furthermore, anaerobic digesters contain mixed microbial communities and besides the methonogenic association described in figure 2.1, other bacteria can be present which can compete with the methanogens for methanogenic substrates. Examples are sulphate reducing bacteria, which will produce hydrogen sulfide instead of methane.

In contrast to aerobic COD removal systems, there is no COD destruction during anaerobic digestion. Complex organic compounds are broken down in more simple intermediates and eventually mineralized to methane and carbon dioxide. All the COD that enters the process ends up in the end product methane, is incorporated in the produced biomass or leaves the system with the effluent. Since a perfect mass balance can be made by only using the COD, the COD is generally taken as a control variable to operate an organic system. Figure 2.2 shows the COD balance.

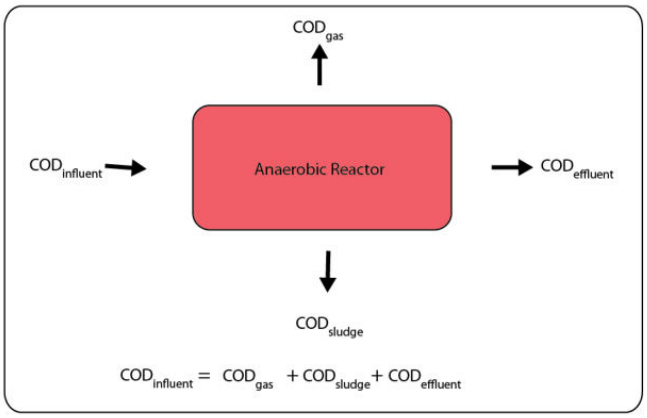

Figure 2.2 The COD Balance

It can be derived that the formation of 1 mole of methane (22.4 Liter according the universal gas law at STP) requires 2 moles of oxygen (COD), which equals 60.05 g COD. Theoretically, one kilo of COD can be converted into 0.35 m^3 CH_4.

It must be noticed that biogas does not only contain biogas. Often 'gaps' in the COD balance occur that can be attributed mostly to the loss of electrons when these are channeled to oxidized anions like SO_4^{2-} and NO_3^- (van Lier et al,200bb). Therefore, for closing the COD balance all reduced gases should be taken into account. Table 2.1 indicates typical biogas compositions. Since the biogas composition varies highly with the influent composition and process conditions, this table should only be considered as an indication.

Table 2.1. Indicative typical composition biogas (Metcalf and Eddy, 2003)

Compound	Molecular formula	%
Methane	CH_4	50–75
Carbon dioxide	CO_2	25–50
Nitrogen	N_2	0–10
Hydrogen	H_2	0–1
Hydrogen sulphide	H_2S	0–3
Oxygen	O_2	0–0

DEGRADATION OF ORGANICALLY BOUND NITROGEN INTO AMMONIUM IONS

Nitrogen is present in sewage in various forms and originates from amino acids in protein and from purines, pyrimidines, free amino acids, vitamins, creatinine, amino sugars and urea (Minnis, 2009). Along with proteins that are flushed into the wastewater from kitchen sources, urea is the prime nitrogen source in wastewater (Minnis, 2009). During the enzymatic hydrolysis processes, proteins are hydrolyzed to amino acids (Van Lier et al, 2008b). The process of acidogenesis results in the further breakdown of the amino acids. The acidogenic conversion of amino acids generally follows the Stickland reaction, in which an amino acid is de-ammonified by anaerobic oxidation, yielding hydrogen, Volatile Fatty Acids (VFA) and ammonia, in conjunction with the reductive de-ammonification of other amino acids (consuming the produced hydrogen) (van Lier et al, 2008b). From both reactions ammonia is released, and ammonia subsequently acts as a proton acceptor. This leads to a pH drop and the creation of ammonium ions.

UASB REACTOR CONFIGURATIONS

Since an Upflow Anearobic Sludge Bed (UASB) reactor is used in this thesis, this type of reactor is described in more detail. The Upflow Anearobic Sludge Bed (UASB) reactor is the best known example following the concept of Anaerobic Sludge Bed Reactors (ASBR). ASBR reactors are undoubtedly the most popular anaerobic wastewater systems so far. The sludge (bacteria) retention in such reactors is based on the formation of easily settling sludge aggregates (flocs or granules), and on the application of an internal gas-liquid-solids separation system (van Lier et al, 2008b). The success of the UASB reactor can be attributed to its capability for retaining a high concentration of sludge, while efficient solids, liquids and water phase separation is achieved. During the passage through the anaerobic sludge the treatment processes take place by solids entrapment and organic matter conversion into biogas, carbon dioxide and sludge. The produced biogas bubbles automatically rise to the top of the reactor, carrying water and solid particles, i.e. sludge and residual solids. The biogas bubbles are directed to an efficient liquid-gas separator (van Lier et al, 2008b). The solid particles drop back down to the sludge blanket. Water flows upwards, carrying some solid materials which settle in the settling area due to the drop in upward velocity owing to the increase in cross sectional area caused by baffles. After settling, the solids slide back to the sludge blanket while water leaves via the effluent weir/tube. Figure 2.3 shows a schematic representation of an UASB reactor.

In an UASB reactor, the wastewater moves in an upward mode through the circular or rectangular reactor. However, contrary to other anaerobic reactor designs, no packing material is present in the reactor vessel (van Lier et al, 2008b). The sludge bed reactor concept is based on the following ideas (van Lier et al, 2008b):

I. Anaerobic sludge has (or acquires) excellent settling characteristics, enabling high superficial liquid velocities (if gentle mixing and good process operation are provided). Thus, mechanical mixing is not applied (reducing costs)

II. The uniform feeding of the wastewater over the bottom of the reactor and the agitation caused by the produced biogas, together provide for the required contact between the sludge and the wastewater.

III. Particularly with low strength wastewater (i.e. diluted wastewaters like sewage) a high height-diameter ratio is used. The small surface area facilitates uniform feeding of the system, whereas the accumulating biogas production over the height of the tower causes a turbulent flow. Moreover, the increased upflow velocity improves contact between the sludge and the pollutants. A liquid recirculation flow can be applied, allowing a more mixed flow pattern and minimizing stratification of the substrate and intermediate products over the heights of the reactor, thereby decreasing potential inhabitation of the anaerobic digestion.

IV. The washout of sludge is prevented by separating the produced biogas using a gas collection dome installed at the top of the reactor. In this way a zone with relatively little turbulence is created in the uppermost part of the reactor. Consequently, the reactor is equipped with an in-built clarifier. The gas collection dome acts like a three phase separation system, facilitating:

- The collection, separation and discharge of the produced biogas
- The reduction of liquid turbulence in the settling compartment in order to enable sludge settling
- The creation of a low solid containing liquid effluent that can be discharged

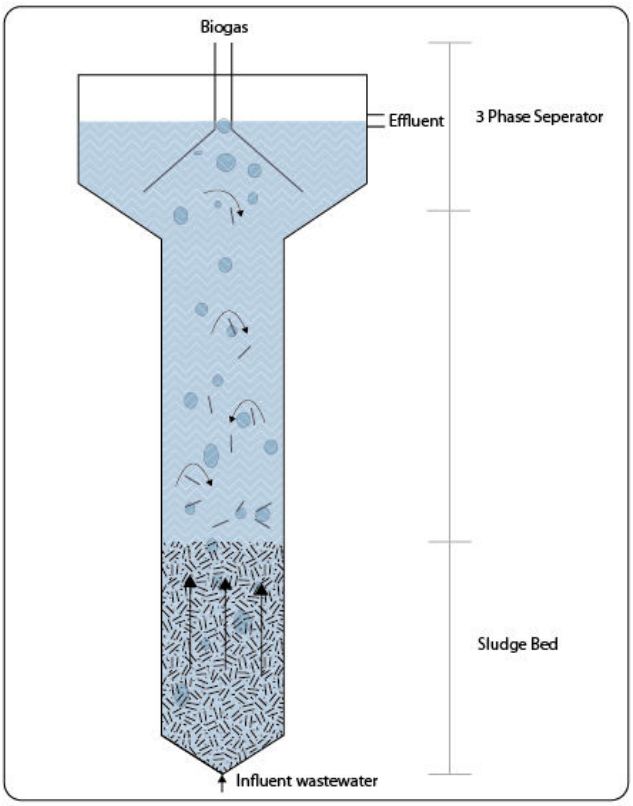

Figure 2.3 Schematic Lay-out of an UASB reactor

The most important UASB reactor internals are the feed inlet distribution (should be designed in order to maximize uniform feed distribution), the effluent outlet and the gas-liquid-solids separator (van Lier et al, 2008b). Ozgun et al (2013b) pioneered research on using an UASB in an AnMBR (thus to combine a membrane with an anaerobic digestion reactor). The argumentation for combining an UASB in an AnMBR is the possible reduced membrane fouling, as the membrane is not in contact with the anaerobic biomass (since in an UASB the biomass is retained within the reactor due to the good settling characteristics of the sludge and the three phase separator).

2.2.2 ULTRA-FILTRATION

Membrane filtration is a treatment process based on the physical separation of compounds from the water phase with the use of a semi-permeable membrane (Crittenden et al, 2012). The role of a membrane is to serve as a selective barrier that will allow the passage of certain constituents and will retain other constituents found in the liquid (Metcalf and Eddy, 2003). The pore size determines the removal of different compounds. Membrane processes include microfiltration (MF), ultrafiltration (UF), nanofiltration (NF), Reversed Osmosis (RO), dialysis and electro-dialysis. These types of membranes are divided based on their pore size. Figure 2.4 shows an overview of the different filtration processes and their membrane process characteristics.

The research of this thesis focused on an ultrafiltration coupled UASB reactor and therefore this type of membrane will be elaborated upon. Ultrafiltration units will remove colloidal substances and micro-organisms and the removal mechanism that is used is primarily sieving (Crittenden et al, 2012). The removal of suspended solids is at least 99% (Crittenden et al, 2012). Figure 2.4 shows that monovalent ions, like NH_4^+, are not removed by ultrafiltration.

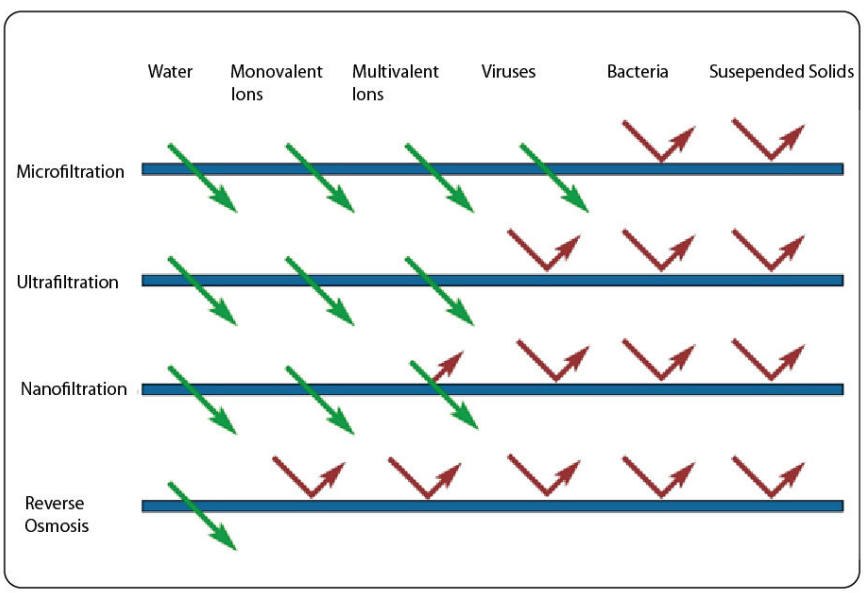

Figure 2.4 Membrane proces scharacteristics (www.zena-membranes.cz)

The most important process parameter in ultrafiltration installations is the flux. The flux is defined as the water flow through a square meter of membrane surface (Crittenden et al, 2012).

$$J = \frac{Q}{A_{mem}} = \frac{TMP}{\mu \cdot R_{tot}} \qquad [2.1]$$

Where:	J	= Flux	[$m^3/(m^2 \cdot s)$]
	Q	= Volume flow	[m^3/s]
	A_{mem}	= Membrane surface area	[m^2]
	TMP	= Trans membrane pressure	[Pa]
	μ	= Dynamic viscosity	[Pa·s]
	R_{tot}	= Total resistance	[m^{-1}]

Water passes through the membrane under the influence of pressure. The pressure difference across the membrane is called the Trans Membrane Pressure (TMP), which is defined as follows (note that TMP can either be expressed in bar of Pascale) (Crittenden et al, 2012):

$$TMP = \frac{P_f + P_c}{2} - P_p \qquad [2.2]$$

Where: TMP	=	Trans Membrane Pressure	[bar]
P_f	=	Feed pressure	[bar]
P_c	=	Concentrate pressure	[bar]
P_p	=	Permeate pressure	[bar]

During filtration the resistance over the membrane increases due to the fouling of the membrane surface. Fouling is defined as the increase in resistance because pore blocking, cake forming, adsorption in the pores and high concentration of dissolved substances near the surface.

Two types of membrane operation are possible: 1. constant flux operation or 2. constant applied pressure operation. When an constant flux is set, the applied pressure to the feed flow has to be increased during the process in order to maintain a constant flux. When a constant applied pressure is used, the flux will decrease during the process due to the fouling of the membrane. Different methods or combinations of methods can be used to minimize the impact of fouling:

- Forward flush
- Backward flush (with permeate)
- Air flush
- Chemical enhanced flush or enhance back flush
- Cleaning in place or chemical soaking
- Physical cleaning ex situ

Membranes can be operated using a dead-end configuration, meaning that all feed water is pushed over the membrane. In cross flow filtration, however, the fluid feed stream runs tangential to the membrane. Particles remaining at the feed side continue to flow across the membrane. Therefore, cross flow filtration is associated with less fouling compared to dead end filtration.

Different membrane module designs are applied. The most typical membrane module types are tubular membranes, cylindrical membranes and flat sheet membranes. It is possible to compare membrane modules based on the specific surface of the modules. Membrane module design is aimed at maximizing the surface area of the membrane in the smallest possible volume. The specific surface area is defined as follows:

$$A_{spec} = \frac{A_{mem}}{V_{module}} = \frac{n \cdot d \cdot L}{\frac{1}{4} \cdot D^2} \qquad [2.3]$$

Where:

A_{spec}	= Specific surface area	[m^{-1}]
A_{mem}	= Membrane area	[m^2]
V_{module}	= Volume module	[m^3]
n	= Membranes in module	[-]
d	= Diameter of membrane	[m]
L	= Length of membrane	[m]

3 ANMBR LABORATORY RESULTS

This chapter describes the laboratory work carried out with the Anaerobic Membrane BioReactor (AnMBR), in the water laboratory of Sanitary Engineering at the technical university of Delft. A membrane coupled UASB reactor was used. Previous research with the same set-up proved the applicability of this particular AnMBR system to the treatment of low concentration sewage. The objective of this thesis research was to use the ammonium present in sewage as a fuel for electricity production, i.e. to purify the water and create a sustainable fuel at the same time. This chapter describes the first step in a chain of technologies used to make the nitrogen content from sewage usable as a fuel for a fuel cell. The focus of the laboratory work as carried out with the AnMBR was more practical than academic. Verification of the capacity of a membrane coupled UASB to remove the Chemical Oxygen Demand (COD) of the incoming sewage, yield biogas and produce a relatively clean ammonium solution, was required. Furthermore, it had to be confirmed that the organically bound nitrogen is indeed converted into ammonium during anaerobic digestion. Once this proved possible, the effluent had to be produced on a long-term to facilitate research on the subsequent steps towards the creation of a fuel out of the nitrogen present in sewage. This chapter describes the used UASB reactor, the operational parameters and the produced effluent characteristics.

3.1 MATERIALS AND METHODS

3.1.1 EXPERIMENTAL SET-UP

A laboratory scale UASB reactor with an effective volume of 7 liter was used, as described in Ozgun et al (2013b). The system was equipped with feed, recycle and effluent pumps, pH and temperature sensors and a gas meter. A three-phase separator was installed at the top part of the reactor to separate the biogas from the mixed liquid as well as to retain suspended particles in the reactor (Ozgun et al, 2013b), allowing for high upflow velocities. The reactor could be connected to an externally placed tubular cross-flow ultrafiltration membrane, with an available internal diameter of 0.8 mm (see appendix 3.1 for details on the membrane).

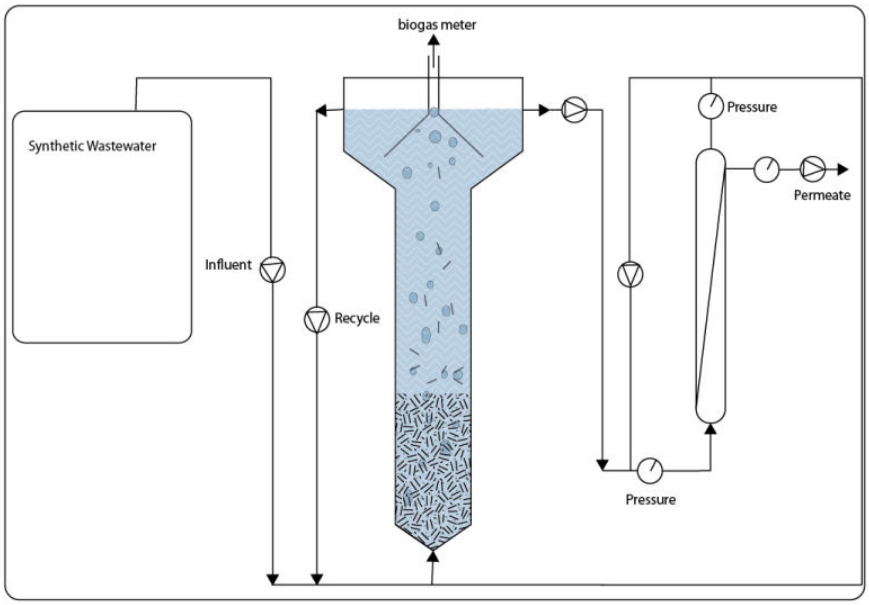

Figure 3.1 schematic layout AnMBR set-up

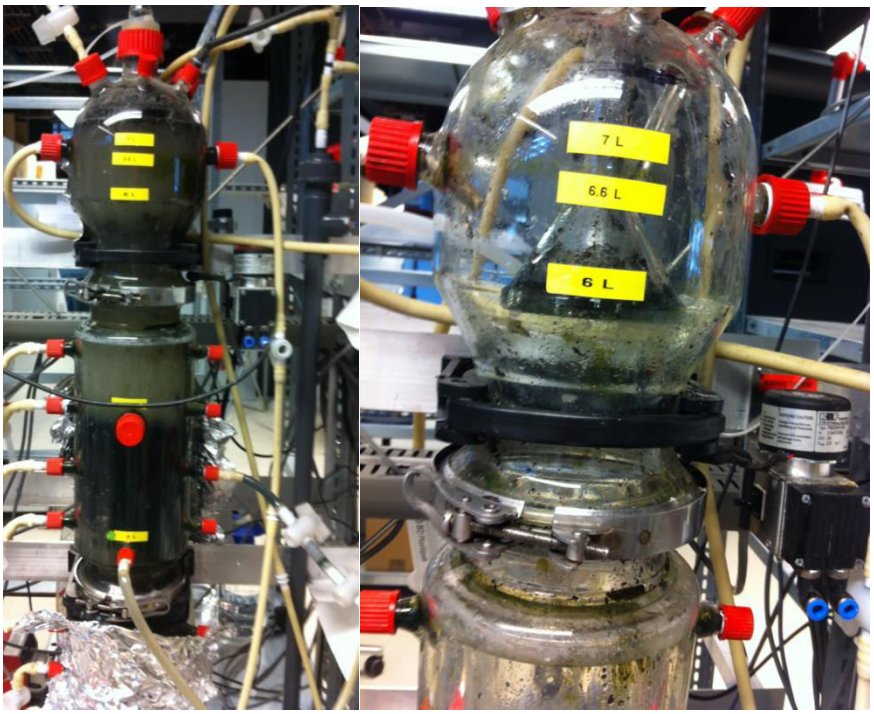

Figure 3.2a (left): Operational UASB reactor with expanded sludge bed. b (right): Three phase separator

3.1.2 SEED SLUDGE

The reactor was seeded with flocculent anaerobic sludge obtained from a pilot scale UASB reactor treating black water in Sneek. This sludge has been collected and stored by Ozgun et al (2013b).

3.1.3 WASTEWATER SOURCE

The reactor was fed with synthetic sewage. The macronutrient and micronutrient composition was based on the recipe as used by Ozgun et al (2013b). The composition of the concentrated synthetic wastewater is presented in table 3.1. The synthetic wastewater was prepared on a weekly basis and stored at 4°C. The feed solution was always completely mixed and diluted with tap water before mixture in a ratio of 1: 15. Table 3.2 shows the chemical properties of the diluted synthetic wastewater as fed to the reactor.

Table 3.1. Composition of the concentration synthetic sewage

Macro nutrients	g/l	Micronutrients	mg/L
Urea	1.2	$FeCl_3.6\ H_2O$	1000
NH_4CL	2	$CoCl_2.\ 6\ H_2O$	1000
$CH_3COONa.3\ H_20$	7.4	$MnCl_2.4H_2O$	250
Ovalbumin	0.45	$CuCl_2.4H_2O$	15
$MgSO_4.7H_2O$	0.18	$ZnCl_2$	25
$KH_2PO_4.3H_2O$	1.4	H_3BO_3	25
$CaCl_2$	0.265	$(NH_4)_6Mo_7O_{24}.4H_2O$	45
Starch	6.4	$Na_2SeO_3.H_2O$	50
Milk powder	1.5	$NiCl_2.6H_2O$	25

Yeast	0.6	EDTA	500
Sunflower Oil	1	HCL 36%	0.5
Micronutrients [ml]	13.3	Resazurin sodium salt	250
		yeast Extract	1000

Table 3.2. Properties synthetic wastewater

	mg/L
Total COD	530 ± 30
soluble COD	159 ±25
Total N	78 ± 5.2
NH_4-N	36 ± 5.5
TP	12 ± 0.8
TSS	230 ± 25

3.1.4 OPERTIONAL PROCEDURE

The reactor has been operational for a period of 123 consecutive days. Before starting the measurements, the seed sludge was acclimated to the synthetic wastewater in the UASB reactor for 40 days with an upflow velocity of 0.6 m/h.

According to Ozgun et al (2013b), the upflow velocity is an important variable which affects the effluent characteristics of an UASB. Considering the recycle flow within the reactor, the upflow velocity can be determined according to equation 3.1:

$$v_{up} = {Q_{in}}/{A} + {Q_r}/{A} \qquad [3.1]$$

Where: v_{up} = upflow velocity in the reactor [m/h]
Q_{in} = Feed flow synthetic wastewater [m^3/h]
Q_r = Recycle flow within reactor [m^3/h]
A = internal surface reactor [m^2]

Ozgun et al (2013b) concluded that an upflow velocity approaching 0.6 m/h resulted in the best results, i.e. the highest filterability and the slowest clogging of the membrane. Therefore, an corresponding upflow velocity was applied (see table 3.3) throughout the experiment, corresponding to a hydraulic retention time (HRT) of 6 hours and a daily effluent production of 30 L/day. The applied flux over the membrane was 12.3 L/m^2/h, as recommended by Ozgun et al (2013b).

Table 3.3. Operational parameters reactor

HRT	6	h
V	7	L
A	0.95	dm^2
Q_r	4.81	l/h
Q_{in}	1.25	l/h
v_{up}	0.64	m/h
J	12.3	l/m^2/h

During the experiments the pH was in the range of 6.5-7.1 and the temperature was controlled at 35°C by a thermostatic water bath. The experimental set-up was connected to a computer running LabView software, controlling all pump and

collecting pH, temperature and biogas flow data online. Influent Total N and NH_4-N concentrations have been measured at random intervals, and the NH_4-N effluent concentration was measured daily using standard methods (APHA, 2005) .

The membrane should have been connected once the biogas production of the UASB had stabilized. However, the measured biogas production did not stabilize (see 3.2 Results and 3.3 Discussion) and due to time pressure the membrane was connected nonetheless, after 81 days of UASB operation. During operations, the membrane was automatically backwashed with permeate during 20 seconds every 3 minutes. Furthermore, the membrane was backwashed during 15 minutes twice a day with tap water. Once clogging over the membrane increased significantly, this resulted in an increased pressure over the membrane. As described in chapter 2.2.2, the Trans Membrane Pressure (TMP) is a measure of how much forces is requires to push permeate through the membrane, so it can be used to indicate the fouling rate of the membrane. Once the TMP exceeded a TMP value of 220 mbar, the membrane was removed from the set-up, backwashed with high pressure tap water and chemically cleaned with an active chlorine solution for 24 hours.

3.2 RESULTS

The NH4-N concentration of the effluent was the most important parameter, since the focus in this research was on recapturing and using this ammonium as a fuel for a fuel cell. Furthermore, the COD removal and biogas production were indicators for proper UASB performance. Therefore, these factors will be elaborated upon separately. Due to the processes taking place in the reactor and the filtration by the membrane, the effluent was characterized by a low SS value and a low COD value, in which most of the nitrogen originally present in the wastewater is present in the form of NH_4.

Figure 3.3a: reactor in operation, clearly showing particles moving up with the biogas and settling continuously. b (right): UASB effluent without membrane (left) and with membrane

NH_4 CONCENTRATION ANMBR EFFLUENT

Table 3.4 shows the measured total nitrogen concentration, the average ammonium concentration of the influent synthetic wastewater and the average ammonium concentration of the AnMBR effluent. The ammonium concentration was indeed significantly increased due to the processes taking place in the reactor. Organically bound nitrogen was converted into ammonium during anaerobic digestion. The difference between the total influent nitrogen and the total effluent nitrogen concentrations can be explained by the nitrogen used for biomass growth and a (less significant) loss of ammonia gas in the

biogas. The nitrogen recovery amounted to 86%, this means that 86% of the total influent nitrogen was available in the form of ammonium in the effluent.

Table 3.4. Average total N, Ammonium influent and ammonium effluent concentrations

TN inf	78.0 ± 5.2	mg/L
NH_4-N inf	35.2 ± 5.5	mg/L
TN eff	68.5 ± 3.3	mg/L
NH_4-N eff	66.6 ± 8	mg/L

COD REMOVAL AND BIOGAS PRODUCTION

Table 3.5 shows the average Chemical Oxygen Demand (COD) of the influent synthetic wastewater and the effluent of the AnMBR. An average total COD removal efficiency of 82% was obtained. Compared to the efficiencies obtained by Ozgun et al (2013) this is a high value, which is probably due to the higher operation temperature.

Table 3.5. Average COD removal

COD in	530	mg/L
COD eff	95	mg/L
Average COD removal	82	%

Figure 3.4 shows the measured biogas production in ml biogas per day. Based on three gas composition measurements, the biogas produced consisted on average of 78,3 % of methane. Compared to literature, this is quite a high value for sewage as the substrate (van Lier, 2008b). The average daily methane yield amounted to 0.11 L CH_4/g $COD_{removed}$, and the average biogas production was 1.86 L/day. The biogas production was very irregular. In appendix 3.2 the COD balance is calculated, and only 49.9% of the incoming COD was (on average) accounted for. Many factors in the COD balance were not measured (biomass yield, other reduced gasses) and assumed instead, but still this is a very unfitting balance. This suggests biogas leakage (see the discussion for a further elaboration).

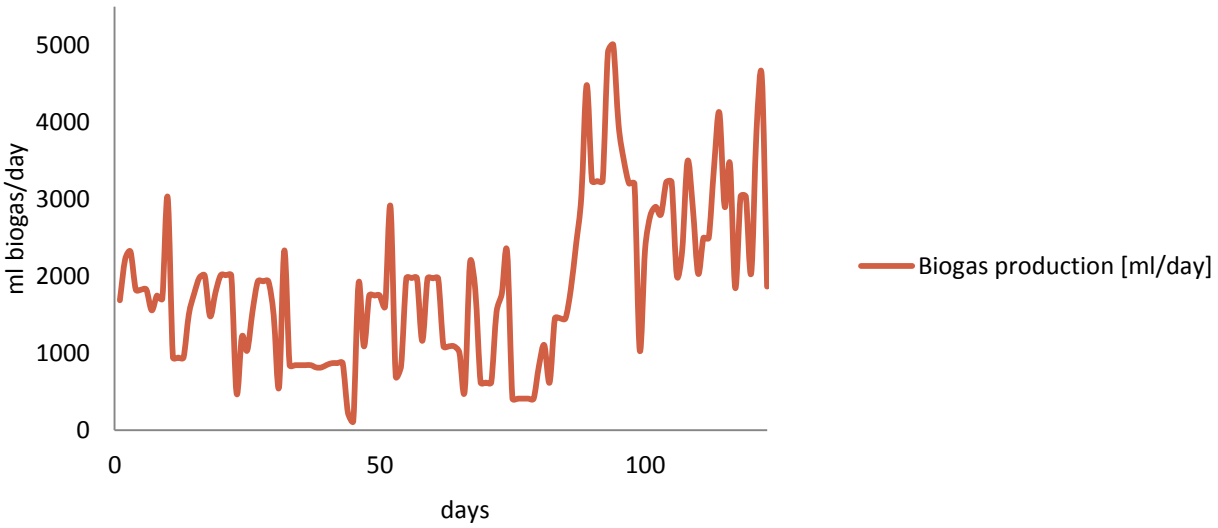

Figure 3.4 Biogas production (mL/day)

3.3 DISCUSSION

The measured biogas production was variable. Especially the extreme low values can be explained by the (many) operational difficulties that have been faced during the operational time of the AnMBR. Clogged tubes, torn tubes and irregular pumps frequently caused the flooding of the reactor, as often as extreme low water levels in the tank that both resulted in the discontinuation of the anaerobic process. This, of course influenced the biogas production negatively.

However, the more stable NH_4-N and COD concentrations of the effluent suggested that the operational difficulties cannot be held responsible for the unstable biogas production alone. Moreover, the COD balance, as described in appendix 3.2, only accounts for 50% of the incoming COD. This balance must be seen as a guidance, since the sludge yield is not measured but assumed. Yet, such a significant part of the COD balance that cannot be accounted for, suggests a biogas leakage. Possibly, the three phase separator did not function perfectly and it is likely that biogas leaked from the headspace out of the UASB reactor without being measured. Furthermore, during operation it was observable that significant amounts of sludge accumulated on top of the three phase separator, making it impossible to collect their produced biogas. However, considering the fact that the COD and NH_4-N concentrations of the effluent were as expected, no major effort has been paid to completely fixing the leakage.

Another discussion point is the analysis of the AnMBR effluent. Since the focus of the AnMBR operation was solely on 1) proper functioning (COD analysis) and 2) ammonium concentration increase (NH_4-N analysis), no other analysis of the AnMBR effluent has been carried out.

3.4 CONCLUSION

Despite of the variable measured biogas production, possibly because of leakage, the AnMBR had a stable COD removal and produced an effluent with an increased ammonium concentration and high nitrogen recovery (86%). Thus, indeed the organic bound nitrogen present in sewage was converted into ammonium, while producing biogas. Since the ammonium ions were not retained by the membrane, an effluent was produced with an average ammonium concentration of 67 mg NH_4-N/L out of a feed flow with 35 mg NH_4-N/L.

Section II: Ion Exchange

4 ION EXCHANGE THEORY

As described in the previous chapter, the AnMBR converts (most of) the organically bound nitrogen present in sewage into ammonium ions (NH_4^+). These ammonium-ions are not retained by the ultrafiltration membrane and thus the AnMBR effluent has an ammonium concentration of approximately 67 mg NH_4-N/L. Since the ammonium ions from the AnMBR effluent are to be used as a fuel for electricity production by a fuel cell, the creation of an ammonia rich gas is required. In order to create a pure ammonia-rich gas, first the ammonium-ions have to be isolated from the AnMBR effluent. Secondly, the ammonium has to be concentrated. The choice has been made to use Ion Exchange (IE) for separating and concentrating the ammonium-ions. This chapter describes how the ion exchange process works. The ion exchange kinetics are elaborated upon and the operational parameters are described. Basically, this chapter holds the background information that is necessary for the actual implementation of an ion exchange column in series with the AnMBR as described in chapter 5. The final part of this chapter describes the choices made for the ion exchange laboratory tests carried out within this thesis research, based on the theory discussed. In appendix 4.1, an elaboration on different types of ion exchangers (zeolites, resins and alternative ion exchangers), their main properties and the influence of wastewater on the ion exchange properties (per type of ion exchange material) can be found.

In addition to the isolation from the anMBR effluent and the concentration of the ammonium ions, the other major objective of ion exchange is the removal of ammonium from the AnMBR effluent up to values that meet the discharge quality standards set for nitrogen (10-15 mg TN/L).

4.1 ION EXCHANGE KINETICS

Ion exchange is a physical-chemical water treatment method, used in order to remove ions from solutions up to low concentrations. The principle of ion exchange is a reversible chemical reaction between a substance (the ion exchanger) and a solution. During the reaction, ions that are electrostatically bound to the surface of the ion exchanger are substituted with dissolved ions of similar charge that are present in the solution (Verkerk, 2003). At the completion of the process, the ion that was originally part of the ion exchanger and the ion that was originally in solution, are found in reversed places. Cationic and anionic exchange refers to respectively the exchange of positively charged ions (cations) and negatively charged ions (anions). For the removal of ammonium, cation-exchangers are used, which exchange sodium-ions for ammonium-ions. Formula 4.1 shows the reversible exchange process, where the cation-exchanger is presented by R (Verkerk, 2003).

$$R\text{-}Na + NH_4^+ \rightarrow R\text{-}NH_4 + Na^+ \qquad [4.1]$$

The most important kinetic property of the ion exchanger is the capacity to move the exchanged ions to the right place, since this defines the exchange rate i.e. the rapidity in which ions are replaced. The exchange from and to the ion exchanger takes place equally, because the electro-neutrality of the exchanger has to be guaranteed (Verkerk, 2003). The actual exchange rate is influenced by several physico-chemical features, like the specific properties of the ion exchanger, the concentration-gradient, gradients of electrical load and the interaction in between the ions (including potential chemical reactions) (Verkerk, 2003). The mechanism of the exchange process is described using the diffusion equation (assuming the diffusion as the rate limiting step in the exchange process). The first law of Fick defines the exchange flux for an ion A through a layer with thickness δ (Jacques and Prahl, 1998):

$$J_A = \frac{D_A \Delta C_A}{\delta} \qquad [4.2]$$

With:			
	J_A	= Exchange flux	[kmole/m^2.s]
	D_A	= Diffusion coefficient	[m^2/s]
	ΔC_A	= Concentration gradient over the layer	[kmol/m^3]
	δ	= Thickness of layer	[m]

Thus, the law of Fick shows that the rate of molecular transport with a constant diffusion coefficient, is proportional to the concentration gradient of the diffusing ion. However, in practice the diffusion coefficient will never be constant (Verkerk, 2003). The diffusion coefficient for ion exchange is in practice influenced by the average velocity of the molecules, the free space, the temperature and the occurrence rate of collisions with the matrix of the ion exchanger. Furthermore, the ion exchange shape is never completely homogeneous. For a more accurate description of the ion exchange rate, diffusion on the inside and outside of the ion exchanger can be looked at (Bolto et al, 1987). Bolto et al (1987) distinguished seven steps in the kinetics of ion exchange (see figure 4.1):

Step 1. Diffusion of ions out of the surrounding solution to the statical layer (the film) around the ion exchanger-grain.

Step 2. Diffusion through the film surround the ion exchanger grain (film diffusion)

Step 3. Diffusion through the ion exchange-matrix to the site of exchange

Step 4. The actual ion exchange reaction (pore diffusion)

Step 5. The diffusion of the disconnected ion through the ion exchanger to the surface of the ion exchange grain

Step 6. The diffusion of the disconnected ion through the film

Step 7. The diffusion of the disconnected ion to the surrounding solution

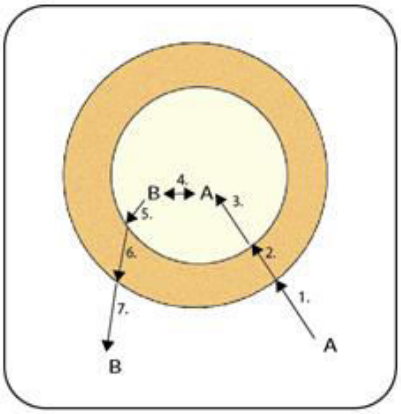

Figure 4.1 Schematic image of the diffusion steps

When there is sufficient turbulence around the ion exchange grain, step 1 can be neglected. Usually, this is ensured by the flow through the ion exchange bed. Thus, the rate limiting step is or the diffusion of the ion through the film (film diffusion, step 2) or the diffusion through the ion exchange matrix (pore diffusion, step 4).

For pore diffusion, the rate of exchange (s^{-1}) is to a large extend determined by the mobility of the ions in the ion exchangers, which is affected by the radius of the grain. The exchange rate v is proportional to the internal diffusion coefficient D (m^2/s) of the ion exchanger and inversely proportional to the square of the grain radius r (m) (Bolto et al, 1987). When it is assumed that the grains are spherical and uniform in size, it follows that:

$$v = \frac{D}{r^2} \qquad [4.3]$$

Out of equation 4.3 it follows that the exchange rate increases with a smaller grain-diameter.

For film diffusion the exchange rate is proportional to the diffusion coefficient of the film *D* and to the concentration of the solution *C*. Also, the exchange rate is inversely proportional to the grain radius *r*, the thickness of the film δ and to the concentration of the competing ion C (as is shown in equation 4.4):

$$v = \frac{DC}{r\delta \underline{C}} \qquad [4.4]$$

The thickness of the film (δ) depends on the flow velocity through the column. A larger flow velocity results in a smaller film thickness and thus a larger exchange rate (assuming film diffusion is the rate limiting step). In diluted solutions (< 0.01M) film diffusion is rate limiting and in concentrated solutions (> 0.1 M) the pore diffusion will determine the rate of ion exchange (Verkerk, 2003). The AnMBR effluent ammonium concentration approximates 0.005M and therefore film diffusion is expected to be rate limiting for the ammonium removal with ion exchange. There is one important factor that does not affect the ion exchange rate itself, but does affect the actual removal of ammonium. This is the competition between ammonium ions and other cations present in the AnMBR effluent (Potassium, Calcium and Magnesium). These competing cations will not cause a lower exchange rate, but they can 'occupy' exchangeable sites on the ion exchanger. This will result in a lower exchange of ammonium (Verkerk, 2003). The influence of competing cations depends on their presence and on the selectivity of the used ion exchanger for ammonium. The selectivity refers to the degree of preference or affinity that an ion exchanger has for a specific cation over other cations. The selectivity differs widely per exchanger and cation combination.

4.2 ION EXCHANGE AND AMMONIUM REMOVAL FROM WASTEWATER

This chapter focusses on the use of ion exchange for ammonium removal from AnMBR effluent. To eventually obtain an ammonia rich gas, the ammonium ions have to be isolated from the AnMBR effluent, to make sure that other components of the anMBR effluent will not be fed to the fuel cell.

In this section, first an overview is given of literature on ammonium removal from wastewater, and afterwards the operational parameters of the ion exchange process are described. The goal of this chapter is to function as a argumentation of the choices that were made concerning the tested operational properties of the ion exchange laboratory scale set up, used in this thesis for separating and concentrating the ammonium from the AnMBR effluent. In appendix 4.2 an elaboration on the properties and behavior of different types of ion exchangers (zeolites and organic resins) can be found, plus an overview of alternatively used ion exchangers.

4.2.1 LITERATURE REVIEWON AMMONIUM REMOVAL FROM WASTEWATER

The traditional method for ammonium removal from wastewater is based on biological treatments (Metcalf and Eddy, 2004, Verkerk and the Graaf, 2001). However, as the discharge limits for treated wastewater became more stringent over time, ion exchange gained momentum as available method for the removal of ammonium from wastewater (Jha and Hayashi, 2009). Moreover, under special circumstances, such as a low organic content/nitrogen ratio in the wastewater or when it is aimed to re-use the ammonium (as is the case in this thesis), the ion exchange process might be more suitable compared to traditional biological nitrification-denitrification where the ammonium is destroyed. The fact that with ion exchange both recovery and removal of ammonium from wastewater is possible, is an obvious advantage over other ammonium removal technologies (Verkerk and de Graaf, 2001). Likewise, the short contact time, the low energy demand

and the relatively simple operation are other mentioned advantages of using ion exchange in wastewater treatment (Malovanyy, 2013).

Much literature can be found on the use of ion exchange for ammonium removal in wastewater treatment. Most literature focuses on the comparison and analysis of different types of ion exchangers. In practice, natural zeolites are used significantly more than resins for ammonium removal.

In the work of Malovanyy et al (2013), Nguyen and Tanner (1998), Jha and Hayashi (2009) and Liberti and Passino (1981) different types of ion exchangers are analyzed and compared on the removal of ammonia from (treated) wastewater using different types of ion exchangers. In spite of the wide range in publication date, these articles are in essence comparing the same types of ion exchangers: artificial resins, e.g. strong acid cation exchangers (SAC) and weak acid cation exchangers (WAC) and natural zeolites (always Clinoptilolite is tested, and sometimes different types of Clinoptilolite). The conclusions of all mentioned studies consist more or less of the following: Due to the high exchange capacity and fast regeneration in clean water, at first glance SAC resins seems to be the best ion exchanger available. However, SAC resins have a very low selectivity for ammonium, thus in the presence of competing anions, the SAC resins perform poorly. The natural zeolites tested, mainly Clinoptilolite, have a bit lower total exchange capacity but feature a very high selectivity for ammonium. Therefore, the conclusion is in the mentioned articles that for removing ammonium from wastewater (with a high incidence of competing ions like K^+, Mg^{2+}, Ca^{2+}) the use of the natural zeolite Clinoptilolite is most suitable. Thus, although the ion exchange capacity and the exchange rate for natural zeolites are relatively low compared with resins, the preference for ammonium above competing cations proves to be the most influential parameter on the obtainable operational capacity for removing ammonium from (treated) wastewater.

It is remarkable that most studies on ammonium removal from wastewater using ion exchange do not include the natural zeolite Chabazite in their studies. The only study that does consider Chabazite for removing ammonium from wastewater is performed by Verkerk (2003). Leyva-Ramos (2010) and Langwaldt (2008) are the only found studies that also investigated Chabazite as an ion exchanger, but these studies do not consider the application of ion exchange in wastewater treatment. Verkerk (2003) compared 5 different types of ion exchangers (2 types of Clinoptilolite, Chabazite, an artificial zeolite, an SAC exchanger and a WAC exchanger), and concluded that in the absence of competing ions, the SAC resins have a highest exchange capacity and the most complete regeneration, but in wastewater it proved that the natural zeolites behaved better. Both in terms of exchange capacity and regeneration. Moreover it was found that in both wastewater and clean water, Chabazite showed the largest operational exchange capacity (9,5 mg NH_4-N per g Chabazite) and the most complete and quickest regeneration.

It is notable that in literature on ion exchange of ammonium, Clinoptilolite has been studied most extensively, whereas Chabazite has such a better exchange capacity, selectivity and stability. This is most probably due to the fact that Clinoptilolite is the most abundant natural zeolite and Chabazite is less available.

Based on the described literature, the choice has been made to compare three types of natural zeolites to see which zeolite functions best for separating and concentrating the ammonium from the AnMBR effluent. These three types of compared zeolites are Chabazite, Clinoptilolite and a thermal pre-treated Clinoptilolite (see appendix 4.2 for specifications).

4.2.2 AMMONIUM REMOVAL FROM 'ANMBR' EFFLUENT USING ION EXCHANGE-OPERATIONAL PARAMETERS

In this section the operational parameters of the ion exchange process are explained. The ion exchange process consists of three phases: loading, backwashing and regeneration. The operations are described of a set up that uses a zeolite as ion exchanger and a NaCl solution for regeneration. Thus, the zeolite will constantly exchange ammonium-ions and sodium-ions (Na^+). During the loading phase, the AnMBR effluent is flowing through a column packed with the zeolite. Before the loading phase starts, the zeolite is saturated with sodium-ions, e.g. all exchangeable sites are occupied by sodium-ions. When the AnMBR effluent is led through the column, the ammonium is bound to the ion exchanger, and the replaced sodium-ions leave the process with the effluent (Verkerk, 2003). As either the exchanger becomes saturated with ammonium (when all exchangeable sites are taken), or the total feed solution passed the column, the zeolite bed is cleaned by means of backwashing with tap water. Hereafter, the zeolite is regenerated chemically by passing a concentrated salt solution through the column. The ammonium-ions are exchanged by sodium-ions, and the ammonium-ions thereby become in solution again (Semmens et al, 1977). The displaced ammonium-ions flow out of the column with the regeneration solution and are collected. Thus, overall, the ion exchange process does not remove the ammonium from the water phase, but concentrates the ammonium in a smaller volume instead (Verkerk, 2003).

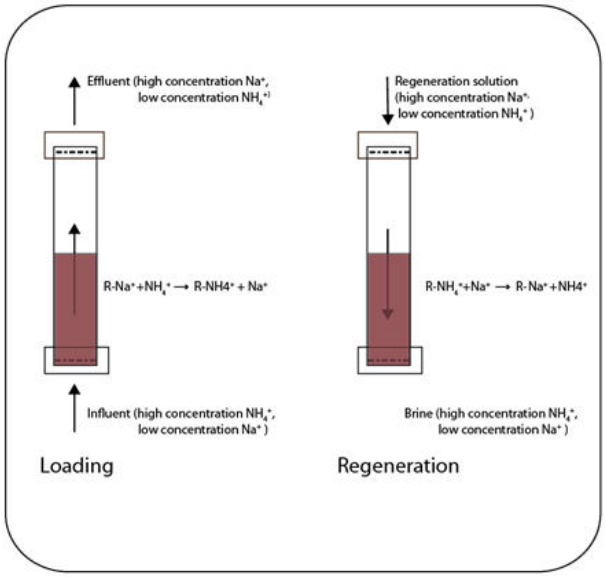

Figure 4.2: Loading and Regeneration

Figure 4.2 schematically shows the loading and the regeneration phases (with a counter-current flow pattern). Several factors influence the ion exchange process used for ammonium removal. In the following sections, subsequently the loading, backwashing and the regeneration processes will be explained, based on the most influential parameters.

4.2.2.1 LOADING

The majority of ion exchange processes is carried out in fixed bed columns with a counter-current flow regime, i.e. an upward flow regime during the loading phase and a downward flow during the regeneration phase (Semmens et al, 1977). Once the treated flow comes into contact with the ion exchanger, in the upper layer an exchange between ammonium and sodium ions will occur according to (Verkerk, 2003):

$$R\text{-}Na + NH_4^+ \rightarrow R\text{-}NH_4 + Na^+ \quad [4.5]$$

The ammonium-free treated water flows through the column without any further exchange taking place. After a while, the first layer of the exchange material will be saturated, i.e. 'full' with ammonium ions. The zone in which the exchange process takes place will thus shift downwards through the column. Below this ion-exchange front, the wastewater is ammonium free and the ion exchanger is still loaded with sodium ions (the ammonium-free wastewater is in equilibrium with the regenerated ion exchanger)(Verkerk, 2003). Figure 4.3 shows this schematically. When during the loading phase a downward flow regime is applied, the ion exchange front moves downward during the loading. When an upward flowing loading regime is applied, the ion exchange front will move upwards.

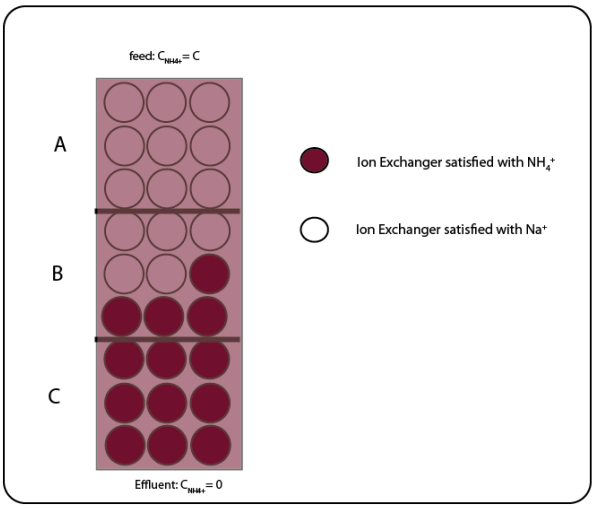

Figure 4.3 Schematic reproduction of the ion exchange bed. A is satisfied with ammonium, in zone B the ion exchange front is located and zone C is still completely in the regenerated state.

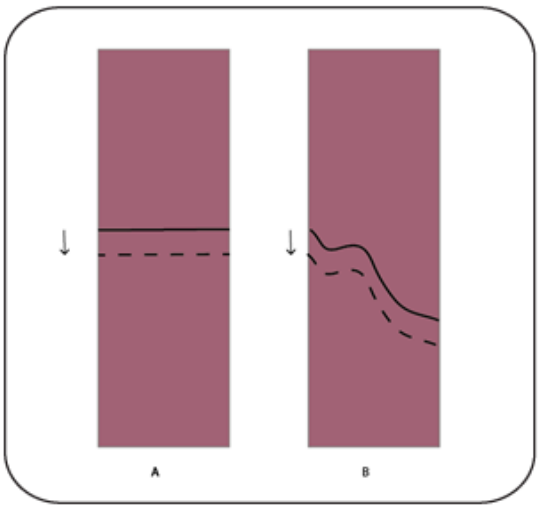

Figure 4.4 A shows a sharp ion exchange Zone front and B a disperse ion exchange front

If the zeolite has a large selectivity for ammonium, the ion exchange front will have a sharp profile because the exchange equilibrium will quickly be set. When a zeolite is used with a low selectivity for ammonium, the ion exchange front will be more diffuse. Once the ion exchange front reaches the end of the zeolite bed, additional ammonium cannot be bound anymore and will end up in the effluent. This is called the break-through of ammonium. If the loading process would continue for a long time after the occurrence of break-through, the effluent ammonium concentration would equal the ammonium concentration of the feed due to the lack of exchange. The loading process should be stopped before breakthrough. The following parameters are influential during the loading process, in random order:

1. Exchange Capacity of the zeolite
2. Flow velocity through the column
3. Effluent concentration of ammonium (break-through point)
4. Grain size of the zeolite
5. Feed characteristics (presence of competing ions)
6. Depth of the ion exchange bed
7. pH
8. Temperature
9. Pre-treatment

In this thesis, the most important (and tested) parameters are the capacity of the ion exchanger, the flow through the column and the depth of the ion exchange bed. Information on all other parameters, and extra information on the described parameters are described in appendix 4.3.

LOADING PARAMETER 1: THE EXCHANGE CAPACITY OF THE ION EXCHANGER

The total exchange capacity describes the total amount of cations that theoretically can be exchanged by the ion exchanger in milligram cation per gram exchanger. So, the capacity refers to the number of free negatively loaded 'sites' located on the exchanger, which are available for ion exchange (Verkerk, 2003). In practice, not all these free sites are available, due to competing ions, a too high loading velocity or incomplete regeneration (Malovanyy, 2013). The capacity that is achieved in practice is called the operational capacity.

For natural zeolites, the capacity depends on the purity of the zeolite-rock. Therefore, the capacity needs to be determined experientially. Usually, the suppliers of natural zeolites supply the total capacity together with the zeolites. For synthetic zeolites, the capacity can be calculated directly based on the chemical formula of the crystal-matrix.

As explained before, this total capacity is hardly ever met. The operational capacity is strongly influenced by the regeneration, the influent-characteristics (concentration and present competing cations), selectivity of the ion exchanger and the flow of the feed (Verkerk, 2003). In theory, after regeneration the original operational capacity should be restored. In practice, however, this does not happen due to incomplete regeneration and accumulation of cations on the ion exchanger (Malovanyy et al, 2003).

The total capacity of natural zeolites ranges from 20-77 mg NH_4-N/g zeolite and the operational capacities range from 4- 50 mg NH_4-N/g zeolite (as found in literature, Green et al, (1996), de la Torre Gutierrez (1999), Chmielewska (1996), Koon et al (1975), Malovanyy et al (2013), Nguyen and Tanner (1998), Jha and Hayashi (2009), Liberti and Passino (1981) and Verkerk (2003)).

LOADING PARAMETER 2: FLOW RATE THROUGH THE COLUMN

In theory the capacity of zeolites decreases as the flow rate increases, due to a decreased contact time (Verkerk, 2003). McLaren et al (1973) did extensive research on the impact of the flow rate, ammonium concentration and temperature on the ion exchange process. They concluded that doubling the flow rate (from 8 to 16 BV/h), results in a decrease in operational capacity of 10%. This impact of the flow rate is independent of the temperature and the ammonium concentration, a larger flow rate does also result in a more dispersed ion exchange front (which can be made undone by a higher selectivity for ammonium). However, the influent ammonium concentration has a more significant effect on the ion exchange process compared to the flow rate (see loading parameter 3).

Due to differences in ammonium influent concentrations, used ion exchangers and the set break through limit (i.e. the maximal ammonium concentration in the effluent) among studies (and the fact that many studies do not report those details explicitly), it is difficult to compare the effect of different flow velocities of regeneration solution through the column. In appendix 4.3, an overview is given of operational parameters as found in literature with corresponding flow velocities (with many lacking data). However, table 4.1 shows the ranges of flow-velocities as applied in found literature.

It can be stated that in practice the influent ammonium concentration of the feed did not influence the chosen flow rates very much in the consulted literature. Almost all studies applied a flow rate in the range of 5 to 15 BV/h, with a few outliers with higher values.

Table 4.1. Researched ranges of flow rates and associated study details

	[BV/h]	Feed Concentration mg NH_4-N/L	Ion Exchanger
Verkerk, 2003	5 -15	50	Clinoptilolite and Chabazite
McLaren et al, 1973	6,7 - 13,3	70	Clinoptilolite
Green et al, 1996	10 - 20	40	Chabazite
Jorgens et al, 1976	5 - 10	25 and 28	Clinoptilolite
Booker et al, 1996	7 - 15	50	Clinoptilolite
Liberti, 1982	15	40	Clinoptilolite
Liberti, 1981	24	28	Clinoptilolite
Koon et al, 1975	10 - 15	20	Clinoptilolite

LOADING PARAMETER 3: FEED CHARACTERISTICS (PRESENCE OF COMPETING IONS)

The ammonium concentration of the feed has a significant influence on the operational exchange capacity of ion exchangers, larger than the flow rate and the temperature (Verkerk, 2003). According to McLaren et al, 1973, increasing the ammonium concentration of the feed from 17 to 70 mg NH_4-N/L, leads to doubling of the operational capacity. However, a high ammonium feed concentration results in a more frequent required regeneration. According to Verkerk (2003), this will make the use of ion exchange for solutions with high ammonium concentrations (> 70 mg NH_4-N/L) undesirable. See appendix 4.3 for a detailed description of the composition of Dutch municipal wastewater and the AnMBR effluent as used in this thesis.

4.2.2.2 BACKWASHING

The aim of backwashing is to clean the zeolite bed from suspended solids, organic matter and trapped air, before and after the loading. Generally, backwashing happens with tap water, but backwashing with in exchange effluent is also possible. Also the potentially created flow patterns and canals through the bed are removed. Optimal backwashing happens with a bed expansion of 30% (Verkerk, 2003).

The backwashing before the loading washes out the trapped regeneration solution. This reduces the risk on ammonium leakage, since the ion exchanger will not absorb ammonium once large amounts of sodium are still available.

4.2.2.3 REGENERATION

After the loading phase, the ion exchange bed is regenerated by passing a concentrated salt or acid solution through the column. Depending on the type of regeneration solution used, the sodium, calcium or hydrogen cations that were bounded to the ion exchanger before the loading, take their place back during regeneration, pushing the previously bounded ammonium ions back into solution. This exchange is possible due to the high concentration of the regeneration-cations, even when the exchanger has a higher selectivity for ammonium. The required concentration in the regeneration solution is determined empirically in literature, there is no fundamental relationship between operational capacity and required

regeneration solution found. Often one certain volume of regeneration solution can be re-used. In order to retrieve and concentrate the ammonium, peak concentration collection is applied, as explained in the following section. In practice it is impossible regenerate the zeolites entirely , thus the initial operational capacity will never be recovered completely (Verkerk, 2003). The quality of the regeneration solution decreases over time due to pollution with other cations and accumulation occurs of the cations that have a larger selectivity with the ion exchanger on the zeolites than ammonium (Verkerk, 2003). Furthermore, per cycle a part of the regeneration solution gets lost due to dilution. This can be minimized by draining the ion exchange bed before and after regeneration. According to Liberti et al, 1981 the capacity loss for Clinoptilolite regenerated with a salt solution (c), amounts to 10% after each regeneration cycle.

PEAK CONCENTRATION COLLECTION

The regeneration phase can be described and compared using a regeneration curve. A regeneration curve shows the course of the ammonium concentration in the regeneration solutions that passes the ion exchange bed against the volume of regeneration solution that passed the ion exchange bed (Figure 4.5). The shape of the regeneration curve is dependent on the type of regeneration solution and the flow velocity during regeneration. The black line in figure 4.5 represents an efficient regeneration, with a steep and high regeneration peak. A steep regeneration curve shows a high exchange rate and a high peak value means that the first few volumes of regeneration solution, regenerated the complete ion exchange bed. The red regeneration curve shows an in-efficient and incomplete regeneration, with nor a steep nor a high regeneration peak (for example this can be case if the regeneration solution is polluted with competing cations).

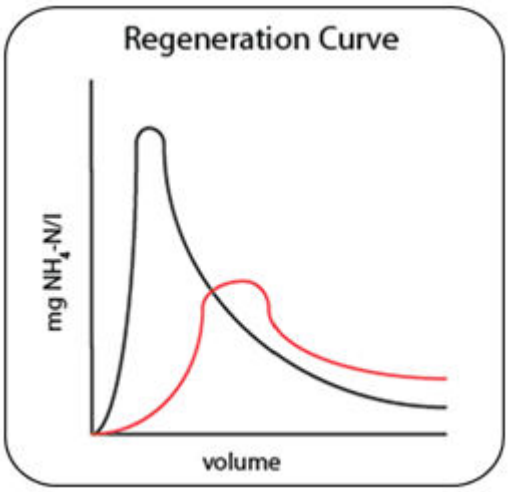

Figure 4.5 Typical regeneration curve

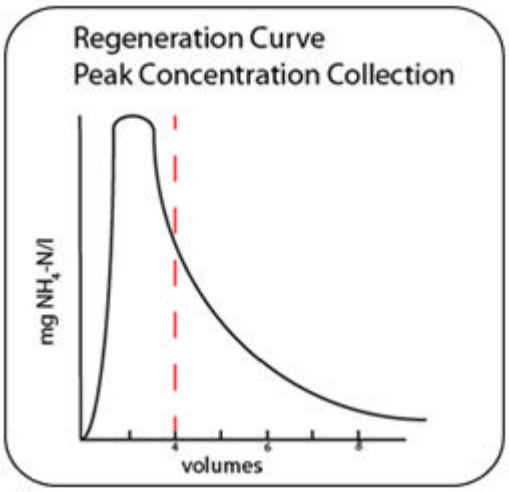

Figure 4.6 schematic Peak Concentration Collection

The objective of the ion exchange step in this thesis is to separate and concentrate the ammonium from the AnMBR effluent. A high ammonium concentration is required for the efficient production of an ammonia rich gas. The concept of Peak Concentration Collection (PCC) will be used to obtain the required ammonium concentration.

The PCC concept basically holds that in order to obtain a high ammonium concentration, only the part of the regeneration solution is collected that holds the ammonium peak (as shown in figure 4.6). For example, the peak in the regeneration curve shown in figure 4.6 falls within the first 4 volumes of regeneration solution leaving the ion exchange bed. Applying the PCC concept implies that these first 4 volumes are collected separately and the rest of the regeneration solution is recycled immediately and reused for future regeneration. Subsequently, the obtained 4 volumes with the high ammonium

concentration are used to create an ammonia rich gas, and a matching volume of fresh (ammonium-free) regeneration solution is added to the total regeneration solution.

When PCC is applied, during the first few ion exchange cycles an accumulation of ammonium in the regeneration solution will occur, but the ammonium accumulation will stabilize. If after stabilization, the total incoming ammonium corresponds to the total ammonium in the obtained 4 volumes as is shown in figure 4.6, no further post treatment or replacement of the regeneration solution is required.

Through PCC, it is tried to 'catch' as much ammonium as possible in a small volume. This will be facilitated by a steep and high peak in the regeneration curve. As said, the shape of the regeneration curve is caused by the type of regeneration solution and the regeneration flow rate.

Properties that affect the regeneration efficiency and thus the shape of the regeneration curve are:

1. Type of regeneration solution
2. The flow rate
3. The pH
4. The flow direction

TYPES OF REGENERATION SOLUTIONS

Sodium-chloride (NaCl) is used in the far majority of practical applications of ion exchange (Verkerk, 2003). However, other salt or acid solutions can also be used. Different regeneration solutions mentioned in literature are sodium nitrate ($NaNO_3$) (Semmens, 1979), calcium chloride ($CaCl_2$) (Koon et al, 1975), calcium hydroxide ($Ca(OH)_2$), sodium hydroxide (NaOH) (Mercer et al, 1970), potassium chloride (KCl) (Kallo, 1995), hydrochloric acid (HCL) or hydrogen sulphate (H_2SO_4) (Verkerk, 2003). The choice of regeneration solution is mainly depending on the type of ion exchanger used. Resins can be regenerated using strong acids, while strong acids will harm the crystal matrix of zeolites. In literature, no information has been found on the regeneration using acids for ammonium removal from wastewater.

Salt solutions on the other hand, are most used for the regeneration when ammonium removal from wastewater is considered (Verkerk, 2003, Koen et al, 1975, Halling-Sorensen, 1993). Salt solutions do not harm the zeolite matrix. Moreover, salt is cheap and easily manageable. Most ion exchanger have a low selectivity for sodium. Therefore, the exchange between sodium and ammonium is relatively easy (Verkerk, 2003). Often, a sodium chloride solution is used. Sodium chloride is cheap, easy to dissolve and the chloride ions do not affect the ion exchange process. The only main disadvantage of using a salt solution for regeneration is the increase of sodium concentration in the effluent. The salt concentration of the regeneration solutions affects the shape of the regeneration curve. Literature shows that a higher salt concentration results in a faster regeneration (and thus a steeper regeneration curve). This corresponds to the ion exchange kinetics. Due to costs and salt-sensitive post-treatment of the regeneration solution, in practice salt concentrations between 20 and 40 g/L are used (Verkerk, 2003). In their own study on ammonium removal from wastewater, Verkerk used a 100 g/L NaCl solution for regeneration (Verkerk, 2003).

Another type of regeneration, is to use calcium solutions. Regeneration with calcium gives a faster break through and a slower regeneration compared to sodium (Mercer et al, 1970). A slower regeneration results in a less steep regeneration curve, making the use of calcium less attractive considering PCC. Regeneration with potassium has also been mentioned.

Natural zeolites have a higher selectivity for potassium compared to ammonium, which can result in permanent bounding of potassium, reducing the exchange capacity of the ion exchanger (Verkerk, 2003).

Liberti et al (1981) and Verkerk (2003) mention the potential regeneration using sea water. Dutch sea water contains approximately 24 g/L NaCl. Within their studies, there is no data reported on the regeneration with sea water, it is only stated that sea water functioned as a regeneration solution with no quantified argumentation. Sea water, if available, would of course be a very cheap solution and is therefore also tested in this thesis. However, a lower regeneration capacity is expected compared to NaCl solutions due to the presence of competing cations.

THE FLOW RATE

In general, comparable loading and regeneration flow rates are used in literature. However, to ensure sufficient contact time, a smaller regeneration flow velocity might be used. According to Jorgensen et al (1993) a flow rate in the range of 4 – 20 BV/hour is desirable. In the research done by Verkerk (2003) on ammonium removal from wastewater, a flow rate of 10 BV/h was used.

PH

According to Koon et al (1976), a high pH (12, 5) leads to regeneration curves with higher and steeper peaks compared to a low pH (when caustic soda (NaOH) and calcium hydroxide (Ca(OH)) are used for regeneration). A disadvantage of the high pH is the degradation of the matrix of zeolites and the high chemical costs (Verkerk, 2003). Moreover, ammonia nitrogen exist in aqueous solution as either the ammonium ion NH_4^+ or the ammonia gas NH_3, depending on the pH of the solution, in accordance with the following equilibrium reaction (Metcalf and Eddy, 2003).

$$NH_4^+ \leftrightarrow NH_3 + H^+ \qquad [4.6]$$

A high pH will cause the ammonium-ammonia equilibrium to shift towards the right and causing the ammonium to escape from the solution in the form of ammonia gas (equation 4.6). This will imply the loss of ammonium, since it is difficult to retrieve the ammonia gas during the ion exchange step.

FLOW DIRECTION

The flow direction during loading and regeneration has a significant impact on the process. The loading and regeneration can be done with a co-current flow direction (both the feed and the regeneration solution flow in the same direction through the column) or in a counter-current direction (the feed flows top-down and the regeneration solution flows bottom-up for example). Verkerk (2003) advices a counter-current flow direction. since a counter-current flow direction protects against leakage by making sure that the ion exchangers that the feed solutions meets the last, are regenerated the best since these layers are the first to come in contact with the fresh regeneration solution.

4.3 THEORY APPLIED

The theoretical background as described in this chapter is used for designing and implementing a laboratory-scale ion exchange column, that can be used to separate and concentrate the ammonium from the AnMBR effluent. This section sums the made decisions.

Ion Exchanger

Based on the literature review, zeolites were chosen as the most suitable type of ion exchanger. Basically all literature reported that natural zeolites were both more selective and stable compared to artificial zeolites and resins, when used for ammonium removal from (pre-treated) wastewater. The most researched zeolite is Clinoptilolite. The natural zeolite Chabazite is hardly mentioned in literature, but in the spare cases that Chabazite it researched it behaves better than Clinoptilolite. Therefore, the choice has been made to do preliminary batch tests with 3 types of natural zeolites: Chabazite, Clinoptilolite and a thermally modified Clinoptilolite. See appendix 4.3 for more characteristics of the tested natural zeolites. The best performing zeolite will be used in the column set-up. See appendix 4.4 for the calculation of the required bed volume of ion exchanger in the column. The objective of the column tests is to identify the most suitable operational conditions for the ion exchange pilot installation, in order to obtain a sufficient amount of a sufficiently concentrated ammonium solution.

Loading flow rate

Almost all literature uses loading flow rates in the range of 5 to 15 BV/h. Since a faster loading velocity results in a less time consuming process, loading with velocities of 10 and 15 BV/h have been tested.

Regeneration solution

Sodium-chloride (NaCl) is chosen as the most suitable regeneration solution. This is because it is cheap, does not harm the zeolites and because natural zeolites have a low selectivity for sodium. The impact of the NaCl concentration on the regeneration curve is investigated. Since a rather quick regeneration is required to enable PCC, the choice has been made to test rather high NaCl concentrations (e.g. 100 g NaCl and 150 g NaCl)

Regeneration flow velocity

The objective of the ion exchange pilot installation is to create a sufficient volume of a concentrated ammonium solution. For obtaining this concentrated ammonium solution, PCC is used. The success of PCC depends on the shape of the regeneration curve. The regeneration curve depends on the regeneration flow velocity, and thus the choice for the tested regeneration flow velocities is quite significant. Two conflicting values must be considered. One the one hand, the regeneration solution has to be in contact with the ion exchangers for sufficient time to enable complete exchange of ammonium with sodium. On the other hand, the velocity must not be chosen too small, since for the An MBR solution the film-diffusion limits the ion exchange rate (see chapter 4.1). A too small flow velocity results in a thicker film around the ion exchangers, leading to a lower exchange rate. Moreover, a very small regeneration flow velocity is also unpractical, since it will result in a more time consuming regeneration. In literature, values ranging from 4 – 20 BV/h are used. The choice was made to do column tests with 10 and 15 BV/h.

5 ION EXCHANGE LABORATORY RESULTS

Production of ammonia gas as fuel for a SOFC out AnMBR effluent requires the separation of ammonium from the rest of the AnMBR effluent and the subsequent concentration of ammonia. As described in chapter 4, ion exchange is a suitable technology for separating cations from a liquid flow and the suspended particles within this liquid flow. Therefore, ammonium ion exchange was applied in this thesis.

Ion exchange experiments were conducted in the water laboratory of the Delft University of Technology to determine the most functional type of ion exchanger and optimal operational parameters for separating an concentrating the ammonium, the production of an effluent that meets the Dutch water quality regulations for nitrogen (< 10 mg TN/L) and ultimately the highest ammonium concentration that could be obtained. Initial batch tests were followed by analysis of the ion exchange process in a column test. This chapter describes the experimental procedures for both tests, the results of the testing and a discussion of the data obtained.

5.1 BATCH TESTS

Different types of materials can be used as an ion exchanger. Based on the literature review described in chapter 4, the choice was made to use a natural zeolite as ion exchanger. The objective of the batch tests is to analyze and compare three types of natural zeolites, in order to find the best behaving natural zeolite. The three natural zeolites that have been compared are Clinoptilolite (Indonesia), a thermally pre-treated Clinoptilolite (USA) and Chabazite (USA) (see appendix 4.2 for the zeolite characteristics). The thermally pre-treated Clinoptilolite will be referred to as Clinoptilolite T in this thesis. The sub-objectives of the batch tests is to provide the following information for all three types of zeolites

- The relative operational capacity
- The relative selectivity of the zeolite for ammonium
- The regeneration efficiency for different regeneration concentrations

The relative operational capacity is mentioned, since the actual operational capacity can only be determined via a breakthrough test in a column. Since the objective is to compare the three zeolites, the determination of the relative operational capacity (the operational capacity as measured in a batch under similar circumstances for all three zeolites) is sufficient.

Figure 5.1 The three types of zeolites (Clinoptilolite (green), Clinoptilolite T (red) and Chabazite (yellow)

5.1.1 THE DETERMINATION OF THE OPERATIONAL LOADING CAPACITIES AND THE RELATIVE SELECTIVITY FOR AMMONIUM.

MATERIALS AND METHODS

The used Chabazite and Clinoptilolite T zeolite types were supplied by st.Cloud Mining, a Connecticut based zeolite mining company and the Clinoptilolite was still available in the water laboratory of Delft University of Technology from the research from Verkerk (2003)(see appendix 4.2 for all the zeolite characteristics as supplied by the supplier). Prior to the batch tests, the three types of zeolites were pre-treated in a 100 g NaCl solution, to ensure that all the exchangeable sites on the zeolites are taken by sodium ions. After pre-treatment, each type of zeolite was added to one 1 L bottle filled with synthetic AnMBR effluent, and one bottle filled with a mixture of demineralized water and ammonium. These two types of solutions had a similar ammonium concentration, however the AnMBR effluent also contained other competing cations, while the clean water solution only contained the cation ammonium. The 6 bottles were mixed homogeneously for 24 hours using a mixer. Before, after and at specific time intervals during this 24 hours, the ammonium concentration in the bottles was measured. Using the initial ammonium concentration in the solution, the measured ammonium concentrations and the mass of the added zeolites, the operational capacity was calculated for each measuring moment. All ammonium concentrations of the samples were measured according to Standard Methods (APHA, 2005), using a Merck Photometer NOVA 60.

RESULTS

Figure 5.2 shows the operational capacities of the different types of zeolites over time. Since the actual implementation of ion exchange in the context of this thesis will not be at batch scale, these batch tests were only used to obtain information on the zeolites relative to each other. Figure 5.2a shows the measured operational capacities of ammonium in clean (demineralized) water, whereas figure 5.2b shows the measured operational capacities of ammonium in the synthetic AnMBR-effluent. Because of the presence of competing cations such as $Ca^{2+,}$ Mg^{2+} and K^{+}, the operational capacity of the zeolites was expected to be lower in the bottles filled with AnMBR effluent. By comparing the operational capacity of one zeolite in clean water with the operational capacity in the synthetic AnMBR effluent, an indication can be given of the selectivity of the zeolite for ammonium. The selectivity is a measure of the preference of the ion-exchanger for a particular ion above other ions in the solution.

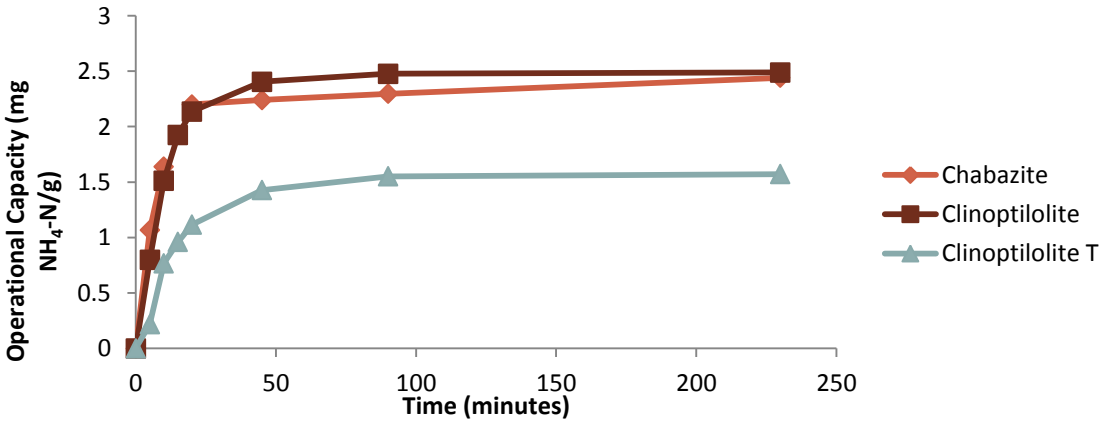

Figure 5.2 a. Operational capacity clean water

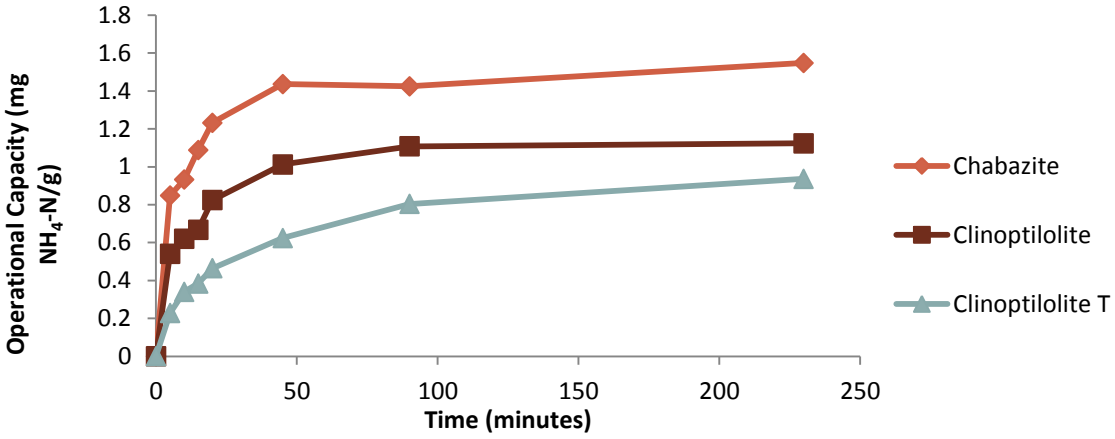

Figure 5.2 b. Operational capacity AnMBR effluent

As can be seen, in the clean water solution the operational capacities of Chabazite and Clinoptilolite were comparable, whereas the operational capacity of Clinoptilolite T was significantly lower. In the AnMBR effluent, all the zeolites show a lower operational capacity compared to the clean water solution. It is however also visible that Chabazite had the highest operational capacity. Chabazite showed the smallest decrease in operational capacity between the clean water solution and the AnMBR effluent. Hence, the negative impact of the competing cations in the AnMBR solution was the smallest for Chabazite. Thus, it can be concluded that Chabazite shows the strongest selectivity for ammonium.

Figure 5.3 The set-up for determination of the operational capacity

5.1.2 THE REGENERATION EFFICIENCY FOR DIFFERENT REGENERATION CONCENTRATIONS

MATERIALS AND METHODS

The regeneration efficiency is a measure that shows the amount of the total absorbed ammonium to the zeolite that is released during the regeneration. Basically it shows the completeness of a regeneration phase. For determining the regeneration efficiencies of the three types of zeolites, the zeolites were pre-treated for 24 hours in a 1000 mg NH_4-N/L solution. Therefore, it can be assumed that all exchangeable sites on the zeolites were bounded to ammonium ions. After the pre-treatment, the bounded ammonium per gram zeolite during pre-treatment was determined by measuring the ammonium concentration. The pre-treated zeolites were added to two types of regeneration solution; 100 g NaCl/L and

150 g NaCl/L (see chapter 4 for an elaboration on the choice of regeneration solution and the salt concentrations). Each type of zeolite was added to one bottle with 100 g NaCl/L and one bottle with 150 g NaCl/L, resulting in 6 bottles. The salt solutions were made using demineralized water. The bottles were mixed in a mixer and the ammonium concentration was measured after 0, 5, 15, 30, 60 and 120 minutes using standard methods (APHA, 2005).

RESULTS

The regeneration of 3 types of zeolites was analyzed, using two types of regeneration solution. One 100 g NaCl/L solution and one 150 g NaCl/L solution. The results are shown in figure 5.4a and 5.4b. Chabazite showed the highest regeneration efficiency, for both regeneration solutions. Also, the regeneration with the 150 g NaCl/L solution was more complete compared to the 100 g/L NaCl-solution. For the other types of zeolites, the effect of the increased salt concentration on the regeneration efficiency was less significant.

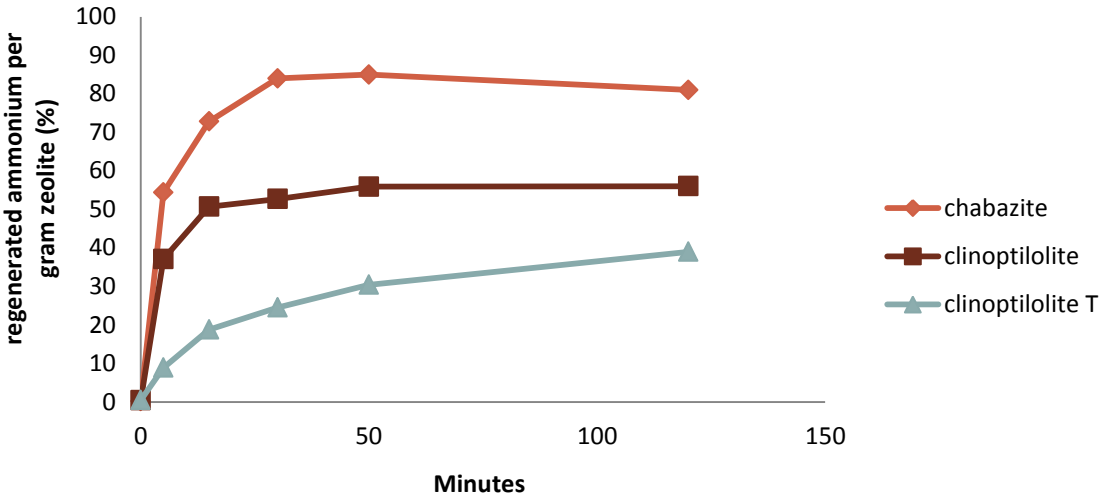

(a)

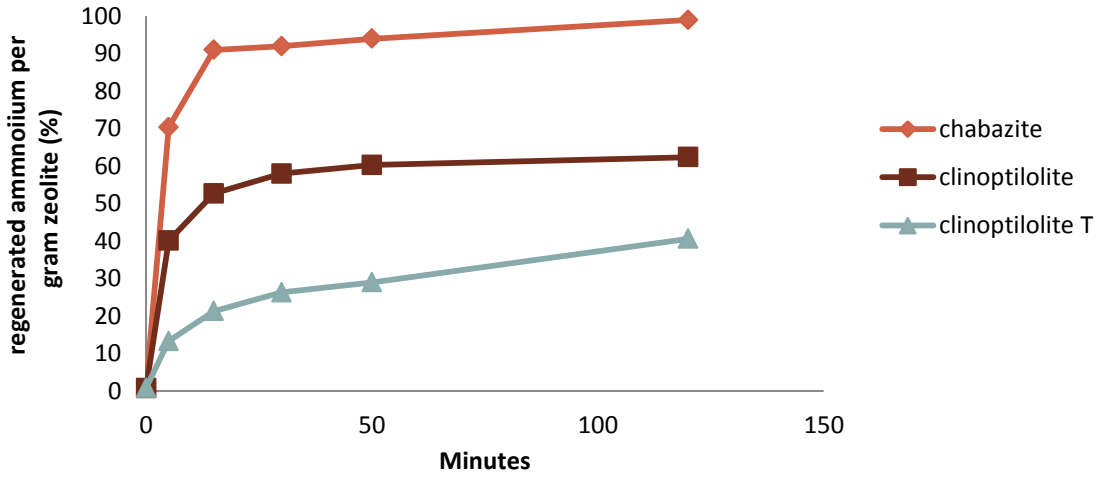

(b)

Figure 5.4 a. Regeneration with 100 g NaCl/L. b. Regeneration with 150 g NaCl/L

5.1.3 THE ISOTHERM OF CHABAZITE

Since Chabazite showed the best absorption and regeneration, the isotherm of Chabazite for ammonium was determined. This isotherm describes the relationship between the ions in solution and the ions attached to the zeolite (Verkerk, 2003). An isotherm is applicable to only one type of ion and exchanger combination and applies solely to the conditions under which it is determined. In theory an isotherm is temperature dependent, in practice the temperature hardly influences the ion-exchange capacity (Verkerk, 2003).

MATERIALS AND METHODS

The isotherm was created by adding a constant mass of Chabazite to increasing ammonium concentrations in 50 ml bottles. The bottles were shaken in a mixer for 24 hours. After equilibrium was reached, the remaining ammonium concentration in the bottle was determined using standard methods (APHA,2005).

RESULTS

Figure 5.5 shows two isotherms, one for Chabazite and ammonium, and one for Chabazite and ammonium under the presence of a 150 g NaCl/L in solution. It must be noted that the black points in the isotherm of Chabazite and ammonium under the presence of 150 g NaCl are not measured values, but extrapolated instead.

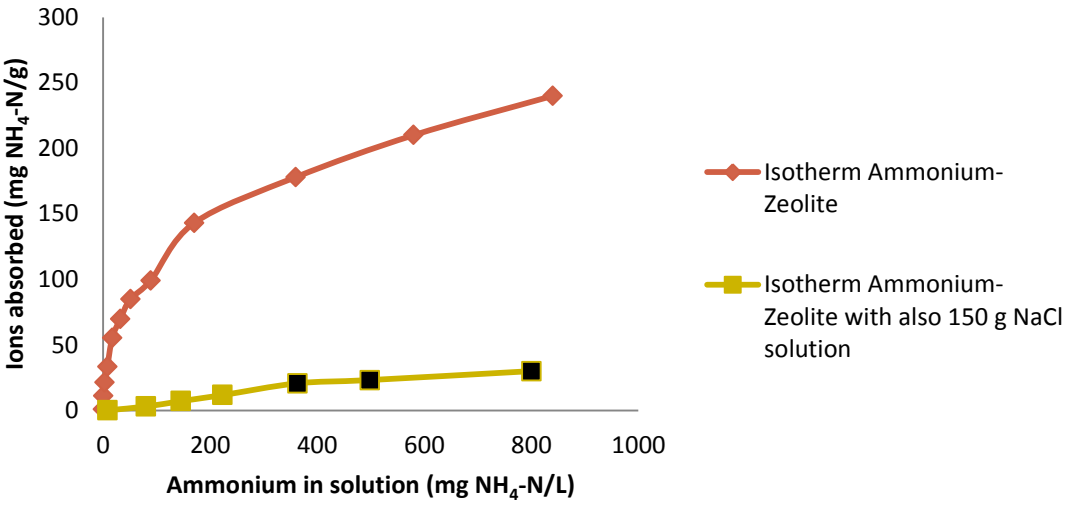

Figure 5.5 Isotherm ammonium-zeolite and ammonium zeolite with 150 g/L NaCL solution

From the concave shape of the ammonium isotherm, it can be concluded that ammonium has a preference of being bounded to Chabazite opposed to being in solution (Verkerk, 2003). Figure 5.5 also shows that once NaCl is present in the solution, ammonium is less likely to be absorbed. This is logical, since ammonium will be in competition with sodium for the absorption sites on the Chabazite.

5.2 COLUMN TESTS

The objective of the column tests is to determine the best functioning ion exchange process conditions in order to firstly achieve the best separation of ammonium from the AnMBR effluent, and secondly to be able to concentrate the separated ammonium. It is tried to concentrate the separated ammonium using Peak Concentration Collection (PCC). The concept of PCC is extensively described in chapter 4.2.2.3 The regeneration of an ion exchange column can be shown using a regeneration curve. A regeneration curve shows the ammonium concentration of the effluent regeneration solution against time. In general, the regeneration curve shows an initial peak, and a slow decrease in the ammonium concentration afterwards (e.g. most of the ammonium is flushed out of the ion exchange bed in the first few volumes of the regeneration effluent, from now on called 'the brine'). When PCC is applied, it is tried to capture only the volume of brine that is containing this peak of ammonium. For a successful PCC, the shape of the peak in the regeneration curve is important. According to literature, the regeneration flow and the NaCl concentration in the regeneration solution are the most influential factors on the height and width of the peak of the regeneration curve (Verkerk, 2003, see chapter 4).

Within this thesis research, different combinations of regeneration flows and salt concentration were tested in order to assess the resulting regeneration curves. These combinations of a regeneration flow and a salt concentration are called 'operational regimes'. For an argumentation on which velocities and salt concentration have been chosen to test, see chapter 4. The first part of the column tests chapter describes the so called 'regime tests'. The main question of the regime tests is the following:

"Considering a daily production of AnMBR effluent of 30 L (with approximately 65 mg NH_4-N/L) and a required daily production of a concentrated ammonium solution, what regime results in the highest obtainable ammonium concentrations using PCC?"

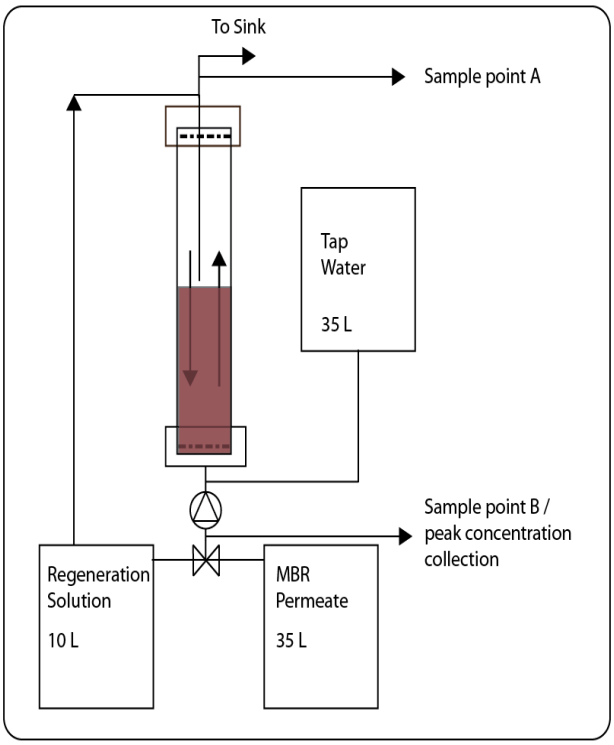

Figure 5.4 Schematic l lay out of the ion exchange laboratory set-up

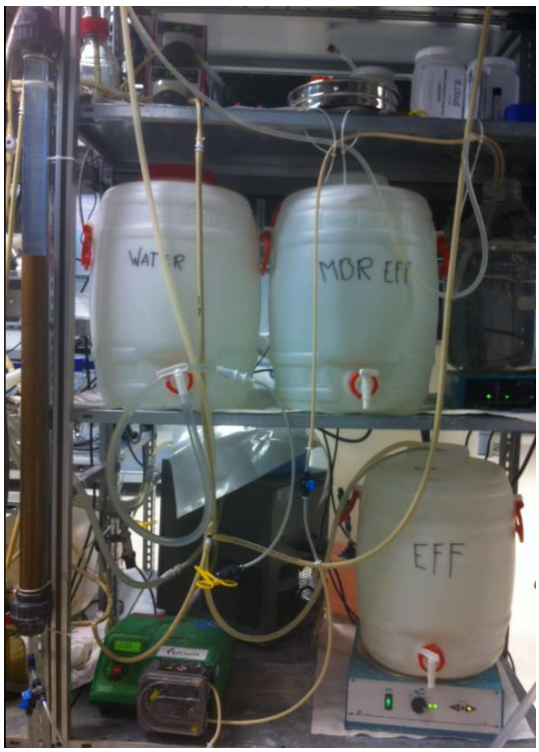

Figure 5.5 Actual laboratory scale set-up

In order to answer this question, column tests were executed and regeneration curves were generated. Based on the shape of the peak in the regeneration curve, PCC was applied and the obtained ammonium concentration was assessed. Besides these regime tests, sea water was also explored as a regeneration solution replacement. Furthermore, column tests have been done with a saturated ion exchange bed, to find out what ammonium concentrations can be maximally achieved using PCC (ignoring the limits set the research question, e.g. using the AnMBR effluent and requiring a concentrated ammonium solution on a daily basis). The results of these additional column tests can be found in appendix 5.1. Figure 5.4 shows the schematic lay-out of the laboratory set-up that has been used for the column tests and figure 5.5 shows a picture of the set-up. In order to explain the operation of the column, one operational cycle is described step by step.

Step 1: Loading.

During the loading, the daily AnMBR effluent (30 liter) was led over the column, with an upwards flow regime. The loading velocity will be referred to as $\mathbf{V_L}$. The loading lasted for approximately 4 - 6 hours.

Step 2: Backwashing.

After loading, the column was backwashed. For backwashing tap water was used, with a backwash flow that leads to an expansion of 30 % of the zeolite bed. The bed was backwashed during 10 minutes. After backwash, the bed was drained completely to minimize dilution of the regeneration solution.

Step 3: Regeneration.

The regeneration solution was led over the column in a downward flow regime, thus a counter current flow regime was used for the loading and the regeneration. The regeneration velocity will be referred to as V_R. As described in chapter 4, a NaCL solution was used as the regeneration solution and the NaCl concentration was represented by $\mathbf{C_S}$. The ammonium concentration in the regeneration solution is described by C_A. The zeolite bed was regenerated with a volume of 30 bed volume, re-used from a collection vessel of 20 bed volumes. During the regeneration, peak concentration collection was practiced. Thus the first few bed volumes of the brine were collected separately and the rest was recycled directly.

Step 4: Backwashing.

After regeneration the column was again backwashed to a bed expansion of 30 %, during 10 minutes.

Step 5: Complementing regeneration solution

Due to the practice of peak concentration collection, a specific volume of the regeneration solution was collected separately, while the rest was flowing back to the collection vessel, to be recycled directly. The volume that was taken away for nitrogen recovery, had to be substituted by an equal volume of fresh regeneration solution.

For a better understanding of the ion exchange cycle, figure 5.6 shows a schematic representation of the ion exchange column during loading and regeneration. Table 5.1 shows the constant operational values of the column. See appendix 4.4 for an elaboration on the calculation of the required bed volume.

Table 5.1: constant operational values

Height column [m]	1
Diameter column [m]	0.04
Bed Volume [ml]	600
V_L [BV/h] , [l/h]	15, 7.5
Feed	Synthetic AnMBR effluent

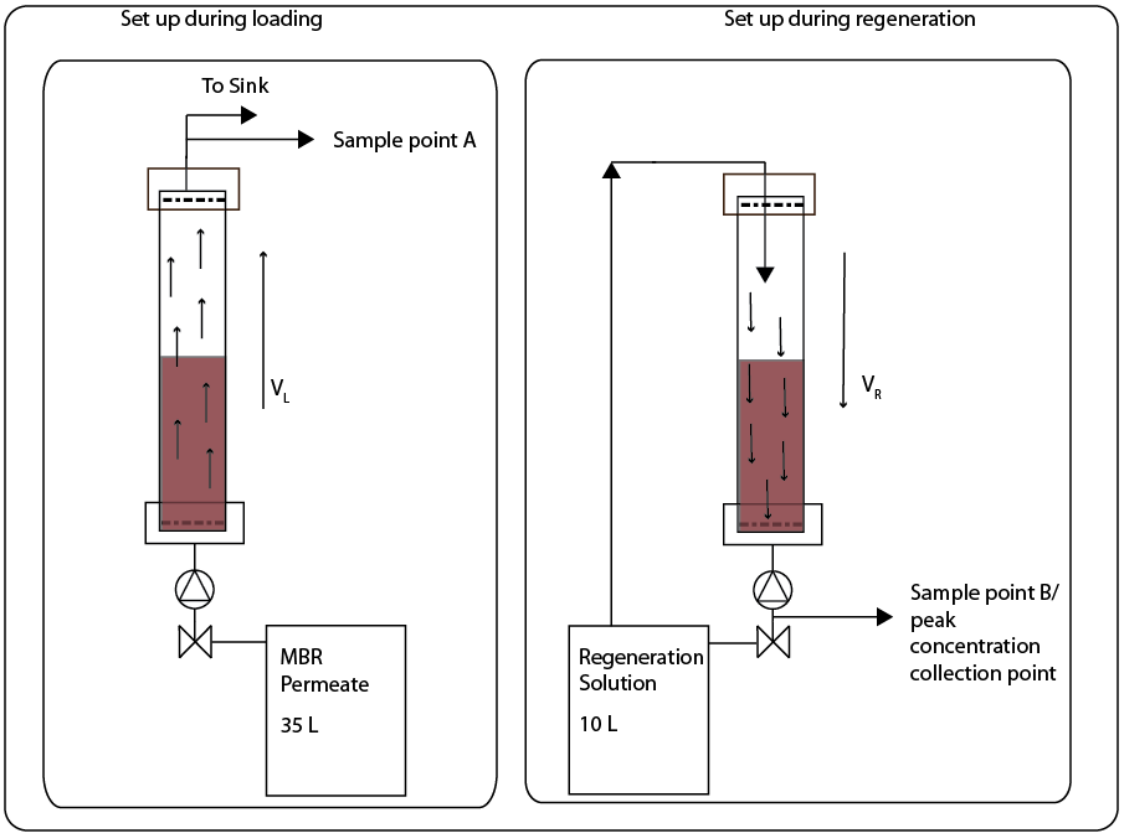

Figure 5.6 Ion Exchange cycle during loading and regeneration

5.2.1 REGIME TESTS

This section describes the search for the most suitable operational regime for ion exchange, in order to separate the ammonium from the AnMBR effluent and to obtain the highest ammonium concentrations using PCC. As mentioned previously, the factors investigated were the regeneration flow velocity and the NaCl concentration in the regeneration solution (see chapter 4 for an elaboration on the choice of factors and the ranges). Table 5.2 shows the operational regimes tested.

Table 5.2: Tested operational regimes

	Regime A	Regime B	Regime C	Regime D
V_R [BV/h] [l/h]	15 , 7.5	15 , 7.5	10 , 5	10 , 5
C_{NaCl} [g NaCl/L]	100	150	100	150

In order to apply PCC, the location of the peak in the regeneration curve had to be determined. Thus, thus the first step in the regime column test was the determination of the regeneration curves of all 4 regimes.

5.2.1.1 OBTAINING THE REGENERATION CURVES

MATERIALS AND METHODS

A regeneration curve shows the change in ammonium concentration of the brine over the volume of regeneration solution that passed the ion exchange bed, during the regeneration of one ion exchange cycle. In order to obtain the regeneration curves of the 4 proposed regimes (table 5.2), the lab set-up shown in figure 5.4 was used.

Next to the production of an ammonia rich gas, the other major objective of ion exchange is the production of an effluent that meets the dutch discharge quality regulations for nitrogen. Therefore an approximate 5 ml sample of the ion exchange effluent was taken from sampling point A as the loading phase finished to check that the ammonium concentration was zero. To obtain the regeneration curves, the change in ammonium concentration of the brine was measured at sample point B over the approximately 2 hour regeneration phase. During the first 15 minutes of regeneration a an approximate 5 ml sample was taken every 2 minutes, and for the rest of the regeneration phase an approximate 5 ml sample was taken every 30 minutes. The ammonium concentrations of the samples were measured according to Standard Methods (APHA, 2005). In accordance with literature, the ion exchange process required a stabilization period of a few cycles in order to show a stable regeneration. In this case a stable regeneration refers to a relatively reproducible regeneration curve and a constant ammonium concentration in the regeneration solution. The initial regeneration curves showed substantially lower ammonium concentrations compared to the regeneration curves of later cycles. Therefore, the choice was made test each regime for a period of 5 cycles to allow for stabilization.

RESULTS

For an overview of all the regeneration curves obtained from all the regenerations of all the four operational regimes, see appendix 5.2. In the same appendix, the measured ammonium concentrations in the ion exchange effluent can be found. The ammonium concentrations of the ion exchange effluent were always lower than the limit of detection (2 mg NH_4-N/L), for each ion exchange cycle. This shows that a constant complete separation of ammonium from the rest of the AnMBR effluent was achieved and that the discharge quality regulation of 10 mg TN/L was easily. Figure 5.7 shows the regeneration curves of the fifth cycle of each operational regime. The regeneration curves from all four operational regimes clearly followed the expected pattern of a steep high peak of ammonia in the initial brine followed by tapering off of the concentration as regeneration continues (see chapter 4). All the four peaks were more or less located within the first 2 liters of brine that passed the ion exchange bed. This means that for peak concentration collection (PCC), at least the first 2 liters needed to be collected. Furthermore, Figure 5.7 shows that regime B and D (those regimes with the relatively high NaCl concentrations) had higher peaks compared to regimes A and C. This leads to the conclusion that regeneration with a higher salt concentration results in a quicker and/or more complete regeneration, which corresponds with ion exchange kinetic theory. According to the theoretical exchange kinetics, the exchange rate increases with an increasing concentration gradient. Additionally, the regimes with a relatively low regeneration flow velocity (regime C and D) show a slightly higher peak compared to the regimes with similar NaCl concentrations, but a higher regeneration flow velocity (regime A and B). This can be attributed to the longer contact time and thus a more complete exchange reaction.

Overall, the influence of the salt concentration appeared to be more significant than the impact of the regeneration flow velocity (regime B and D have the highest peaks), however, since the regeneration curves of all four regimes are quite similar, it can be assumed that the differences between them are not great.

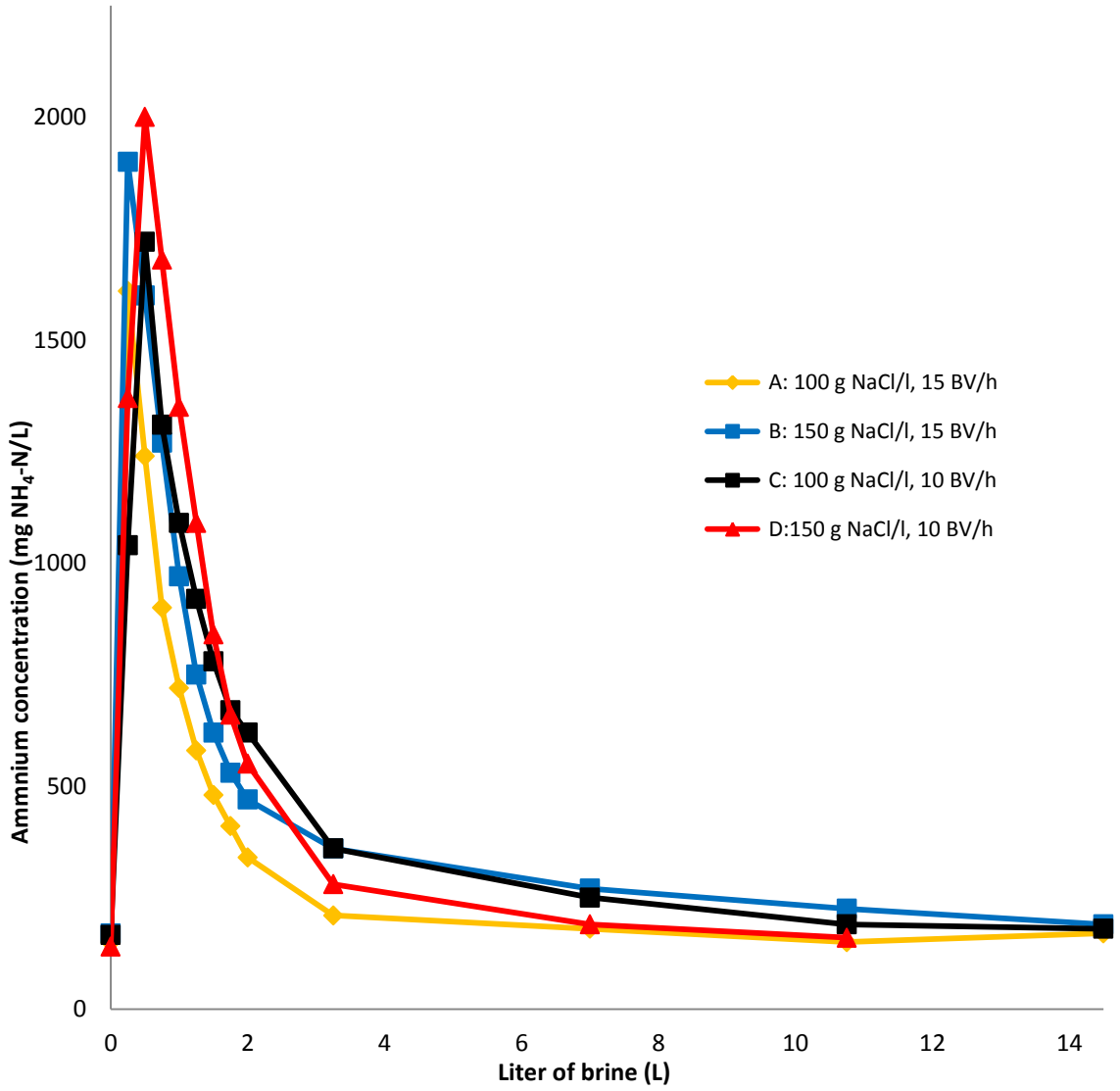

Figure 5.7 Regeneration of fifth cycle of all four regimes

5.2.1.2 CONCENTRATING THE AMMONIUM USING PEAK CONCENTRATION COLLECTION

As discussed in the previous section, the measured regeneration curves of all the four regimes followed the expected peak-pattern and all four of the peaks were situated more or less within the first 2 liters of the collected brine. To obtain a high concentration of the ammonium that was separated by the ion exchanger from the AnMBR effluent, Peak Concentration Collection (PCC) was employed. PCC refers to the separate collection of the first volumes of brine with the intention to capture as much ammonium as possible in a small volume.

The concentration factor was used to measure the increase in concentration between the AnMBR effluent and the brine. Considering the daily input of 30 liter AnMBR effluent with an average ammonium concentration of 67 mg NH_4-N/L , the total ammonium input fed to the ion exchange installation was approximately 2010 mg NH_4-N per day. A perfect ion exchange cycle (e.g. a perfect ion exchange cycle consists of the following 3 features: 1. a perfect separation of ammonium from the rest of the AnMBR effluent, 2. a complete regeneration, and 3. a perfect PCC, thus managing to capture all the

ammonium input into these 2 separately collected liter of brine) would produce 2 liters of brine with an ammonium concentration of 1005 mg NH_4-N/L. This perfect ion exchange cycle would increase the concentration from 67 mg NH_4-N/L to 1005 mg NH_4-N/L, which corresponds to a concentration factor of 15. Thus implementation of PCC during the regeneration of the ion exchange column that is fed with the AnMBR of one day, can theoretically achieve a concentration factor of 15, e.g. a solution with 67 mg NH_4-N/L is concentrated to a 1005 mg NH_4-N/L solution. The actual achievable concentration factors were measured as described below.

MATERIALS AND METHODS

The achievable ammonium concentrations applying PCC were assessed simultaneously with the analysis of the regeneration curves, after the initial verification of the location of peak the regeneration curves' peak. As described previously, 5 cycles were executed using the ion exchange set up for each of the 4 regimes. Normal operation, without PCC, consists of a constant circulation of regeneration solution, where the regeneration solution is pumped from its vessel over the ion exchange bed, and then returns to the vessel to be recycled. During PCC however, the 2 liters of brine were collected separately via sample point B (figure 5.4). The ammonium concentrations of the collected 2 liter were analyzed using standard methods (APHA, 2005). After the separate collection of the first four bed volumes, the rest of the brine flowed back into the regeneration solution vessel and for recycling. During PCC, the first 2 liter of the brine removed from the cycle was replaced with 2 liter of ammonium-free NaCl solution. The ammonium concentration within the regeneration solution vessel was sampled and measured after each ion exchange cycle, both before and after the refill with the ammonium-free NaCl solution.

RESULTS

Table 5.3 shows the percentage of recovered ammonium, applying PCC during the fifth ion exchange cycle. Graph 5.8 shows the measured ammonium concentrations in the first four bed volumes of regeneration solution collected for PCC for each regime (see table 5.2)after 5 cycles of loading and regeneration. The results showed that application of PCC was an effective method of concentrating the ammonium. For each regime the ammonium concentration factor was at least 11. As described, the theoretical maximum concentration factor for a perfect ion exchange process was calculated as 15. Figure 5.8 shows that regime B resulted in the maximum obtainable concentration factor. This high concentration value shows that the ion exchange system was functioning very well and that the ammonium concentration was concentrated up to the highest theoretically possible value when regime B is applied. In other words, when regime B is applied, all ammonium that is fed to the ion exchange installation is collected in the first two liter, thus the ammonium is concentrated with negligible ammonium loss.

Table 5.3: Percentage of ammonium recovered using PCC

Regime A	Regime B	Regime C	Regime D
76	100	92	97

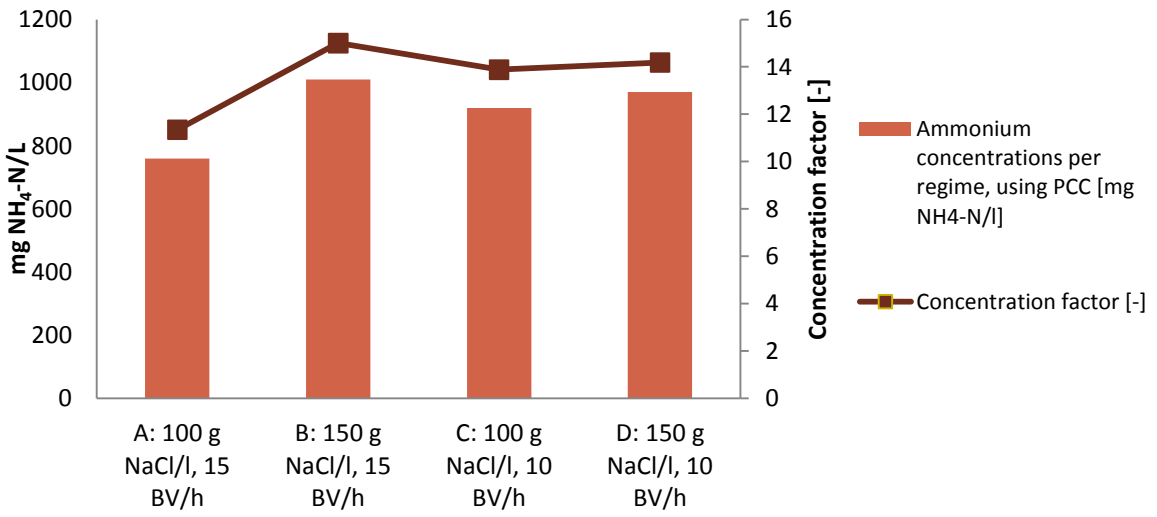

Figure 5.8 Measured ammonium concentrations using PCC and the achieved concentration factors

Table 5.3 shows the percentage of the influent ammonium, i.e. all the ammonium in the AnMBR effluent fed to the ion exchange installation in one day, which was recovered in the first two separately collected liters when applying PCC. It must be noted that the ammonium not "recovered" was not lost, but remained present in the regeneration solution passing after the first 2 liters. In the following paragraph 5.2.1.3 the impact of the accumulating ammonium in the regeneration solution on the regeneration is assessed.

The observed differences in the concentration factor and the recovery concentration between the four regimes (and mainly between regime B, C and D) were smaller than expected. Regime B and D show slightly higher ammonium concentrations compared to the other regimes and regime B showeds a slightly higher value than regime D, but considering the relatively small amount of executed cycles and the potential errors in the measurements ($\sigma = \pm 85$ mg NH_4-N/L at high concentrations), it can be said that regime B and regime D can be expected to function equally well.

5.2.1.3 THE IMPACT OF ACCUMULATED AMMONIUM CONCENTRATION IN THE REGENERATION SOLUTION

In the context of the research described in this thesis, the concept of PCC is used to concentrate the ammonium. This implies that only the first volumes of the brine are collected and substituted by fresh regeneration solution, while the rest of the brine is recycled directly as regeneration solution. In conventional ion exchange operations, generally the total volume of brine is post-treated before recycling (Verkerk, 2003), while in this case only the first few bed volumes were post-treated. This leaded to an accumulation of ammonium in the regeneration solution.

This accumulation of ammonium was, in the context of this thesis, an advantage, because it lead to higher obtainable ammonium concentrations in the separately collected first volumes of brine. This can be understood by looking at figure 5.7. Figure 5.7 shows an equal ammonium concentration at 0 L (the very start of regeneration) and at 14 L. This is the ammonium concentration in the regeneration solution, i.e. the background ammonium concentration, and this concentration becomes constant after a few regeneration cycles. If this ammonium concentration would be zero, the obtained regeneration peak would be lower, and the obtained ammonium concentration in the separately collected first volumes using PCC would be lower.

Yet, a high concentration of ammonium in the regeneration solution can theoretically negatively affect the regeneration, since the ammonium will compete with the sodium for absorption sites on the zeolite. However, not much is known about the extent to which ammonium in the regeneration solution negatively affects the regeneration. Maximum allowable ammonium concentrations are also not known. Only Verkerk (2003) mentions a maximum ammonium concentration of 300 mg NH_4-N/L, but without a clear argumentation or reference. In order to understand if accumulated ammonium in the regeneration solution can indeed form a disadvantage for the long term operation of the ion exchange installation while applying PCC, the impact of ammonium on the regeneration efficiency was analyzed.

MATERIALS AND METHODS

Batch tests were used to assess the impact of accumulated ammonium in the regeneration solution. The test used to assess the impact of ammonium on the regeneration efficiency, is comparable with the tests executed for making the isotherm (see chapter 5.1.3), but in reverse. First, a specific mass of Chabazite was pre-treated for 24 hours in a 1000 mg NH_4-N/L solution and the ammonium concentration before and after the pre-treatment was measured. Twelve (12) bottles of 50 ml were used (figure 5.9) and 10 gram of the 'saturated' Chabazite was added to each bottle. Subsequently, these bottles were filled with regeneration solution. Six (6) bottles were filled with a 100 g NaCl/L regeneration solution and the other 6 with a 150 g NaCl/L solution. The regeneration solution added to each of the 6 bottles with the same NaCl concentration had varying ammonium concentrations which ranged from 0 – 1000 mg NH_4-N/L. The bottles were mixed continually for 24 hours. The ammonium concentrations of the regeneration solutions were measured before and after the 24 hours of mixing. Each ammonium concentration was measured according to the Standard Methods (APHA, 2005).

Figure 5.9 The bottles used for assessing the impact of ammonium on the regeneration

The amount of ammonium absorbed per gram Chabazite can be calculated from the ammonium concentrations measured before and after pre-treatment. The amount of regenerated ammonium can be calculated from the measured ammonium concentrations before and after the mixing in the regeneration solution. With these two values, the completeness of regeneration can be calculated as a percentage.

RESULTS

Figure 5.10 shows the completeness of the regeneration of Chabazite, in the presence of increasing concentrations of ammonium in the regeneration solution. It is shown that the regeneration was more complete when the regeneration solution consisted of 150 g NaCl/L compared to 100 g NaCl/L (As also seen in chapter 5.1). Moreover, the figure shows that up to concentrations of 600 mg NH_4-N/L in the regeneration solution, the regeneration was not significantly affected by the presence of ammonium. Above 600 mg NH_4-N/L in the regeneration solution there were relatively few measuring points. However, even when over 1000 mg NH_4-N/L was present, still more than 80% of the absorbed ammonium was regenerated.

Based on figure 5.10, the conclusion can be drawn that the accumulation of ammonium in the regeneration solution did not have a strong negative effect on the regeneration efficiency, and certainly not in the range of ammonium concentrations that was found during the regime tests, i.e. the maximum ammonium concentration found in the regeneration solution

during the regime tests was 230 mg NH_4-N/L. Especially for regeneration with a 150 g NaCl/L solution, there was no significant negative effect observed at that ammonium concentration, according to figure 5.10.

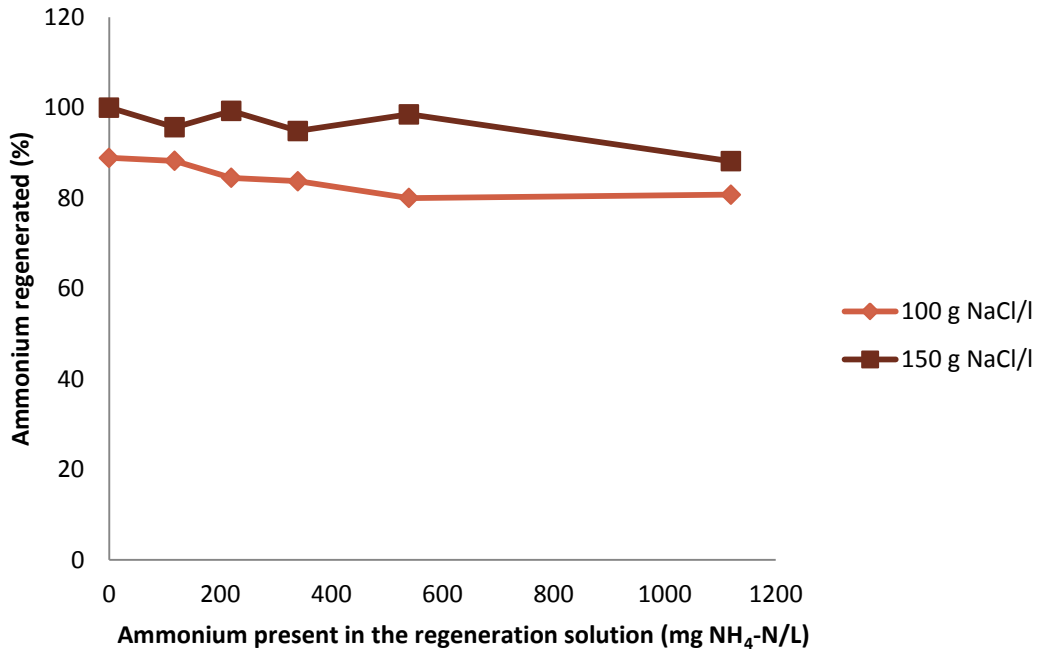

Figure 5.10 Influence of ammonium concentration on the regeneration efficiency

5.2.2 LONG-TERM ION EXCHANGE OPERATION

After the determination of the most functional operational regime (regime B), the ion exchange installation was operated for 15 days under this best-proven regime.

MATERIALS AND METHODS

For the long term operation, the ion exchange set-up as described in section 5.2 was used. Table 5.4 summarizes the operational parameters used and figure 5.11 shows the ion exchange set-up. The AnMBR effluent can be recognized by its outstanding color. The long term operation test was executed with operational regime B (which implies a regeneration flow velocity of 15 BV/h and a regeneration solution with 150 g NaCl/L).

Table 5.4: Long term ion exchange operations

Height column [m]	1
Bed Volume [ml]	600
V_L [BV/h] , [l/h]	15 , 7.5
V_R [BV/h] , [l/h]	15 , 7.5
Ion exchange feed [-]	AnMBR effluent
C_R	150 g NaCl/L
Test period [cycles]	15

Figure 5.11 Ion Exchange set up, treating actual AnMBR effluent

During the long term operation, 15 ion exchange cycles were carried out (one ion exchange cycle per day). During the loading phase, the AnMBR effluent production of one day was led over the ion exchange column. Data for regeneration curves and ammonium concentrations using PCC were collected every third day. All ammonium concentrations were analyzed using standard methods (APHA, 2005).

RESULTS

During each cycle, the ammonium was completely removed from the AnMBR effluent, resulting in low ammonium concentrations in the ion exchange effluent (<2 mg NH_4-N/L). Considering the 2 mg total N/L in the anMBR effluent that was not converted into ammonium (chapter 3), the total N concentration of the ion exchange effluent is < 4 mg total N/L. This concentration easily meets the regulation of 10-15 mg Total N/L. this indicates a successful isolation of ammonium from the rest of the ion exchange effluent. In appendix 5.4 all obtained data of the long term operation can be found.

Figure 5.13 shows the regeneration curves obtained from the long-term operation of the ion exchange column, using the real AnMBR effluent as the feed. It can be seen that the regeneration curve of the first cycle is a bit aberrant, while the shapes of all other curves are very similar (both similar to each other, and to the expected values based on the regime tests). This indicates a stable ion exchange process, after a short stabilization period. Apparently, the potential differences between the artificial and the real AnMBR effluent (see chapter 2.3) do not significantly affect the ion exchange process on the measured time-scale.

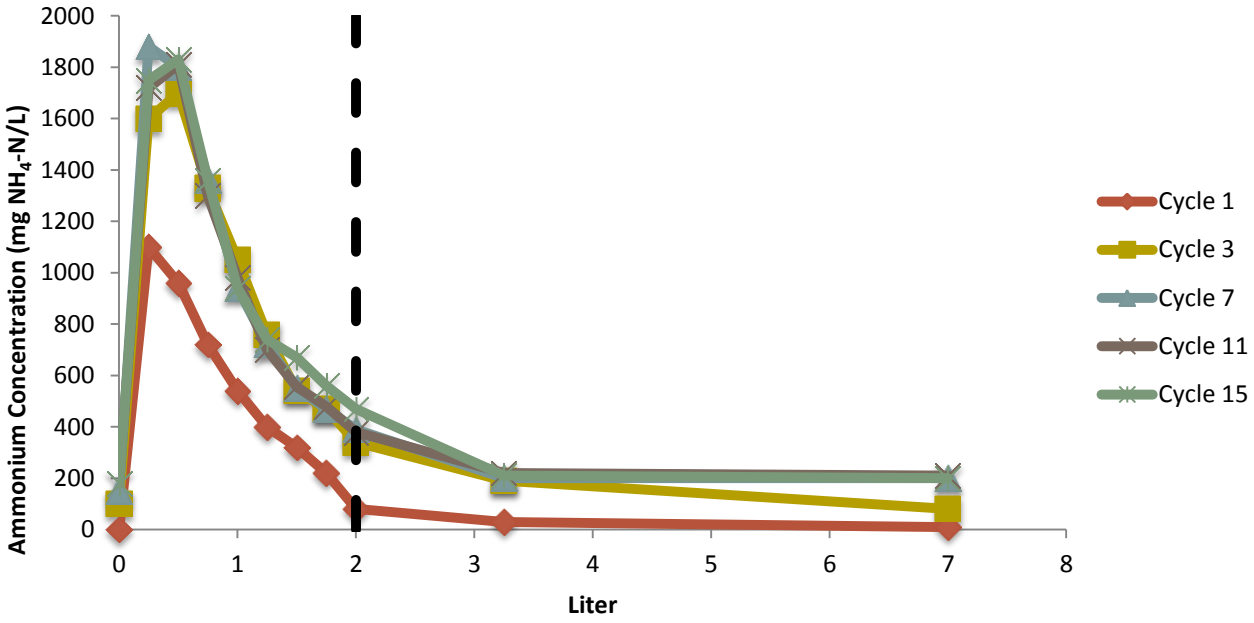

Figure 5.12 Regeneration curve long term operation

Figure 5.12 shows that the peak of all regeneration curves fits in the first 2 liter of brine, just like the regeneration curves of the regime tests. Therefore, PCC was again applied by separately collecting the first 2 liter of brine. In figure 5.12, the volume that is collected separately by applying PCC is indicated with a dashed black line.

Figure 5.13 shows the measured ammonium concentrations, obtained by using PCC. Also the concentration factors are shown. It can be seen that the first cycle resulted in odd values, but all ammonium concentrations and concentration factors of subsequent cycles were quite constant. All values but the first were quite similar to what was expected based on the regime tests results. The small variations are most likely due to a slightly varying ammonium concentration in the AnMBR effluent. The high concentrations (approximately 1000 mg NH_4-N/L) and concentration factors imply that the ion exchange installation was effective for separating the ammonium and creating a concentrated ammonium solution on a long term, while applying the operational regime that proved best during the regime tests.

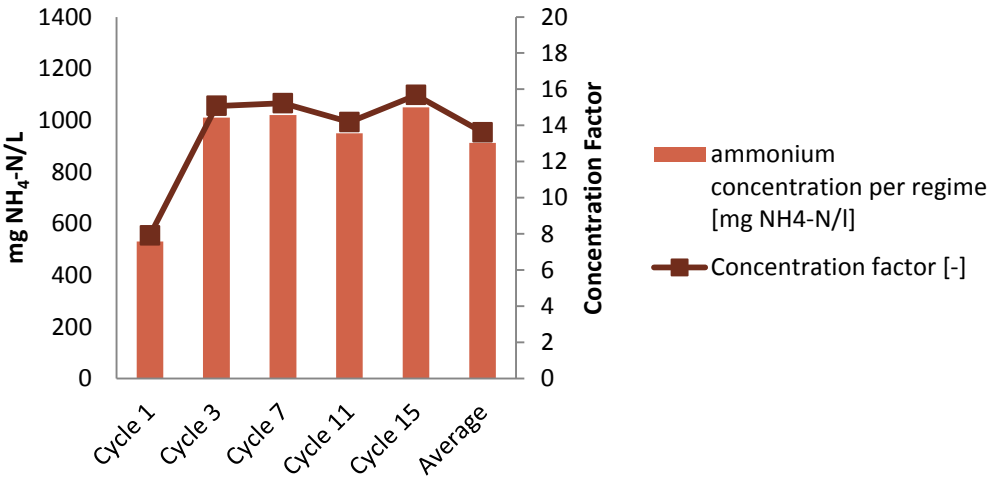

Figure 5.13 Measured ammonium concentrations using PCC and the achieved concentration factors

Table 5.5: Percentage of recovered ammonium using PCC [%]

Cycle 1	Cycle 3	Cycle 7	Cycle 11	Cycle 15
53	100	99	95	99

Table 5.5 shows the percentage of the ammonium that enters the ion exchange on a daily basis via the AnMBR effluent that is recovered in the first 2 liter using PCC. It is shown that simply almost all ammonium is recovered and concentrated within this first 2 liter of brine. This was the case during the regime tests, and apparently also for the long term ion exchange operation.

During the first 3 ion exchange cycles, the ammonium concentration in the regeneration solution stabilized at a concentration of 180 mg NH_4-N/L (See appendix 5.4). According to the results of section 5.2.1.3, this ammonium concentration within the regeneration solution will not impact the regeneration efficiency negatively.

5.3 GENERAL DISCUSSION

During the described laboratory work, a number of problems have been faced. In this chapter, the points that require a discussion are elaborated upon.

5.3.1 GENERAL DISCUSSION BATCH TESTS AND REGIME TESTS

When the batch tests and the regime tests were done, the AnMBR was not yet fully operational. The membrane was not in operation because the anaerobic sludge was not yet stable. Therefore, there was no AnMBR effluent available to be used as the feed for the ion exchange tests. A synthetic AnMBR effluent had to be used instead. The composition of the synthetic AnMBR effluent has been determined as follows:

Firstly, the composition of the synthetic AnMBR effluent was based on the composition of the synthetic wastewater that is fed to the AnMBR (see chapter 3). It has been assumed that the AnMBR effluent holds no suspended solids, since these compounds are all retained by the membrane. Moreover, it was also assumed that compared to other components present in real AnMBR effluent (like humic acids, fatty acids and oil-like compounds), the cations are considered the most influential on the ion exchange process and therefore the most important components of the synthetic AnMBR effluent. Other cations are considered influential because of their potential competition with ammonium and sodium over the exchangeable sites on the Chabazite (see chapter 4). Thus, an estimation of the concentrations of competing cations is required for making a synthetic AnMBR effluent. Based on the influent COD, the anaerobic biomass yield (van Lier et al, 2008), the elemental composition of biomass and the elemental composition of the AnMBR substrate, the concentrations of Potassium (K^+), Magnesium (Mg^{2+}) and Calcium (Ca^{2+}) in the AnMBR effluent have been estimated. In short, the cations that are expected to be incorporated in the new grown biomass were subtracted from the influent amount of cations. The remaining cations were assumed to be present in the AnMBR effluent. The ammonium is of course the most important component of the synthetic AnMBR effluent in the context of this thesis. Fortunately, the ammonium concentration of the real AnMBR effluent was known from earlier research with the same AnMBR set-up (Ozgun et al, 2013). Although attention has been paid to the composition of the AnMBR effluent, it can still not be stated that the results would have been exactly the same

if the real AnMBR effluent could have been used. However, the fact that the data from the long term operation of the column, using the real AnMBR effluent (chapter 5.2.2) is similar to the data of the regime tests with artificial AnMBR effluent, suggests no significant differences on the (relative) short term. Longer term operations are required to be able to investigate possible problems like biological fouling.

5.3.2 DISCUSSION BATCH TESTS

During the batch tests, problems were faced with the mixing of the bottles. The initial plan was to mix the content of the bottles by means of magnetic mixers. However, the porous zeolite grains were physically damaged by these magnets, and dissolved into the solution. During the first attempts, only 4 gram of Chabazite could be retrieved after mixing, from the 25 gram added to the bottle.

All tests have been repeated, using a shaker instead of magnetic mixers. Since this shaker was not made for the type of bottles used, the bottles were not stable in the mixer. Thus, all bottles might not have been mixed equally. It has been tried to diminish the inequality in shaking, by replacing and turning the bottles as often as possible during pre-treatment and during the loading/regeneration.

5.3.3 DISCUSSION COLUMN TESTS

ACCUMULATION OF COMPETING CATIONS NOT ANALYZED IN REGENERATION SOLUTION

Ion exchange separates cations from the liquid phase and from the suspended particles present in the liquid phase. Ammonia is a cation and therefore ion exchange is used to separate ammonium from the rest of the AnMBR effluent. However, it might be case that competing cations present in the AnMBR are also isolated through ion exchange. Thus, ion exchange is not isolating ammonium from the rest of the AnMBR but it might be isolation ammonium and other cations from the rest of the AnMBR effluent. Considering the strong selectivity of the used ion exchanger (chabazite) for ammonium, it is assumed that the accumulation of competing cations is low. However, in future research this assumption should be validated.

MEASUREMENT OF HIGH AMMONIUM CONCENTRATIONS

During the column tests, the measured ammonium concentrations often exceededed the measurable range of the used measuring equipment. Since the goal of the ion exchange set up was to concentrate the ammonium, this was expected and wanted. However, to measure ammonium concentrations that exceeded the measuring range, dilution of the samples was required. A required dilution of a factor 100 has occurred. This high dilution factors might have affected the accuracy of especially the high concentrations among the measured data negatively, resulting in a standard deviation up to ± 85 mg NH_4-N/L for high concentrations.

TIME LIMITED MEASURING PERIOD DURING REGIME TESTS

Initially it was planned to test each operational regime for 3 cycles, but it showed that the ion exchange process did not always stabilize within 3 cycles. Therefore, the choice was made to test 5 cycles per regime. Although it showed that the differences between the third and the fifth were smaller than between the first and the third, still it is a relatively small

number of cycles and there is no academic reason why the regimes are tested 5 times and not 10. However, testing one regime for 5 cycles would take one complete working week and the available time was limited. The choice has been made to start as quickly as possible with the regime that proved to be best, in order to assess the behavior of the ion exchange process under long-term operations.

THE IMPLEMENTATION OF PEAK CONCENTRATION COLLECTION (PCC)

Peak concentration collection (PCC), was used to concentrate the ammonium that was separated by the ion exchanger from the AnMBR effluent. The peak in the regeneration curves of all tested regimes was located within the first 2 liter of brine. Therefore, the choice was made to separately collect the first 2 liter of brine, and thus to try to capture as much ammonium as possible in these 2 liter. At the start of the research, the assumption was made that 2 liter would be a convenient volume to concentrate the ammonium in. At the moment of this assumption, the process used for creating an ammonia-rich gas was not yet known, so also the minimum required volume and required concentration of the concentrated ammonium solution was not yet known. Taking away the first two liter (and not more or less) seemed the most logical way to go. On the one hand, a volume of 2 liter seemed small enough for a proper concentration factor (taking away a larger volume than 2 liter by applying PCC automatically leads in a lower concentration, because the peak of the regeneration curve is located within these first 2 liter). On the other hand, 2 liter also did not seem to be a too small volume. Since the minimum required volume for the follow up step of the ion exchange was not yet known, it seemed unwise to focus on a very small volume.

Consequently, the choice was made to take away the first two liter of the brine and to try to collect as much ammonium as possible within these two liter. During the tests it appeared that after a few ion exchange cycles, the ammonium that was captured within these first 2 liter of the brine, equaled the total daily input of ammonium. Figure 5.15 shows the regeneration curve of the fifth cycle of the long term operation of the ion exchange installation. Next to the regeneration curve (the red line), also the ammonium concentration in the regeneration solution is shown (the yellow line). This ammonium concentration can be considered as the ‘black ground’ ammonium concentration, that enters and leaves the ion exchange bed together with the regeneration solution. Because the ammonium concentration of the brine is plotted against the volume of brine, the surface under the regeneration curve indicates the mass of ammonium that passed the ion exchange bed (mg/L * L = mg). Likewise, the surface under the yellow line shows the mass of ammonium that enters and leaves the ion exchange bed together with the regeneration solution.

The black dashed line indicates the volume that was collected separately by applying PCC. Figure 5.14 shows that the separately collected mass of ammonium equals the absolute mass of regenerated ammonium, since the two green dashed areas cancel each other out. Due to the ammonium right of the black dotted line, the ammonium concentration in the regeneration solution remains the same after the collected first 2 liter are replaced by fresh regeneration solution.

During the research it was shown that a high ammonium concentration in the regeneration solution does not negatively affect the regeneration efficiency. Knowing that, it might have been preferable to collect only the first liter instead of the first 2 liter of brine. If only the first liter of brine would have been collected, a higher ammonium background concentration in the regeneration solution would be set and a concentration of 2000 mg NH_4-N/L would be possible to collect (assuming that this higher background ammonium concentration does not negatively affect the regeneration capacity). However, in an early stage of the research, the decision was made to collect the first two liter, and therefore a concentration of 1000 mg NH_4-N/L was the maximum obtainable value.

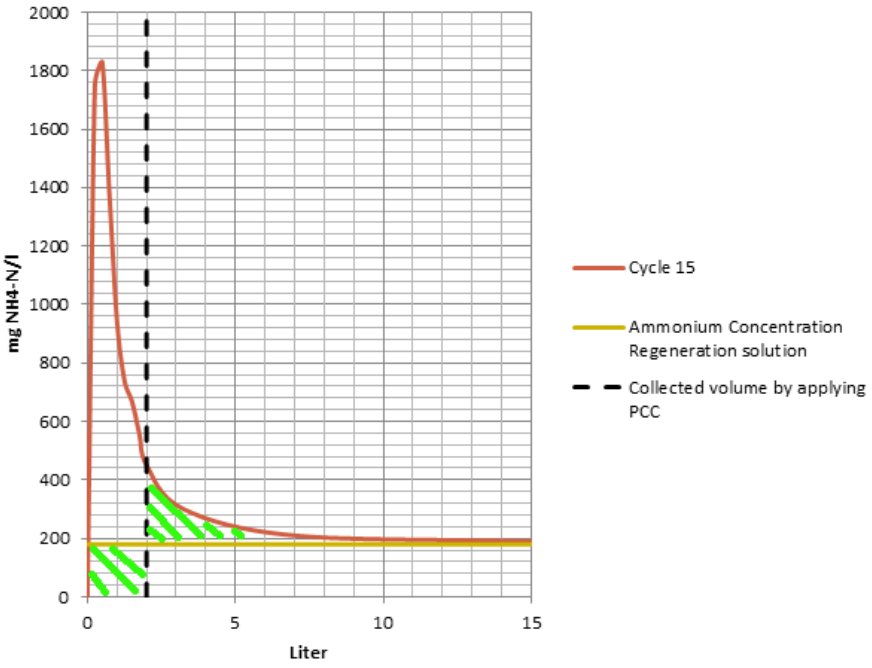

Figure 5.14 Regeneration curve long term operation, 15th cycle

LOADING THE DAILY ANMBR EFFLUENT PRODUCTION IN ONE CYCLE

In view of a continuing ammonia rich gas production, the decision was made to carry out one cycle per day, feeding the daily AnMBR effluent production of 30 L per loading phase. This decision caused limitations in the operational regime possibilities. Appendix 5.2 shows results of the application of PCC after the regeneration of a ion exchange bed saturated with ammonium. By regenerating a saturated ion exchange bed, it was possible to obtain 2 liters with 6 g NH_4-N/L, instead of 1 g NH_4-N/L as is obtained when the AnMBR effluent of one day is treated (and thus the bed is not saturated). More research is necessary on the optimization of ion exchange, focusing on obtaining the highest ammonium concentration by applying PCC.

WASH OUT OF ION EXCHANGE BED AFTER START-UP

During the regime tests, for each regime a new ion exchange bed was used. For each regime, 600 ml of the zeolite as delivered by supplier was placed in the ion exchange set up. During the start-up however, the ion exchange beds showed a significant wash-out of dissolved zeolite material (see figure 5.16a). Before start up, minimal 10 bed volumes of water (2,5 liter) had to be led over the ion exchange bed before the effluent was clear and without dissolved zeolites. The volume of zeolites that has been added to the column is known, but the amount of washed out material is not known exactly. It is assumed that the amount of washed out zeolite is comparable for all regimes. This is not tested however, thus it might be the case that for some regimes the test have been executed with a slightly larger or smaller ion exchange bed.

LONG TERM OPERATION WITH REAL ANMBR EFFLUENT WAS RELATIVELY SHORT

The long term ion exchange operation was measured for a period of 15 cycles. It is questionable whether 15 cycles delivered enough data for long term observation of the ion exchange system. However, due to the sometimes problematic process of AnMBR effluent production (due to clogging, flooding or other issues with the AnMBR), it was often not possible

to produce enough AnMBR effluent for one cycle in 3 days. Therefore, the long term operation became quite time consuming. It is assumed that the storage of the AnMBR effluent for 3 days did not change its characteristics. Obviously, longer term operations with the AnMBR effluent as a feed are required to assess, for example, the impact of bio-fouling. Also the regeneration capacity has to be evaluated under long term operations including PCC. It might be that at some stage, a regeneration with ammonium-free regeneration solution is required.

SCALE RELATED ISSUES

During the execution of the described experiments, a multiple of issues were faced that were caused merely by the small laboratory-scale of the ion exchange set up. For the ion exchange there was one main scale-related problem, namely the formation of air bubbles. During the process of backwashing, draining the ion exchange bed and changing of pumping directions, apparently air got trapped within the ion exchange system. At the start of the loading phase, this air usually formed air bubbles and resulted in a washout of zeolites (if no intervention took place). In a bigger column, air bubbles will never manage to get big enough to be able to move a layer of zeolites upwards and therefore the ion exchange process in a bigger column will be less sensitive for bubbles pushing the zeolites out of the column.

5.4 GENERAL CONCLUSIONS

5.4.1 CONCLUSIONS OF THE BATCH EXPERIMENTS

- Chabazite shows the highest relative operational capacity for ammonium
- Chabazite has the highest selectivity for ammonium
- Chabazite regenerates the most complete and the fastest
- The NaCl concentration of the regeneration solution has a significant impact on the regeneration process when Chabazite is used as the ion exchanger (a higher NaCL concentration results in a faster and more complete regeneration).

54.2 CONCLUSION REGIME TESTS

- A laboratory-scale ion exchange column is a successful method for isolating the ammonium from the rest of the AnMBR effluent. The ion exchange column was capable of retaining all ammonium that was fed via the AnMBR effluent, resulting in no ammonium washing out with the ion exchange effluent (< 2 mg NH_4-N/L). Thus, there is zero ammonium loss in the separation step. Moreover, this makes ion exchange a competing method for meeting strict environmental regulations for discharge quality.
- Applying PCC is an effective way of concentrating the ammonium. Operational regime B results in the highest ammonium concentration using PCC, namely 1010 mg NH_4-N/L which corresponds with a concentration factor of 15. This is the case when PCC is applied by separately collecting the first four bed volumes which corresponds to 2 liter. Two (2) liters with an ammonium concentration of 1010 mg NH_4-N/L equals the incoming 30 liter of AnMBR with an average of 67 mg NH_4-N/L. Consequently there is almost no loss of ammonium in the concentrating step.
- The differences between the different regimes were small. Impacts of the flow velocity and the salt concentration in the regeneration solution are minor. This is not considered an issue since all regimes functioned well.

- Regime B was selected for further use in the project. The choice is made to continue with regime B since a faster regeneration velocity is less time consuming.
- Due to the application of PCC, not all the regeneration solution is post-treated to remove the ammonium before it is recycled. Batch tests executed to assess the potential negative influence of a high ammonium concentration in the regeneration solution concluded that the negative impact is not significant, especially not in the ammonium concentration ranges found during the regime tests.

Overall, it can be stated that if the ion exchange installation is operated with one cycle per day, treating the total daily AnMBR effluent, operational regime B is the most suitable in order to separate ammonium from the rest of the AnMBR effluent and to concentrate the ammonium. It has been proven that a concentration factor of 15 is possible, concentrating the ammonium up to 1010 mg NH_4-N/L.

Two additional column tests have been done, besides the regime tests.

- Sea water has been tested as a regeneration agent. Sea water can be used for the regeneration of an ion exchange bed, consisting out of ammonium exchanging Chabazite (appendix 5.1). However, the regeneration capacity of sea water is less than a pure NaCl concentration in the range of 100- 150 g NaCl. This is logical, considering the lower NaCl concentration and the presence of competing cations.
- The regeneration of an ion exchange bed that is saturated with ammonium has been analyzed (appendix 5.2). The tests with the saturated bed showed that it can be interesting to look at a saturated bed operation of the ion exchange installation. Because it is indeed possible to obtain very high ammonium concentrations (by applying PCC) when the ion exchange bed is saturated, compared to a bed that is only fed with the daily AnMBR effluent.

5.4.3 CONCLUSION LONG TERM OPERATION

- Ion exchange is a successful technology for separating ammonium from the rest of the AnMBR effluent. Hereby, the AnMBR effluent is treated for ammonium, and extremely low effluent ammonium concentrations can be reached. Taking also the 2 mg TN/L into account that was not converted into ammonium during the AnMBR step, the ion exchange effluent has a total nitrogen concentration of maximal 4 mg TN/L, which easily meets the regulations.
- After a short stabilization period of 2 cycles, the obtained data shows a stable and constant functioning of the ion exchange installation.
- The ion exchange technology in combination with the implementation of PCC, is also successful for concentrating the ammonium. Two liter with a concentration of aprox. 1000 mg NH_4-N/L could be reached, out of an average influent concentration of 67 mg NH_4-N/L. That amounts to a concentration factor of around 15. Moreover, more than 95% of the fed ammonium was retrieved in the separately collected 2 liter (using PCC). This means that in the overall process of separating the ammonium from the AnMBR effluent and concentrating the ammonium, not much ammonium is lost. Hereby, almost all influent ammonium was available for the generation of an ammonia-rich gas.
- Considering a period of 15 cycles, the ion exchange installation worked almost exactly the same for the synthetic AnMBR effluent as the real AnMBR effluent . And the accumulation of ammonium in the regeneration solution stabilizes at a concentration of 180 mg NH_4-N/l. According to the results in section 5.2.1.3, this concentration will not have negative impact on the regeneration efficiency.

Section III: The Distillation Tower

6 DISTILLATION TOWER THEORY

The research presented in this thesis describes the process in which ammonium from sewage is used for electricity production. In order to use this ammonium as a fuel, it has to be available in the substance of an ammonia-rich gas. The used fuel cell has an incorporated gasifier, which enables the direct feeding of a liquid fuel. Therefore the objective of the step described in this chapter is 1) to convert the ammonium ions from the ion exchange brine into ammonia, and 2) to create a mixture sufficiently rich in ammonia so that it can be fed directly as a fuel to a fuel cell.

The idea of this thesis research was to feed sewage to an AnMBR (chapter 3) and to separate and concentrate the ammonium from the AnMBR effluent using Ion exchange (chapter 5), creating 2 liter per day with a high ammonium concentration. Thereafter, the idea was to increase the pH of this ammonium concentration, converting the ammonium into ammonia, which then easily could be 'stripped' from the solution into an ammonia-rich gas. Stripping is a physical separation process, used to remove components from a liquid stream by being brought in contact with a gas stream. When the stripping of ammonia from a solution is considered, ammonia will be taken out of solution and will be incorporated in the stripping-gas. In the context of this thesis, it was attempted to apply this stripping concept in order to obtain an ammonia-rich gas out of the ammonium solution that resulted from the work described in the previous chapters.

However, the ammonium concentration obtained with ion exchange was not sufficient for creating an ammonia-rich gas and a further increase in the ammonium concentration was required. Moreover, because it was not possible to easily produce a pure ammonia gas, a new important parameter came into view: the carrying gas. The carrying gas is the gas that is used as a stripping agent and is fed to the fuel cell together with the ammonia. The fact that a carrying gas was inevitable, introduced a new range of specific limitations (a minimal fuel percentage in the fuel mixture, and the fact that some gasses are harmful to the fuel cell).

A distillation tower is used to create an ammonia-water mixture, rich enough in ammonia to be fed as a fuel to a fuel cell. This chapter describes the theory behind the distillation tower, which is eventually used in order to create an ammonia-water mixture with a sufficient ammonia concentration for creating an ammonia-rich gas. In order to explain the faced problems profoundly and to argue the choice for the distillation tower, first a short introduction is given on the theory of ammonia stripping. Afterwards, the considered methods for creating an ammonia-rich solution out of the produced ammonium solution are described and the eventually used technology is described in more detail.

6.1 PRINCIPLES OF AMMONIA STRIPPING

Ammonia stripping is a successful and proven technology for removing ammonium from waste flows (Verkerk, 2003). Ammonium removal up to 95% is possible (STOWA, 1995). Ammonia stripping is a type of gas stripping. Gas stripping is a physical separation process, where components of a liquid stream are removed by being placed in contact with a gas stream that is insoluble with the liquid stream (Dahdal, 1999).

The kinetic theory of gases states that molecules of dissolved gasses can readily move between the gas and the liquid phases (Kavanaugh and Trussel, 1980). Consequently, if water contains a volatile contaminant in excess of its equilibrium level, the contaminant will move from the liquid phase (water) to the gas phase (air/steam) until equilibrium is reached. Thus, stripping involves a gas-liquid mass-transfer process in which the driving force is created by a departure from equilibrium (Halling-Sorensen and Jorgensen, 1993). In more detail, the driving force in the gas phase is a concentration gradient, and in the liquid phase this force is caused by a concentration gradient. If the stripping gas in contact with the

water is continuously replenished with fresh, contaminant free gas, eventually all of the contaminant will be removed from the solution (Kavanaugh and Trussel, 1980). This is the basic operating principle of the air stripping process. When talking about air-stripping the gas phase refers to air (i.e. air is the stripping agent), and with steam-stripping the gas phase refers to steam (i.e. steam is the stripping agent). Considering the creation of an ammonia-rich gas out of the concentrated ammonium solution, two equilibriums are influential and are therefore discussed in the following paragraphs.

6.1.1 DISSOCIATION EQUILIBRIUM

The rate at which ammonia can be removed by stripping is highly dependent on the pH, because the exchange between the two forms, ammonium, which is ionic, and ammonia, which is a highly water soluble-gas, is an acid-base reaction (Halling-Sorensen and Jorgensen, 1993). In aqueous solutions, the following equilibrium exists between ammonium and ammonia (Metcalf and Eddy, 2003):

$$NH_4^+ + OH^- \leftrightarrow NH_3 + H_2O \qquad [6.1]$$

This equilibrium depends on the pH and temperature, defined by the following equation (STOWA, 1995):

$$NH_3 - N = NH_4^+ - N \cdot \frac{10^{pH}}{e^{\left(\frac{6344}{273+T}\right)} + 10^{pH}} \qquad [6.2]$$

As described in equation 6.2, the equilibrium will shift towards a higher ammonia concentration with an increasing pH and/or temperature (See figure 6.1). The more the equilibrium shifts towards the right, the more efficient the stripping process can be.

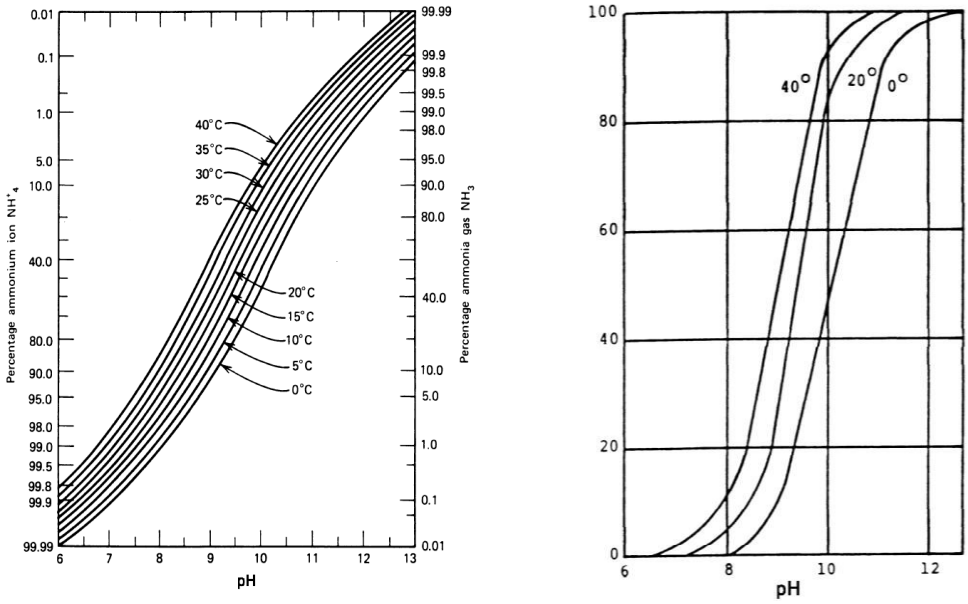

Figure 6.1 a (left) Distribution of ammonia and ammonium for pH and temperature. b (right) Stripping efficiency as function of pH at three temperatures (Halling-Sorensen and Jorgensen, 1993)

As the temperature and the pH of the ammonium-holding water is increased to 10-12, the equilibrium is shifted to the right and most ammonium ions are converted into ammonia, which may be removed by gas stripping. (Metcalf and Eddy,2003) Caustic soda is often applied in order to increase pH in solutions, since it is cheap and easily available (van Dijk, 1984). Moreover, in the context of this thesis, there is a need to refresh the regeneration solution of the ion exchange set-up (chapter 5) with fresh sodium. When caustic soda is added to the 2 liter of separately collected brine, the hydroxide is used

for increasing the pH of the solution and thus for converting the ammonium ions into ammonia, while the sodium is used for refreshing the regeneration solution in order to maintain its regeneration capacity. Afterwards, the ammonia can be stripped and the post-treated brine can be re-used in the ion exchange process.

6.1.2 PHASE EQUILIBRIUM

The next equilibrium that is significant for the stripping of ammonia from an aqueous solution is the phase equilibrium. When a gas phase is led through an ammonia-rich solution, an equilibrium will be formed between the ammonia in the gas phase and the ammonia in solution. Since the gas that is used for the stripping process (the stripping agent) has a low ammonia concentration, the ammonia will come out of solution and enter the gas phase to satisfy the Henry's law equilibrium. Henry's law describes the relationship between de mole fraction of a gas in the atmosphere above a liquid and the mole fraction of the same gas in the liquid (Metcalf and Eddy, 2003):

$$p_g = \frac{H}{P_T} x_g \qquad [6.3]$$

Where	p_g	=	The mole fraction of a gas in air	[mole gas / mole of air]
	H	=	Henry's law constant	[atm (mole gas/mole air)/ (mole gas/ mole water)]
	P_T	=	Total pressure	[usually 1 atm]
	x_g	=	mole fraction of gas in water	[mole gas / (mole gas + mole water)]

The larger the Henry's law constant, the greater the equilibrium concentration of A in the stripping agent will be. Thus, contaminants with large Henry's law constants are more easily removed by gas stripping (Kavanaugh and Trussel, 1980). The Henry's law constant is component specific and temperature dependent. A higher temperature results in a higher Henry's law constant, which implies that with a higher temperature more ammonia can convert into the gas phase (STOWA, 1995). Thus a higher temperature will have a positive effect on the efficiency of the stripping process. Components such as benzene, toluene, and vinyl chloride that have a Henry's law constants greater than 500 atm (mole H_2O/mole air) are readily strippable, compounds such as ammonia with a Henry's law constant of 0.75 atm (mole H_2O/mole air) are marginally strippable, and compounds with Henry's law constant lower than 0.1 (mole H_2O/mole air) are essentially not strippable (Metcalf and Eddy, 2003). Next to the Henry's law constant, the ammonia concentration difference between the gas and solution phase and the contact surface, are influencing the efficiency of the stripping process (STOWA, 1995).

6.2 CREATION OF AN AMMONIA RICH SOLUTION

The objective of the stripping step described in this chapter is 1) to convert the ammonium ions in the ion exchange brine into ammonia, and 2) to create a mixture that can be fed directly as a fuel to a fuel cell. In this process, several problems were faced.

1. The first problem was the realization that the obtained brine with the 'high' ammonium concentration of 1 g NH_4-N/L (chapter 3), is still an ammonium-water mixture with a low absolute ammonium concentration. By using the ion exchange set-up, ammonium is separated from the rest of the AnMBR effluent and concentrated from 67 mg NH_4-N/L to 1000 mg NH_4-N/L. An ammonium concentration of 1000 mg NH_4-N/L is a significant increase, and especially for wastewater engineers who are used to removing ammonium concentrations up to 1 mg NH_4-N/L, 1000 mg NH_4-N is a very high concentration. However, from the more chemical engineering point of view, a water solution with 1000 mg NH_4-N/L is chemically speaking still only a mixture of 0.1 mole% ammonium and 99.9

mole% water. Thus, it was attempted to produce an ammonia-rich gas out of a solution that, absolutely speaking, consisted for only a very small part out of ammonium and mainly out of water.

2. The second problem has to do with the fact that if a fuel cell is fed with a gas mixture that exists only partly out of a gas that can be used as a fuel, there exists a minimum concentration in which this fuel gas has to be present. It is possible to feed a fuel cell with a gas mixture that does not purely consists of a fuel, as long at the other (non-fuel) gas components are not harmful to the fuel cell. For example, a gas mixture of ammonia and steam can be fed to a fuel cell. Steam is (within a certain range) not harmful to the fuel cell, but can also not be used as a fuel. Therefore, there is a minimum percentage of ammonia (the fuel) required to produce electricity with this gas mixture. Although this is an area that still requires research and it is difficult to make well-founded statements, it was assumed that the fuel cell is only capable of producing electricity out of a feed liquid mixture that consists for at least 5 mole% out of fuel (R. Ihringer, personal communications, July 2014). This corresponds to 38.85 g NH_3-N/L. Thus, to be able to use the ammonium mixture produced with the AnMBR and the Ion Exchange as a fuel, it has to be available in a solution with at least a concentration of 38.85 g NH_3-N/L.

3. The third problem concerning the creation of an ammonia-rich gas is the fact that the properties of the compound ammonia ensure that ammonia prefers to be in solution above being present in the gas phase. This makes it difficult to separate ammonia and water (which is required for creating a gas mixture with at least 5 mole percent of ammonia).

4. The fourth faced problem was the fact that air (a mixture of nitrogen-gas, oxygen, water vapor and carbon dioxide) cannot be used as a carrying-gas for ammonia, since the oxygen will damage the (anode side of the) fuel cell. This will be elaborated upon in chapter 8.

For the transformation from the ion exchange brine into a sufficiently ammonia rich solution that can be directly used as a fuel for a fuel cell, air stripping and stream stripping/distillation were considered.

OPTION 1: AIR STRIPPING

The initial plan of stripping ammonia out of the concentrated solution, which resulted from the ion exchange, using air as a stripping-agent and thus creating an ammonia-rich gas, is not feasible due to the following facts:

It is impossible to create an ammonia-rich gas, when ammonia is stripped out of the used solution with air as the stripping-agent. This is due to the low Henry's law constant of ammonia. This seems to be a strange conclusion, since ammonia stripping is a widely applied technology in industries and wastewater treatment (Halling-Sorensen and Jorgensen, 1993, Liao et al, 1995, Budzianowski and Koziol, 2005, Metcalf and Eddy, 2003). However, in general when ammonia air stripping is applied, the focus is on the removal of ammonia out of the solution and not on the re-capturing of this ammonia. Elements with the lowest Henry's law constants can still be stripped out of a solution, as long as enormous amounts of air are used. Thus, it is actually possible to remove ammonia up to high percentages out of liquids using air stripping. However, it is not possible to obtain a gas-mixture with a sufficient concentration of ammonia, in order to be used as a fuel by a fuel cell. Moreover, air is harmful to the anode site of a fuel cell and cannot be used as the carrying gas for ammonia.

OPTION 2: STEAM STRIPPING COMBINED WITH DISTILLATION

Steam stripping in a distillation tower is similar to air stripping, with the exception that the process requires temperatures in excess of 95°C, steam (gaseous water) is used as a stripping agent and no gas-mixture is formed, but a concentrated stream of water and ammonia (Kister, 1992). Components that dissolve well in water, like ammonia, which cannot easily be removed with classic air stripping, can be separated using stream stripping (Hwang et al, 1992). This is because the volatility (the tendency of a compound to vaporize), i.e. the Henry's law constant, is a very strong function of temperature. The principle of steam stripping is comparable to the discussed conventional air stripping. Due to the higher temperature and due to steam as a stripping agent (instead of air), the Henry's law constant of ammonia is increased, creating a positive mass transport from the water to the gas phase. In this sense, the gas phase refers to steam. This steam can be either injected, or created by the vaporization of the water itself. Thus, by applying steam stripping instead of air-stripping, the problem of the harmful carrying gas (air) is prevented, since steam as a carrying gas does not have a negative effect on the fuel cell (R. Ihringer, personal communication, July 2014). However, by just applying steam stripping, it will still be difficult to achieve a minimal of 5 mole% ammonia in the steam-ammonia mixture.

Steam stripping, also known as steam distillation, is essentially a distillation process. Distillation is the process of separating components of a mixture by evaporating and then condensing the vapor into liquid, taking advantage of the fact that different elements or compounds have different boiling points (Metcalf and Eddy, 2003). By combining the steam stripping process and the process of distillation, a volume of purified water and a significantly smaller volume of water and concentrated ammonia will be the result. Thus, in this way, the ammonium is separated from the ion exchange brine, ammonium is converted into ammonia and the concentration of ammonia in the volume is increased.

6.3.1 OPERATING PRINCIPLES OF A DISTILLATION TOWER

Steam stripping and distillation can be combined using a packed distillation tower. The difference between a distillation tower and a steam stripping unit is the input of steam and the absence of a condenser and a re-flux in a steam stripping unit. In a steam stripping unit, steam is constantly added to the unit. In a distillation tower, the steam is originating from the influent water-ammonia mixture.

Distillation is an equilibrium stage operation (Henley et al, 2011). In each stage, a gas phase is brought into contact with a liquid phase. The less volatile components concentrate in the liquid phase (in this case the water) and the more volatile components concentrate in the gas (which is the ammonia). By using multiple stages in series with a reflux, separation can be accomplished (Henley et al, 2011). A distillation column is build up out of a series of stages (Henley, 2011). These correspond to a cascade of equilibrium stages. Liquid flows down the column from stage to stage and is contacted by gas flowing upwards. Traditionally, most columns have literary been built from a set of distinct trays or plates, designed to maximize contact between the ascending gas and the descending liquid (Henley et al, 2011). During this contact, the equilibrium described in equation 6.2 is approached. Some of the ammonia in the entering liquid is gasified and leaves with the gas (as shown in figure 6.2a). By definition, an ideal stage is one where the gas and liquid leave the stage in equilibrium. Consequently, the gas composition functionally depends on the incoming liquid composition (Henley et al, 2011). In theory, if enough stages are provided and enough reflux is available, any desired purity of the liquid (water) and gas phase (ammonia) can be obtained. In practice, there are limits to the number of stages, the provided reflux and ideal stages are not assured (Henley et al, 2011). Newer columns are designed with packings instead of trays. Packings typically consists of thin corrugated metal plates or gauzes arranges in a way that they force fluids and steams to take complicated paths

through the column, thereby creating a large surface area for contact between different phases (Moritz and Hasse, 1999). For comparing packed column with trayed columns, an equivalent concept has been introduced: the Height Equivalent to a Theoretical Plate (HETP). The HETP equals the absorption bed length divided by the number of theoretical plats in the absorption bed. It thus corresponds to the required height in a column that equals to one theoretical equilibrium stages .

$$N_t = \frac{H}{HETP} \qquad [6.4]$$

Where: Nt = Number of theoretical equilibrium stages in a column [-]

H = Actual height of a column [m]

HETP = Height equivalent to a theoretical plate [m]

The HETP is specific for the packing material.

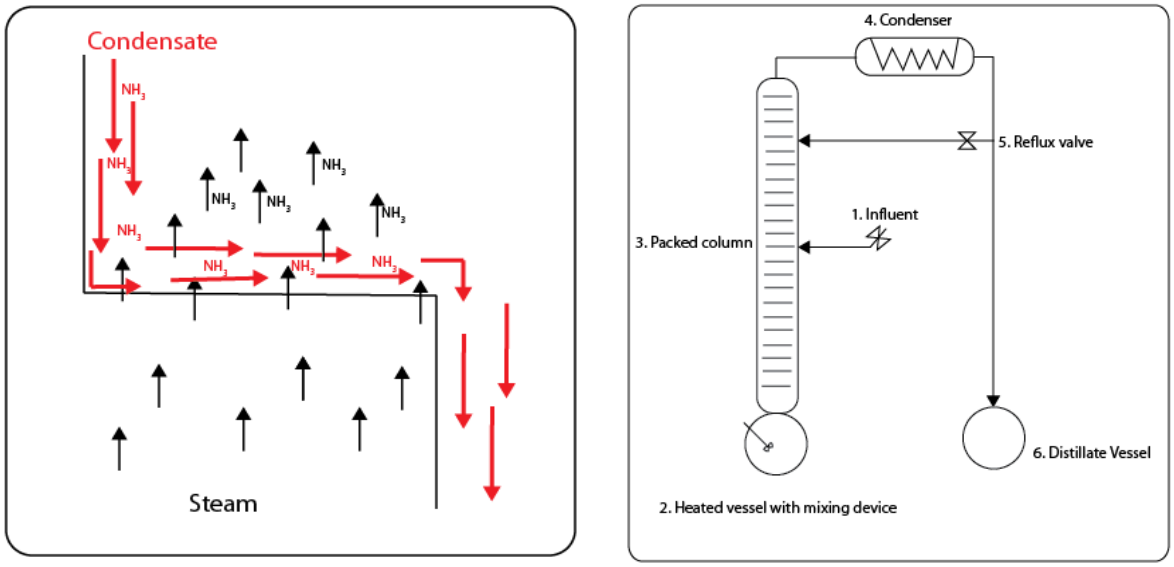

Figure 6.2 a (left) simplified tray as an equilibrium stage b (right) Schematic reproduction of distillation tower

6.3.2 CONFIGURATION OF A DISTILLATION TOWER

A typical distillation tower is shown in figure 6.2b. Regarding the separation of water and ammonium as required for the process described, the distillation tower works as follows: First, the mixture of ammonium and water enters the tower at the influent (1.) and is collected in the vessel (2). In the vessel the pH is increased, to create ammonia out of ammonium. Due to the heating, the mixture is gasified and ascends through the packed column. At the top, the gasified mixture is condensed (4) and the condensed mixture flows back into the column (5). Within the column, the packing material ensures maximal contact between the ascending steam and the descending condensate, allowing the steam to strip the ammonia out of the condensate. The portion of the column above the feed tray is called the rectification section. In this section, the gas is enriched with ammonia by contact with the reflux. The portion of the column below the feed tray is called the stripping section. The liquid feed serves as the reflux for this section. If a batch operation is applied (no continuous feeding), both sections are used as a rectification section.

7 DISTILLATION LABORATORY RESULTS

As described in chapter 6, in order to produce a gas that can be used as a fuel for a solid oxide fuel cell from ammonium present in sewage, ammonium has to be converted into ammonia and it has to be concentrated (in order to produce a sufficiently pure gas).To use ammonium present in sewage as a fuel for a fuel cell, a concentration of at least 38 gram NH_3-N/L in a water solution is required. 38 g NH_3-N/L corresponds to approximately 5 mole% in an ammonia-water mixture. The goal of the laboratory work with the distillation tower is to produce an ammonia-water mixture with at least 5 mole% of ammonia. By operating the ion exchange column as described in chapter 5, a brine of 2 liter per day with an ammonium concentration of 1 g NH_4-N/L is produced out of sewage. Thus a minimal concentration factor of 38 is required.

First, the ammonium ions (NH_4^+) present in the ion exchange brine had to be converted into ammonia (NH_3). This was achieved by increasing the pH, by adding NaOH, and thus causing the (already in chapter 6 discussed) equilibrium shown in equation 6.1 to shift to the right:

$$NH_4^+ + OH^- \leftrightarrow NH_3 + H_2O \qquad [6.1]$$

Afterwards, an ammonia-water mixture with a larger ammonia content is obtained through a combination of distillation and steam stripping in a distillation tower.

The objective of this laboratory work was more practical than academic. In order to reach the ultimate goal of this thesis a further increase in the ammonium concentration of the ion exchange effluent was required and the ammonium needed to be converted into ammonia. A distillation tower was used to achieve this further concentration, and there was no intention nor time to do further research on the distillation tower. Therefore, the work done related to the distillation tower is described as brief as possible. Because no suitable-scaled distillation set up was available at short notice, a significant over-dimensioned distillation tower was used which was available in the laboratory of the Process and Energy department at the Technical University Delft. Due to the size of this set-up, ion exchange brine of 7 days was collected and distilled all together.

7.1 MATERIALS AND METHODS

The used set up is shown schematically in figure 7.1a and a picture is shown in figure 7.1b. The parameters of the column can be found in table 7.1. It is difficult to make a good picture of the used distillation tower due to the installation that is build surrounding it for protection. However, it is possible to get an idea of the scale.

Table 7.1: Characteristic Distillation Tower

Volume Vessel		22.5	l
Effective height tower	Rectification section(above influent valve)	2.20	m
	Stripping section	1.20	m
Diameter tower		5	cm
packing material		MellapakPlus™	[-]
HETP		0.05	m
Theoretical equilibrium stages		68	[-]

The number of theoretical equilibrium stages present in the distillation tower has been calculated according to the HETP (Height Equivalent to a Theoretical Plate) supplied by the supplier (Sulzer, 2013). Based on the supplied data, a HETP of 0.05 meter is assumed (see appendix 7.1). Thus, every 0.05 meter of the packing equals one equilibrium tray. Since the distillation tower has a height of 3,40 meter, the tower consists of 68 theoretical equilibrium stages.

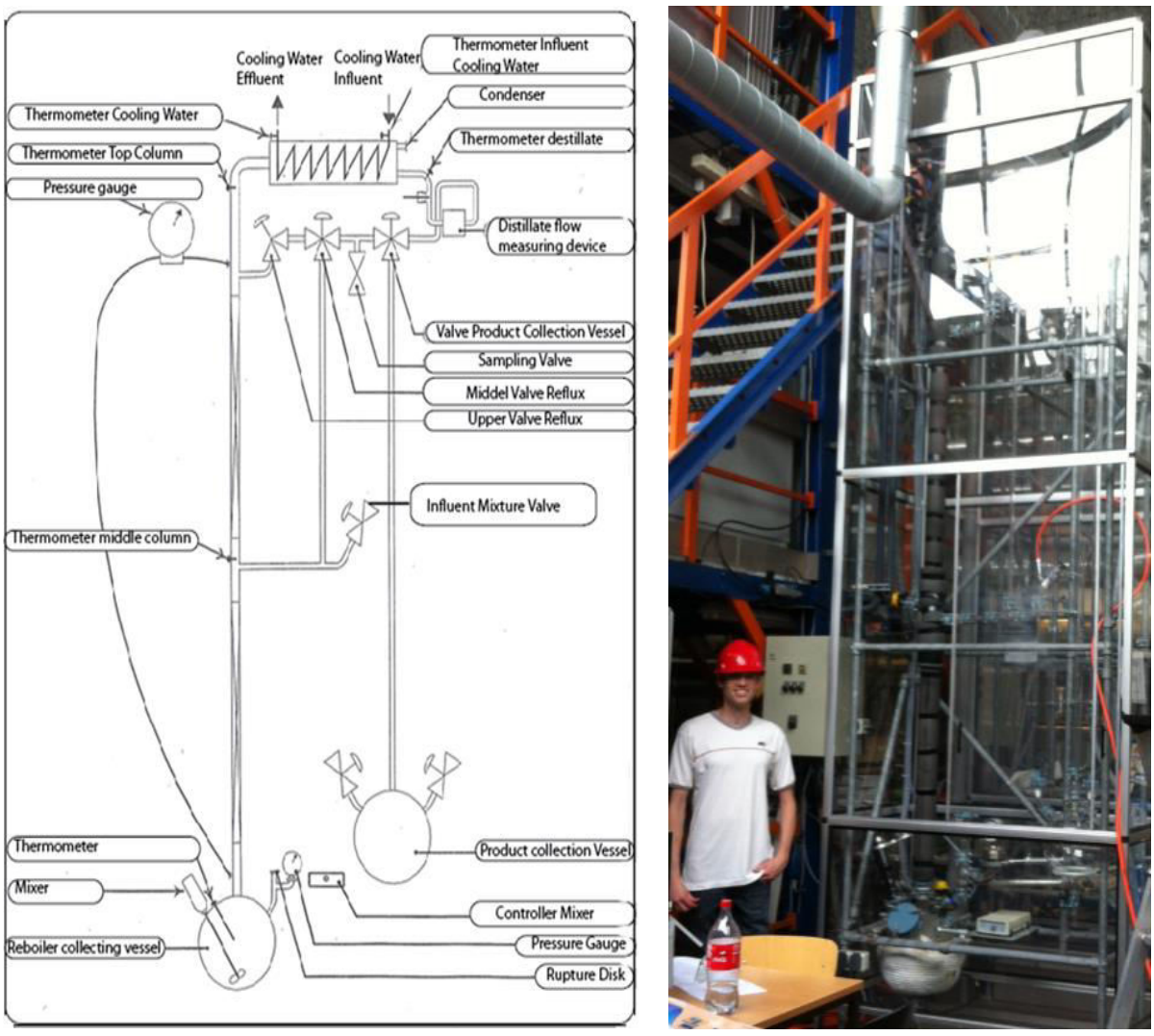

Figure 7.1 a (left) Schematic lay-out of distillation tower. b (right) The used distillation tower

7.2 EXPERIMENTAL PROCEDURE

Prior to the distillation of the ion exchange brine, multiple test distillation rounds were carried out with artificial ammonia-water mixtures to fine-tune the operational conditions. Only the experimental procedure of the distillation of the actual brine from the treated wastewater will be discussed. At the start of the distillation, a sodium hydroxide (NaOH) solution was added to the installation via the influent valve. This solution contained sufficient hydroxide to shift the equilibrium 6.1 completely to the right. Afterwards, a negative pressure of 0.5 bar was created, by connecting the distillation tower to a

vacuum pomp. Once the negative pressure was created, the vacuum in the installation was used to suck the collected ion exchange brine into the re-boiler collecting vessel. The main purpose of the vacuum was the prevention of an overpressure during operation, which could have resulted in severe leakage. Furthermore, the vacuum was created before the merging of the sodium hydroxide to make sure that no directly formed ammonia gas was sucked out of the column during the creation of the vacuum and that no ammonia gas would dissolve in the air present in the column. After all solution was collected in the re-boiler collecting vessel, the power of the heating mantle was switched on completely. Meanwhile, the cooling water flow was turned on. The solution was left boiling for a period of 4 hours, while ammonia accumulated in the highest part of the distillation tower. Due to the pressure of the steam in the re-boiler collecting vessel, the pressure inside the column slowly turned into a positive pressure of 0.3 bar. All this time, the distillation tower was operated at a total re-flux of the condensate. After 4 hours, the valve of the product collecting vessel was switched, and the first 50 ml of product was collected. By means of a density measuring device and the use of Fluidprop, the ammonia concentration of the produced ammonia-water mixture was obtained. Fluidprop is a freeware software package for thermodynamic calculations. Fluidprop was used to calculate the ammonia concentration using the measured density of the distillate.

7.3 RESULTS AND DISCUSSION

50 ml with a mole% of 5,5 NH_3 was collected after the distillation of the ion exchange brine of 7 days.

Table 7.2: distillation ammonia recovery efficiency

	In	Out	
Volume	14	0.05	[l]
concentration	1	42.7	[NH_4-N g/L]
Total ammonia	14	2.1	[g]
Ammonia recovery		15.3	[%]

As can be seen from table 7.2, only an ammonia recovery of 15,3% is achieved. This is significantly lower than expected.

7.3.1 LOW EFFICIENCY

In appendix 7.2, the calculation of the theoretical required stages is described, concluding that 3 theoretical equilibrium stages are required for obtaining an ammonia-water mixture with at least 38 g NH_3-N/L, in case only distillation was applied. As described in section 7.1, the used distillation tower consists of approximately 68 theoretical equilibrium stages. Obviously, this is more than the required 3 equilibrium stages and thus a larger ammonia concentration was expected in the product than was measured. There are multiple factors that might have contributed to this low ammonia recovery and the lower obtained ammonia concentration:

- Relative low heating capacity

The distillation tower has been out of use for at least 10 years and this influenced the operations of the tower negatively. The mixer, installed in the re-boiler collecting vessel was causing a leakage and had to be removed. Consequently, the heat distribution within the collecting vessel was sub-optimal. Moreover, the actual operating capacity is not known, but it is likely that the current available heating capacity does not equal the design capacity anymore, due to lack of maintenance. A too low heating capacity can lead to a too small upward steam flow, resulting in less contact between the steam and the condensate. This might have decreased the mass transfer of ammonia.

- Temperature limits

The boiling point of an ammonia-water mixture decreases if the ammonia mass fraction increases, i.e. a mixture with a higher ammonia concentration tends to evaporate at lower temperatures. For example, for a gas mixture with an ammonia mole fraction of 85%, the boiling temperature of the correlated saturated liquid is -25°C . Thus, if this gas mixture is cooled to -25°C, a liquid with an equal ammonia mole percentage of 85% can be obtained. However, during the laboratory work the distillation product was collected at 20°C. During the product collection process, the product collection valve was opened resulting in a direct pressure loss and contact of the product with 20°C air. Since a saturated liquid with approximately 35 mole % ammonia has its boiling point at 20°C, it is very plausible that a lot of the concentrated ammonia evaporated back into gas during the product collection. Accordingly, it is likely that after distillation a gas was created with very high ammonia concentration within the column, but that after condensation and during the product collection a lot of this ammonia evaporated back into gas, instead of staying dissolved in the water solution.

- Minor leakage losses

As described previously, the used distillation tower is old and has not been used for a long time. Prior to the experiment, a lot of effort was paid to repair the installation, and to some extend the initial leakages were indeed fixed. However, during the operations several minor leakages occurred, which might have caused ammonia to leave the tower in gas phase. During a carried out test distillation, the pressure within the system increased such that the sampling valve was pushed off, resulting initially in a fountain of ammonia-water, and afterwards in a leakage. This leakage was sealed, though it is very likely that the tower was not completely leak-proof afterwards.

7.3.2 ENERGY DEMAND

Distillation is a high energy demanding technology. The maximum energy requirement of the heating device is 2900 W as indicated on the heating device. During the experiment, the maximal power was used for heating. Due to the lack of a mixing device in the used set-up, this is not representative. However, a distillation tower always requires the energy required to heat up the influent to the boiling point, which is 4186 joule per liter per kelvin (Gambhir and Banerjee, 1993)

7.4 CONCLUSION

By using the described distillation column, the ammonium from the ion exchange regeneration solution was successfully converted into ammonia and concentrated up to a sufficient ammonia concentration for functioning as a fuel for a fuel cell. However, the distillation process has a high energy demand, a low ammonia recovery and also a low volume recovery. From the 14 liter of ion exchange brine, only 50 ml was collected with a sufficient ammonia concentration.

Section IV: The Solid Oxide Fuel Cell

8 SOLID OXIDE FUEL CELL THEORY

The main goal of this thesis is to produce electricity with ammonia from sewage as a fuel. Fuel cells are devices that are able of electro-chemically converting the chemical energy of ammonia into electrical energy and heat. Thus, a fuel cell is used as the last step in the chain described in this thesis. This chapter gives a concise introduction into the theory of fuel cells. Fuel cells are complex devices and the scope of this thesis could easily get lost, while going into the details of electricity production with fuel cells. In order to keep this chapter readable, it has been tried to only introduce the theory and parameters which are directly necessary for understanding the performed laboratory work. Since a Solid Oxide Fuel Cell (SOFC) is used within this thesis, the focus in this chapter will be on SOFCs.

8.1 THE PRINCIPLES OF FUEL CELLS

Fuel cells are devices which electrochemically convert the chemical free energy of gaseous or liquid reactants into electrical energy through a chemical reaction with oxygen or another oxidizing agent (Kreuer, 2003). The first successful conversion of chemical energy into electrical energy in a primitive fuel cell was first demonstrated over 160 years ago (Steele and Heinzel, 2001). Figure 8.1 shows the four main components of a fuel cell: the anode, the cathode, an electrolyte in between the two electrodes and an external circuit connecting the cathode and anode.

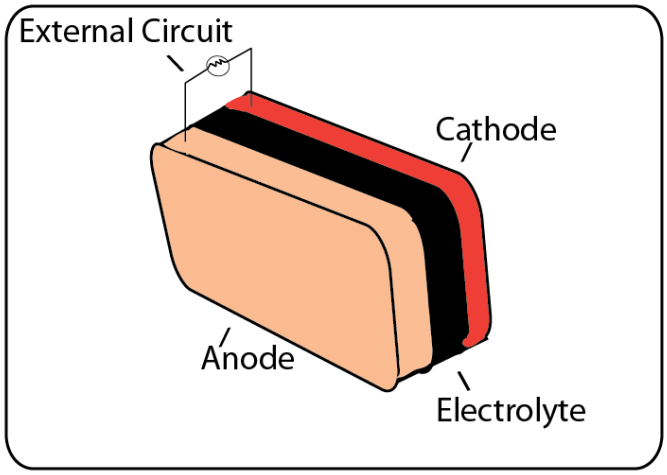

Figure 8.1 Main components of a fuel cell

Apart from effectively separating the anode and the cathode gasses/liquids (e.g. the fuel and the air) the electrolyte mediates the electrochemical reaction by allowing protons/oxides to move between the anode and the cathode, while the electrons however, are blocked by the electrolyte, and drawn from the anode to the cathode through an external circuit, producing direct current electricity (Kreuer, 2013).

The electrolyte is the most important component of a fuel cell (Kreuer et al, 2003). There are many different types of fuel cells, defined by the type of electrolyte that they use. The reactions that take place at the anode and cathode site of a fuel cell, while producing electricity, different for each electrolyte. Furthermore, the details of the reactions at the anode and cathode differ also with the fuel used. In this research, a Solid Oxide Fuel Cell (SOFC) is used, see 8.2 for an argumentation on why SOFC are considered as the most suitable type of fuel cell to use in the context of this thesis research. A SOFC is a

fuel cell with a solid oxide or ceramic non-porous electrolyte. SOFCs use this solid oxide electrolyte to conduct negative oxygen ions from the cathode to the anode.

To understand how the reaction between a fuel and oxygen produces an electric current in a SOFC and to understand where these electrons come from, it is required to consider the separate reactions taking place at each electrode (Larminie and Dicks, 2003). For the sake of explanation, first a SOFC using hydrogen as a fuel is explained. Afterwards, the reactions taking place once ammonia is used as a fuel will be elaborated upon.

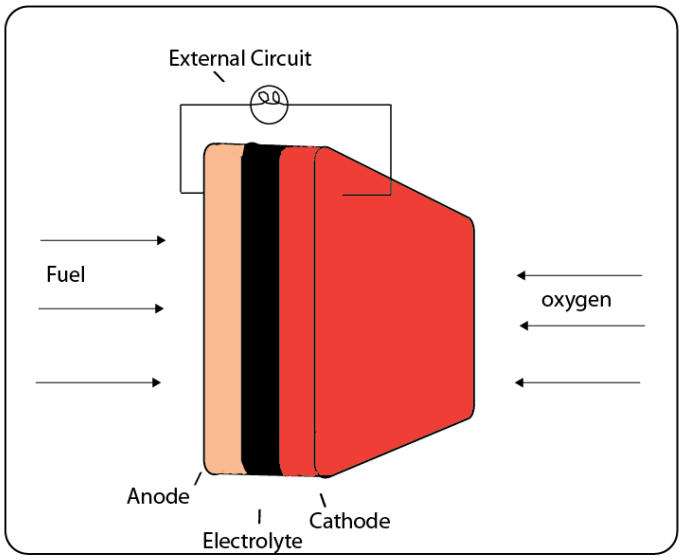

Figure 8.2 basic components of fuel cell with reacting gases

At the anode of a SOFC, the oxidation of hydrogen takes place. Hydrogen reacts with the oxygen ions which are formed at the cathode and allowed to pass through the electrolyte.

$$H_2 + O^{2-} \rightarrow H_2O + 2e^- \qquad [8.1]$$

At the cathode, the reduction of oxygen occurs, and thus the oxygen ions required for equation 8.1 are formed.

$$\frac{1}{2}\, O_2 + 2e^- \rightarrow O^{2-} \qquad [8.2]$$

When the two reactions at the anode and cathode are combined, this leads to the following total equation:

$$H_2 + \frac{1}{2}\, O_2 \rightarrow\ H_2O \qquad [8.3]$$

For these reactions to proceed continuously, O^{2-} ions must be able to pass through the electrolyte easily, and there must be an electrical circuit for the electrons to go from the anode to the cathode. Thus an electric current is produced (see figure 8.3).

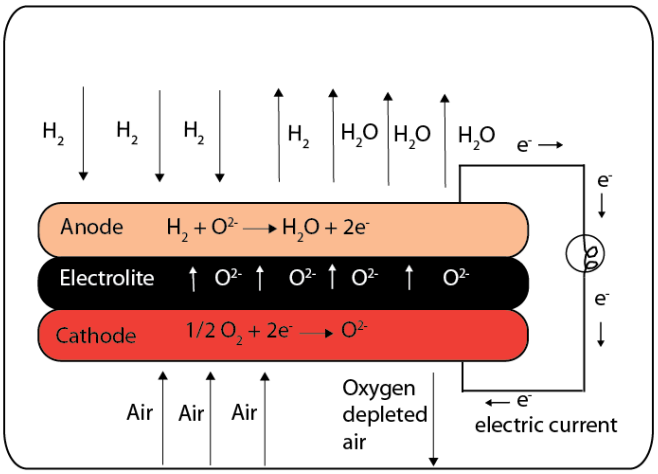

Figure 8.3 schematic representation of the reactions occurring in a hydrogen-fed SOFC

8.1.1 WHAT LIMITS THE CURRENT?

At the anode side, the fuel reacts (in the discussed case the fuel refers to hydrogen), releasing energy (Larminie and Dicks, 2003). However, this reaction has the 'classical' energy form (see figure 8.4) and thus cannot proceed at an unlimited rate. Though energy is released, first the activation energy has to be supplied to get over the energy hill. If the probability of a molecule having enough energy is low, the reaction will only proceed slowly (Larminie and Dicks, 2003). The three main ways of dealing with slow reaction rates are:

- The use of catalysts
- Operating the fuel cell at very high temperatures
- Increasing the electrode area

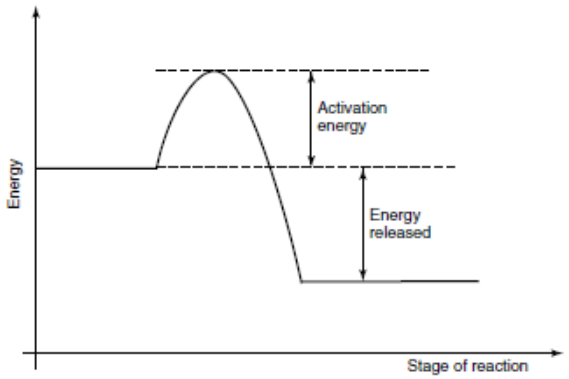

Figure 8.4: Classical energy diagram for a simple exothermic chemical reaction (Larminie and Dicks, 2003)

To prevent slow reaction rates, in the design of fuel cells major attention has been put in increasing the surface of the electrodes, by making them highly porous. In addition to these surface area considerations, often catalytic material is incorporated in the electrode or a catalytic material is used as electrode (Larminie and Dicks, 2003). Because SOFCs are usually operated at high temperatures, the low reaction rate is typically a larger problem for other types of fuel cells. This is an advantage of the SOFC.

8.1.2 THE ELECTROMOTIVE FORCE

The purpose of a fuel cell is to produce an electrical current that can be directed outside the cell to do work (such as powering an electric motor). This electrical current is driven by a potential difference, e.g. the voltage, developed by fuel cell. The electromotive force (EMF) is the voltage developed by any source of electrical energy. The EMF can be defined around a closed loop as the electromagnetic work that would be transferred to a unit of charge if it travels once around that loop (Cook, 1975). In a two-terminal device (such as fuel cells), the EMF can be measured as the open-circuit potential difference (OCV) across the two terminals (e.g. electrodes). The potential difference thus created drives current flow if an external circuit is attached to the source of the EMF (when current flows however, this potential difference will no longer equal the EMF, due to the voltage drop within the device).

The driving force of this created potential difference is the Gibbs free energy (ΔGr) of the reaction that takes place in a SOFC:

$$H_2 + \frac{1}{2}\, O_2 \rightarrow\ H_2O \qquad [8.4]$$

The Gibbs free energy can be defined as the energy available to do external work, at a constant temperature and pressure (Greiner et al, 1999). In the context of a fuel cell, this 'external work' involves moving electrons round an external circuit. The Gibbs function of a system is defined in terms of the enthalpy (total energy of a system) and entropy (measure of disorder of a system).

$$\Delta G = \Delta H - T\Delta S \qquad [8.5]$$

Where	G =	Gibbs free energy	[J/mol]
	H =	Enthalpy	[J/mol]
	T =	Temperature	[K]
	S =	Entropy	[J/mol]

Note that all these forms of chemical energy are rather like mechanical potential energies. Firstly because the point of zero energy (reference point) can be defined almost anywhere. When working with chemical reactions, the zero energy point is defined as normal elements, in the normal state, at standard temperature and pressure (25 °C and 1 bar). When this convention is adopted, 'Gibbs free energy of formation' is used (ΔG_f) instead of 'Gibbs free energy' (ΔG). The second parallel with mechanical potential energy is that the change in energy is more important than the absolute value. The change in the Gibbs free energy of formation, gives the amount of energy that is released. In fuel cells, this change is the difference between the Gibbs free energy of the products and the Gibbs free energy of the inputs (e.g. the reactants). (Larminie and Dicks, 2003)

$$\Delta G_f = G_{f-Products} - G_{f-reactants} \qquad [8.6]$$

Back to the definition of the Gibbs free energy of formation. Enthalpy (H) is defined as the sum of the energy required to create the system (the internal energy) and the energy required to make room for the system (the product of pressure and volume of the system) (Wang, 2011).

$$H = U + PV \qquad [8.7]$$

Where	H =	Enthalpy	[J]
	U =	Internal energy	[J]
	P =	Pressure	[Pa]
	V =	Volume	[m^3]

Just like the Gibbs free energy, enthalpy can be expressed as the enthalpy of formation (ΔH_f). The enthalpy of a specific reaction is obtained by the differences between the enthalpy of formation of the products and the enthalpy of formation of the reactants. The enthalpy of formation of a fuel describes the heat produced when burning the fuel (Larminie and Dicks, 2003). To visualize the relation between the enthalpy (H), the entropy (S) and the Gibb's free energy (G), figure 8.5 is helpful.

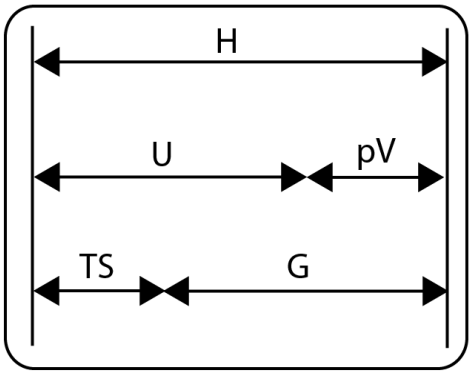

Figure 8.5 Relations between thermodynamic functions

If there are no losses in the fuel cell (e.g. if the process in reversible), then all the Gibbs free energy is converted into electrical energy (later will be shown that this is not true in practice).In section 8.1 it was shown that in the simplest fuel cell working on hydrogen, per hydrogen molecule consumed, 2 electrons pass round the external circuit. So, for one mole of hydrogen used, 2N electrons pass round the external circuit (where N is the Avogadro's number) (Larminie and Dicks, 2003). If –e is the charge on one electron, then the charge that flows per mole of hydrogen through the external circuit is:

$$-2Ne = -2F \text{ coloumbs} \qquad [8.9]$$

While F is the Faraday constant, e.g. the electric charge per mole of electrons (Mohr et al, 2008). If E is set as the voltage of one fuel cell [V], e.g. the electrical potential difference, then the electrical work done moving this charge round the circuit is (Larminie and Dicks, 2003).

$$\text{Electrical work done} = \text{charge} \cdot \text{voltage} = -2FE \quad [J] \qquad [8.10]$$

As mentioned before, if the system is reversible, then this electrical work done will be equal to the Gibbs free energy released (ΔG_f). Consequently:

$$\Delta G_f = -\mathrm{n}\, F \cdot E \qquad [8.11]$$

If the amount of electrons that travel around the circuit per mole of fuel is substituted by the value *n,* and equation 8.11 is re-written, the fundamental equation for the electromotive force (EMF) or reversible open circuit voltage of a fuel cell is deducted:

$$E = \frac{-\Delta G_f}{n\,F} \qquad [8.12]$$

Where:	E	=reversible open circuit voltage	[V]
	ΔG_f	= Gibbs free energy of formation	[J/mol]
	n	= The amount of electrons that travel around the circuit per mole of fuel	[-]
	F	= Faraday constant (9,64853399*10^4) (Mohr et al, 2008)	[C/mol]

Equation 8.12 gives the theoretical reversible open circuit voltage (OCV) or electromotive force (EMF) of a fuel cell. However, it does so for a constant Gibbs free energy value. The Gibbs free energy is not constant value and varies with temperature, reactant pressure and concentration. An equation that gives the reversible voltage [V], including the activities of the reactants and products which modify the Gibbs free change of reaction, is called the Nernst equation (assuming an ideal gas) (O'hayre et al, 2006). Equation 8.14 shows the Nernst equation for the described reaction of hydrogen in a fuel cell.

$$E = \frac{-\Delta G_0}{n\,F} + \frac{RT}{nF} ln \left[\frac{P_{H_2} . P_{O_2}^{\frac{1}{2}}}{P_{H_2O}} \right] \qquad [8.13]$$

So,

$$E = E^0 + \frac{RT}{nF} ln \left[\frac{P_{H_2} . P_{O_2}^{\frac{1}{2}}}{P_{H_2O}} \right] \qquad [8.14]$$

Where	E	= EMF or open circuit voltage	[V]
	E^0	= EMF at standard temperature and pressure, and with pure reactants	[V]
	ΔG_0	= Gibbs free energy of formation	[J]
	n	= The amount of electrons that travel around the circuit per mole of fuel	[-]
	F	= Faraday constant (9,64853399*10^4) (Mohr et al, 2008)	[C mol^{-1}]
	R	= The universal gas constant (8,3144621)	[J· $(mol·K)^{-1}$]
	T	= Temperature	[K]
	P_x	= Partial pressure of gas X	[bar]

The EMF calculated from equation 8.14 is known as the 'Nernst voltage' and is the theoretical reversible voltage that would exist at a given temperature and pressure (Larminie and Dicks, 2003). Although it is not a very friendly-looking formula, it is a useful one. It can easily been seen that if the activity of the reactants increases (e.g. an increasing partial pressure of H_2 and O_2), more energy is released. Conversely, if the activity of the product increases (e.g. an increasing partial pressure of H_20), less energy is released.

8.1.3 MEASURE OF EFFICIENCY: THE FUEL UTILIZATION

To compare a fuel cell with fuel-burning devices, it makes sense to compare the electrical energy produced with the heat that would be produced by burning the fuel (Larminie and Dicks, 2003). This heat is previously extended described as the enthalpy of formation (ΔH_f). Just like the Gibbs free energy, the enthalpy of formation negative for an exothermal reaction (when energy is released).

Thus, to compare with other fuel-using technologies, the efficiency of a fuel cell is usually defined as:

$$\eta = \frac{\text{Electrical energy produced per mole of fuel}}{-\Delta H_f} \quad [8.15]$$

Considering equation 8.11, it can be seen that:

$$\eta_{max} = \frac{\Delta G_f}{\Delta H_f} \cdot 100\ \% \quad [8.16]$$

From reaction 8.15 and 8.16, it shows that there is a connection between the maximum OCV (open circuit voltage) of a cell and its maximum efficiency. This maximum efficiency limit is known as the thermodynamic efficiency (Larminie and Dicks, 2003). If the definition of the Gibbs free energy of formation and the enthalpy of formation are filled in, the following equation q is required.

$$\eta_{max} = \frac{\Delta G_f}{\Delta H_f} = \frac{\Delta H_f - T\Delta s_f}{\Delta H_f} = 1 - \frac{T\Delta s_f}{\Delta H_f} \quad [8.17]$$

Provided that the reaction entropy Δs_f is positive (and ΔH_f is negative for an exothermal reaction), this efficiency limit can even be higher than unity (Kreuer, 2013). Looking at fuel cells in such a principle way, can lead to the conclusion that fuel cells are the perfect energy conversion system, superior to any heat engine, for which the efficiency is limited to the limit of the Carnot cycle (Feynman et al, 2013). Because, according to equation 8.17, the efficiency of a fuel cell is not limited by the Carnot cycle. Unfortunately, the issue is more complex. In practice it is found that not all the fuel fed to a fuel cell can be used, for reasons that will be discussed later. Moreover, the electrical efficiency of a single cell set-up is difficult up-scalable, due to the fact that the heating mechanism is not integrated in an single cell set-up (P.V. Aravind, personal communication, August 2014). A more significant parameter for describing the behavior of a fuel cell is the fuel utilization factor. This fuel usage can be expressed as follows:

$$\mu_f = \frac{\text{mass of fuel reacted in cell}}{\text{mass of fuel input to cell}} \cdot 100\% \quad [8.18]$$

This can be written as follows:

$$\mu_f = \frac{I * S_{1A}}{Q_{in}} \cdot 100\ \% \quad [8.19]$$

Where:	μ_f	= Fuel utilization	[%]
	I	= Drawn Current	[A]
	S_{1A}	= flow of fuel required to obtain 1 A	[ml/(min*A]
	Q_{in}	= total input flow of fuel to SOFC	[ml/min]

The flow of fuel required for obtaining one 1 A (S_{1A}) is calculated as follows:

$$S_{1A} = M \cdot \frac{R \cdot T \cdot 60}{P} \qquad M = \frac{C}{n \cdot L} \quad [8.20 \text{ and } 8.21]$$

Where:	S_{1A}	= flow of fuel required to obtain 1 A	[ml/(min*A)]
	M	= moles of fuel required to obtain 1 A	[mol]
	R	= Universal gas constant (8,3144621)	[J/(mol*K)]
	T	= Temperature	[K]
	P	= Pressure	[MPa]

C	= Electrons required for 1 A (6.241×10^{18})	[-]
n	= Electrons produced by 1 mole of fuel in SOFC	[-]
L	= Avogadro's Constant (6.02214129×10^{23})	[mol^{-1}]

Equation 8.21 is basically a form of the universal gas law (pV = nRT), rewritten in order to obtain the fuel volume required for producing 1 ampere of current (assuming an ideal gas). Factor n is derived from the chemical reaction 8.3 that takes place in a SOFC.

8.1.4 OPERATIONAL FUEL CELL VOLTAGE

In practice, the operational fuel cell voltage is considerable less than the theoretical value calculated with the Nernst equation (equation 8.14). Figure 8.6 shows the performance of a typical SOFC (Larminie and Dicks, 2003). In figure 8.6, the obtainable cell voltage is shown as a function of the current density. The relationship between the applied voltage and the resulting current (expressed in current density), the I-V characteristic curve, defines the electricity producing device.

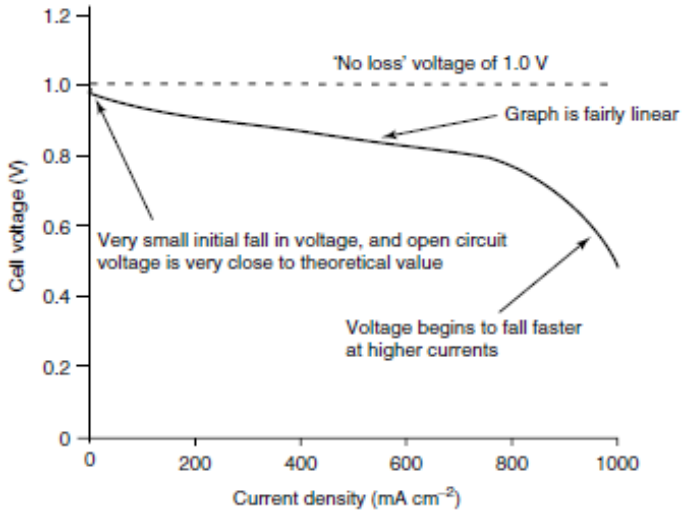

Figure 8.6 Typical behavior of a SOFC cell operating at 800 C (Larminie and Dicks, 2003)

Observations made on the behavior of the fuel cell are included in figure 8.6. Typical for SOFCs is the general small difference between the theoretical OCV (based on the Nernst equation) and the actual measured open circuit voltage (which is represented as the voltage when the current density is zero, thus when there is no closed circuit between the anode and the cathode). Other types of fuel cells generally have higher theoretical OCV value, but also a larger initial fall. This is mainly due to the activation losses (described in 8.1.1), which are more significant for reactions at lower temperatures. SOFC's function on very high temperatures and therefore suffer less from activation losses. The characteristic shape of the I-V curve as shown in figure 8.6, results from four major causes of voltage drop. These four irreversibilities are (Larminie and Dicks, 2003):

- Activation losses

  Activation losses are causes by the slowness of reactions taking place on the surface of electrodes. As discussed in section 5.1.1, a proportion of the voltage generated is lost in driving the chemical reaction that transfers electrons

between the electrodes. The voltage drop caused by activation losses is highly non-linear (Larminie and Dicks, 2003).

- Fuel crossover and internal current
  Energy is lost by fuel passing through the electrolyte, and to a lesser extent, from electron conduction by the electrolyte. As described in figure 8.3, in theory electrolytes only transport ions through the cell. In practice however, a certain amount of fuel diffusion and electron flow will always occur. In general, the fuel losses and internal currents are small, and its impact on the overall voltage drop is usually not very important, especially not for high temperature SOFCs.

- Ohmic losses
  Ohmic losses are caused by the straightforward resistance to the flow of electrons through the material of the electrodes and the various interconnections within the external circuit, as well as the resistance to the flow of the ions through the electrolyte. Essentially, the voltage drop caused by ohmic losses is proportional to the current density. The linear decrease in figure 8.6 can be assigned to ohmic losses.
- Mass transport or Concentration losses
  The change in concentration of the reactants at the surface of the electrodes, due to the chemical reactions taking place, cause a voltage drop. Because this type of irreversibility is a results of failing transport of sufficient reactant to the electrode surface, this kind of loss is also called ‘mass transport loss’.

8.2 AMMONIA-FED SOLID OXIDE FUEL CELLS

Hydrogen is currently the common choice of fuel for fuel cells, but due to its low energy density storage and safety concerns related to its high flammability, the exploration of alternative fuels seems to be crucial for the commercialization and feasible up-scaling of fuel cell technology (Ma et al, 2006, Dekker and Rietveld, 2006).

In the research on multi-fuel fuel cells, Solid Oxide Fuel Cells (SOFCs) offer potential advantages over other types of fuel cells in terms of efficiency, flexibility and cost because of their high operating temperatures (Staniforth and Ormerod, 2003a, Steele and Heizel, 2001). These high operating temperatures allow the possibility of directly internally reforming multiple fuels into hydrogen within the fuel cell itself, in other words, fuels may be directly fed to the SOFC without any pre-treatment (Wojcik et al, 2003).

During their study on the feasibility of operating a SOFC on biogas, Staniforth and Ormerod (2003a) found that the electricity production of the fuel cell was not at all hindered by the ammonia present in the biogas. The SOFCs proved not only to tolerate the ammonia, but to actually utilize the ammonia present in biogas to produce electrical power, at the same time acting as an environmental clean-up device breaking down the ammonia pollutant to nitrogen and water (Staniforth and Ormerod, 2003b). Subsequently, several studies indicated the potential of running SOFCs using ammonia as a fuel (Chachuat et al, 2010, Fuerte et al, 2009, Meng et al, 2007, Dekker and Rietveld, 2006, Fournier et al, 2006). The general mindset in all these studies is that ammonia as a fuel for the SOFC appears to be very attractive, since ammonia is a good hydrogen carrier and carbon free. It can be easily liquefied, the volumetric energy density of liquefied ammonia is higher than that of liquid hydrogen, which is useful in transport and storage (Dekker and Rietveld, 2006). Furthermore, ammonia is less flammable than hydrogen, leaks are easily observable because of the smell, there are no problems with coking and the by-products of its cell reaction are merely nitrogen and water, so no greenhouse gases are emitted (Fuerte et al, 2009).

8.2.1 WORKING PRINCIPLE OF AMMONIA-FED SOFC

The working principles of an ammonia fed SOFC based on a proton-conducting electrolyte are shown in figure 8.7. The oxidation of ammonia in a SOFC is a two-staged process (Fuerte et al, 2009). Initially, decomposition of ammonia into nitrogen and hydrogen occurs (equation 8.22). This reaction is called the reforming of ammonia. The reforming is followed by the oxidation of hydrogen to water (8.23).

$$2\,NH_3 \rightarrow\ N_2 + 3H_2 \qquad [8.22]$$

$$H_2 + O^{2-} \rightarrow H_2O + 2e^- \qquad [8.23]$$

Coincidently, nickel, the traditional anode material for SOFCs, is an excellent catalyst for reaction 8.22 (Qianly et al, 2006). Thus, ammonia undergoes a catalytic thermal decomposition over Ni catalysts at the anode. The combined anodic reaction is:

$$2NH_3 + 3O^{2-} = N_2 + 3H_2O + 6e^- \qquad [8.24]$$

The corresponding cathodic reaction is the reduction of oxygen from air (Wojcik et al, 2003):

$$\frac{1}{2}\,O_2 + 2e^- \rightarrow O^{2-} \qquad [8.25]$$

The overall reaction for complete combustion of ammonia is:

$$4NH_3 + 3O_2 = 2N_2 + 6H_2O \qquad [8.26]$$

The nitrogen gas and steam produced are removed from the anode chamber (Meng et al, 2007).

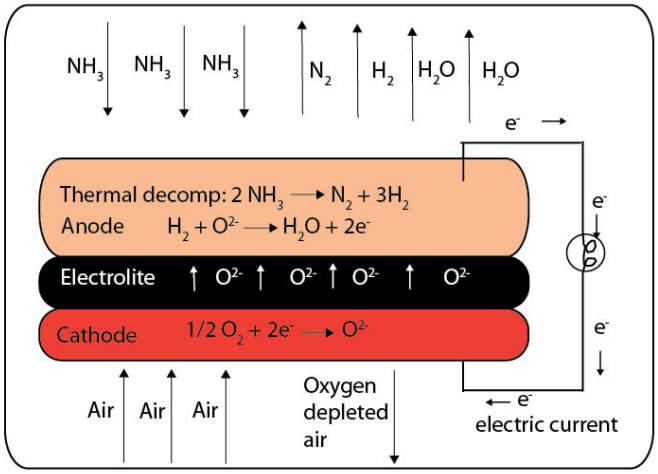

Figure 8.7 schematic representation of the reactions occurring in an ammonia-fed SOFC

As mentioned in chapter 6, some gasses or liquids can be harmful for a fuel cell. Oxygen is harmful for the anode side of a fuel cell, since it will oxidize the anode material.

8.2.2 AMMONIA-FED SOFC BEHAVIOUR COMPARED TO HYDROGEN-FED SOFC

Several studies compared the activity of SOFCs fuelled with ammonia and the equivalent amount of hydrogen. Wojcik et all (2003) reported similar electricity production with ammonia as a fuel for a SOFC, as was obtained with hydrogen. This data was obtained with a SOFC with a platinum anode. Platinum is not a practical solution for a commercial SOFC system, due to high costs. Therefore, Wojcik et al (2003) concluded with the recommendation to look into the use of nickel-anodes, due to their large surface area's and catalytic ability for reforming ammonia in hydrogen.

Qianly et al (2006), found the I-V curve shown in figure 8.8. Ammonia and hydrogen were fed in the same quantities to a SOFC set up (which used SDC as electrolyte, SDC-NO as anode (nickel!) and SSC-SDC cathode). It can be seen in figure 8.8 that the performances for ammonia and hydrogen were quite similar. The difference of cell performances for ammonia and hydrogen decreased with temperature (in figure 8.8 the I-V curve at 700°C is shown, in their work Qianly et al (2006) also reported I-V curves obtained at lower temperatures). Ammonia functions more comparable with hydrogen at higher temperatures because the ammonia-reforming reaction is more complete at a higher temperature (Qianly et al, 2006).

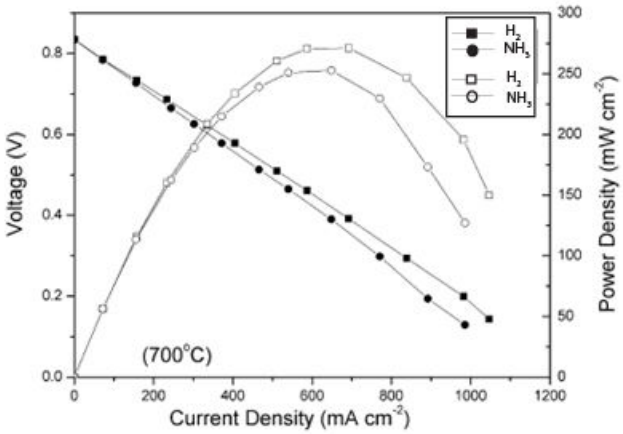

Figure 8.8 I-V curve ammonia-fed SOFC (Qianly et al, 2006)

Furthermore, Xie et al (2007) came to similar conclusions as the previous mentioned studies, i.e. that ammonia and hydrogen have a quite similar behavior for energy production, especially at high operation temperatures. Dekker and Rietveld (2004) came up with the same results. Based on this small literature review, it can be concluded that pure ammonia-fed SOFCs give a power performance similar to that obtained from an equivalent supply of pure hydrogen.

Initially, in ammonia-fed SOFC research, it was assumed that the energetically less favorable partial oxidation reaction forming NO would complicate the operations of the SOFC on ammonia (reaction shown in equation 8.27):

$$4NH_3 + 5O_2 = 4NO + 6H_2O \qquad [8.27]$$

However, Wojcik et al (2003), Dekker and Rietveld (2004), Qianly et al (2006) and Meng et al (2007) all found negligible NO_x concentrations in the SOFC of-gas.

9 FUEL CELL LABORATORY RESULTS

The performance of a SOFC was examined, when fed with the ammonia-water mixture obtained from the work described in this thesis. Single cell experiments were carried out, in the laboratory of Fiaxell, situated in Lausanne, Switzerland. The initial goal of these experiments was to verify the possibility of using the ammonia-water mixture as produced within this thesis as a fuel for electricity production with a SOFC. Single cell tests with hydrogen as a fuel were carried out as a reference. Furthermore, additional single cell tests were done with an artificial ammonia-water mixture as a fuel, in order to study the impact of the ammonia concentration in the fuel on the obtainable electricity production.

The data obtained during the cell tests has been used to create and evaluate I-V curves, in order to obtain information on the behavior of the fuel cell. Furthermore, the fuel utilization during the tests has been analyzed.

Additionally, it was tried to carry out single cell tests with biogas produced by the AnMBR described in chapter 3, as a fuel. Unfortunately, this test was unsuccessful. Due to a leakage in the gas pump, it was not possible to feed the biogas adequately to the fuel cell. The ammonia-water mixture that was produced within this thesis, will be referred to in this chapter as Ammonia 5.5% solution. This ammonia 5.5% solution consist out of 5.5 mole% ammonia (e.g. 38.85 g NH_3-N/L) and 94.5 mole% water.

9.1 MATERIAL AND METHODS

In the Laboratory of Fiaxell, the 'Open Flanges Set up^{TM}' was used for all tests. This is a single cell Solid Oxide Fuell Cell (SOFC) set up, shown in figure 9.1. An oven is required since a SOFC functions on high temperatures. The used cell, a 'redox 2R-cell^{TM}', consists out of an anode supported thin Yttria Stabilized Zirconia (8YSZ) electrolyte and a 60LSC-40GDC cathode (Ihringer, 2011). This cell is shown in figure 9.2a. More details and an elaboration of all advantages of the 'redox 2R-cell^{TM}' above conventional SOFC's can be found in appendix 9.1.

Figure 9.1 a. (left)The Open Flanges Set up in oven b. (right) the Open Flanges set up without oven

Next to the cell itself, the open flange set-up existed of a golden grid for collecting current at the cathode site, a nickel paste for current collection at the anode side, and a foam ring for equal weight. A ceramic cartridge steamer/diffuser is integrated in the 'Open Flanges Set up^{TM}, enabling the creation of a constant steam flux out of a liquid fuel. Due to this steamer, it is possible to directly feed a liquid fuel to the SOFC. Furthermore, it is possible to impregnate the steamer with a catalyst of choice, when for example steam reforming is required. Because the 'Open Flanges Set up^{TM}' is not sealed, mounting (preparing) the cell is easy and quick, which made it possible to do all tests within 2 days.

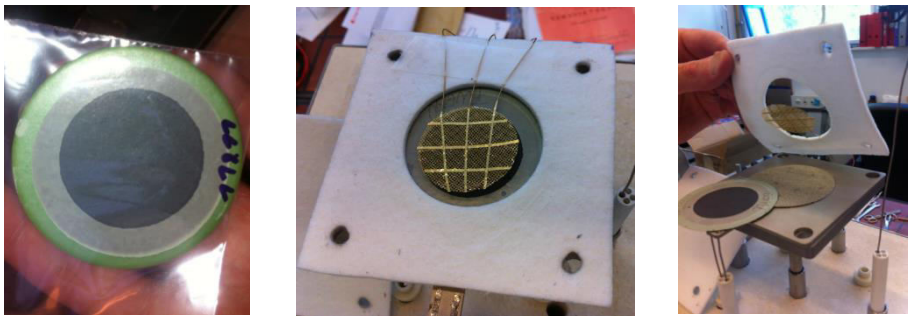

Figure 9.2a Redox 2R-Cell TM, b. golden grid and c. Nickel foam

Table 9.1. Properties of the redox 2R-cell, 143.31

Element	Material	Thickness	Cell Diameter (mm)
Anode	NiO-8YSZ	0.3 mm (functional layer 5-30 µm)	60
Electrolyte	8YSZ (with 2.5 µm GDC buffer layer)	10 micron	60
Cathode	60% LSC-40 % GDC	20 micron	36

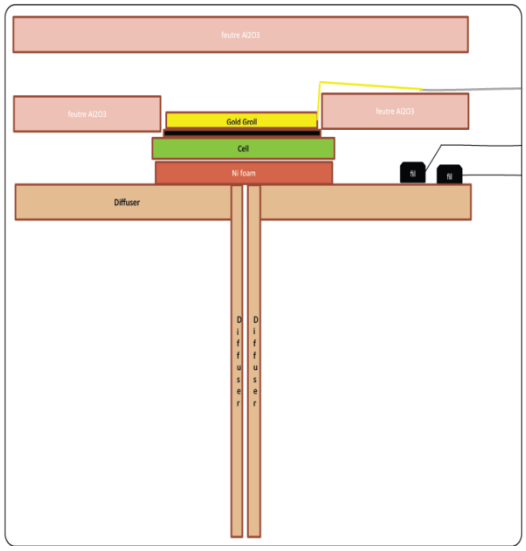

Figure 9.3. schematic lay-out of 2R-Cell set up

Figure 9.4 shows the specifications of a ⌀ 6 cm cell, as supplied by the supplier, Fiaxell. The I-V curve is shown for a range of operating temperatures, for a hydrogen flow of 182 ml/min. As shown, the open circuit voltage (OCV) equals more then 1,1 V. The highest temperature shows the best results, with a current density of 1 A/cm^2 and a power density of over 450 mW/cm^2 achieved at 0.8 V.

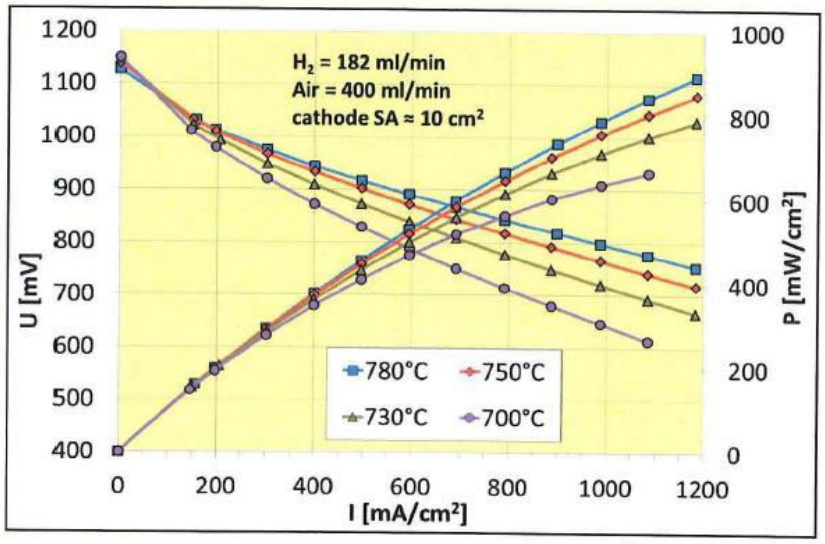

Figure 9.4. I-V curve of a single 2r-Cell

9.2 EXPERIMENTAL PROCEDURE

If no experiment is done, the SOFC was continuously fed with Formier gas (92 % N_2 and 8% H_2). At the start of the experiment, the oven was turned on. When the required temperature was reached, gradually the Formier gas flow was substituted with the tested fuel. As mentioned, tests were done with three different types of fuels as indicated in table 9.2. Firstly, the ammonia solution produced within this thesis (ammonia 5.5% solution) was tested as a fuel. Secondly, tests were done with pure hydrogen as a fuel. This was done to validate the behavior of the fuel cell, by comparing it with the supplied I-V curve . Furthermore, also the behavior of the fuel cell when fed with an artificially made solution with a higher concentration of ammonia was tested (Ammonia 25% solution). This solution consisted for 25 mole% of ammonia and 75 mole% of water. This ammonia 25% solution was tested since it was expected that large potential improvements are possible within the chain of installations described in this thesis research. Therefore, it is useful to see the effect of a larger ammonia concentration in the fuel on the behavior of the fuel cell, since an optimization of the installation described in this thesis might result in a mixture with higher ammonia concentrations.

Table 9.2 Fuels tested for the SOFC

Fuel	Origin
Ammonia 5.5 % Solution	Originating out of synthetic sewage
Ammonia 25% solution	Locally made
Pure Hydrogen	Locally available

For obtaining I-V curves for different fuels, an increasing current was drawn from the cell by means of a adjustable resistance and the corresponding voltage over the cell was measured. Steps of 1 A have been taken for the tests using hydrogen as a fuel and steps of 0.2 A were taken for the tests with Ammonia 5.5 % solution as a fuel and steps of 0.5 A were taken for the Ammonia 25% solution. After each current increase, the cell was allowed to stabilize the voltage output for some time. Once the voltage output had stabilized, the voltage output was measured and recorded. In figure 9.5, the complete set-up for the tests with hydrogen as a fuel is shown.

Figure 9.5 Test set up for hydrogen tests

The Ammonia 5.5% solution was fed to the SOFC with a liquid pomp to the incorporated steamer and fed directly to the cell. The artificial 25% ammonia-water mixture was also fed to the fuel cell in this way.

For creating the I-V curves, the set drawn currents for which the corresponding voltages have been measured, need to be converted into the current density according to formula 9.1:

$$I_d = \frac{I}{A_{cell}} \qquad [9.1]$$

Where:	I_d	=	The current density	[mA/cm^2]
	I	=	The drawn current	[mA]
	A_{cell}	=	Active cell surface	[cm^2]

The active cell surface in the used set up is the surface of the cathode, which is 10.18 cm^2. Other used parameters have already been described in chapter 8.

9.3 RESULTS

The obtained I-V curves of the tests with all three fuels are shown in figure 9.6. figure 9.6 shows the measured voltages, for different fuels, corresponding with set currents. Also the produced power density, calculated as the power density multiplied with the voltage ($I_d \cdot V$),is plotted in the same graph. The most important observation from figure 9.6 is that indeed electricity could be produced when the ammonia 5.5% solution, as produced out of sewage, was used as fuel. As expected, it was possible to draw more current from the artificial ammonia 25% solution, because of the larger availability of fuel. The OCV of the ammonia 25 % solution was higher than the ammonia 5.5 % solution, which was also expected and in agreement with the Nernst equation. According to equation 8.13, a larger partial pressure of the fuel leads to a larger OCV and larger measured voltage values. This is logical, since if more fuel is available, a larger voltage can be produced.

Furthermore, it can be seen that the behavior of the fuel cell while fed with pure hydrogen is indeed similar to the reference values, based on the I-V curve provided by Fiaxell (see figure 9.4). This means that the cell was functioning properly. The supplied I-V curve and the measured I-V curve for the fuel cell while fed with hydrogen, both show an OCV very similar to the calculated value of the pure hydrogen of 1,27 Volt (see appendix 9.2 for calculation).

Based on the lower availability of fuel, it was expected that when ammonia 5.5% solution was used, it would be possible to draw less current compared to the other fuels. However, according to personal communication with R. Ihringer (June 2014), the developer of the fuel cell test set up, it should have been possible to draw a bit more than measured. This might be caused by a leakage of the fuel, a not completely equal distribution of the fuel to the cell or the occurrence of back diffusion of oxygen into the cell.

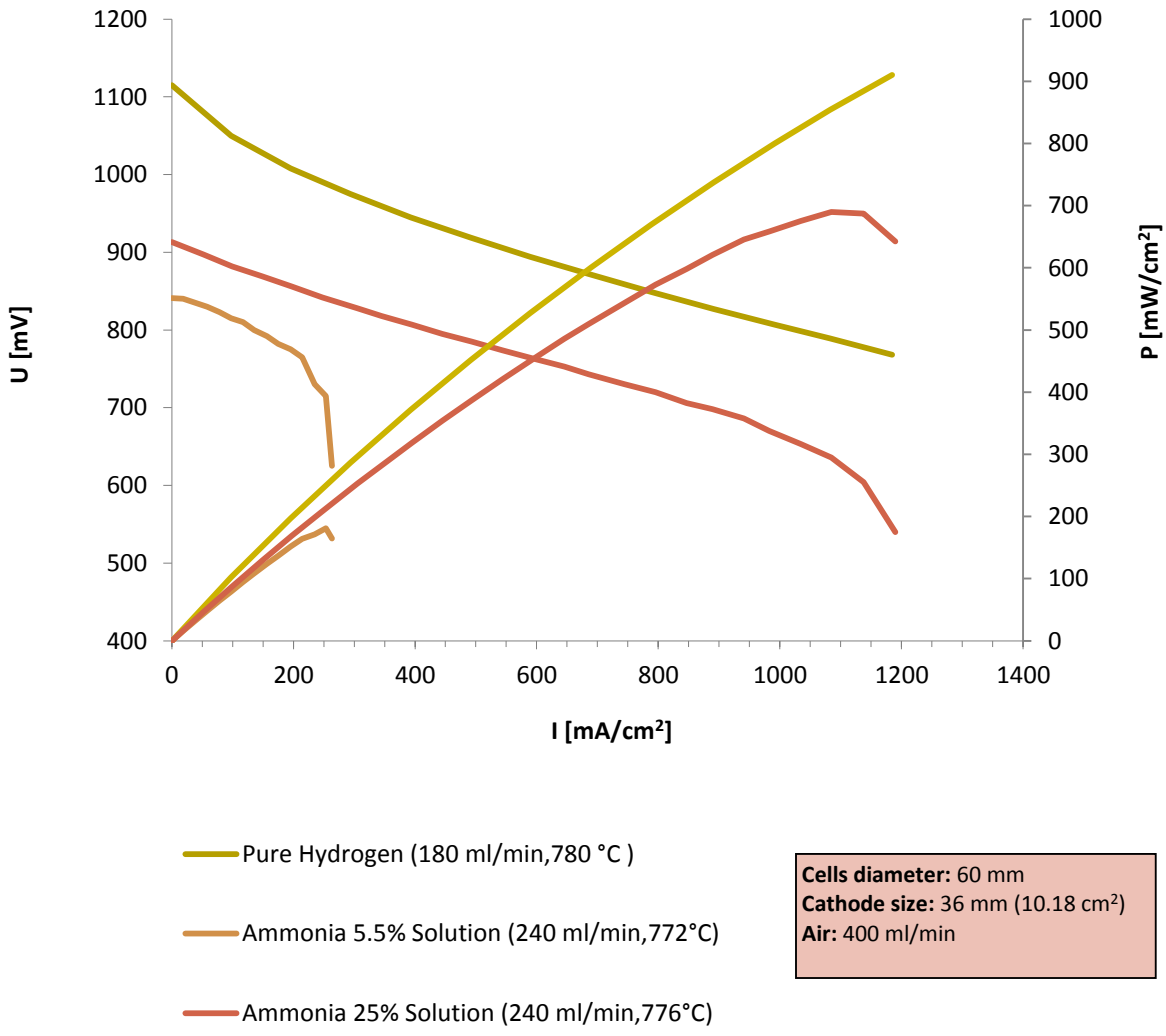

Figure 9.6 2R-Cell™ N° 143.31 tested with fuel diffuser

Figure 9.7 shows the calculated fuel utilization plotted against the power production. For calculating the fuel utilization, equation 8.18 and 8.19 have been used (section 8.1.3). The pure hydrogen results in the highest power production, but also in the smallest fuel utilization. Ammonia 5.5% solution produces the smallest power production, but with the highest fuel utilization. This is due to relative high fuel flow of hydrogen.

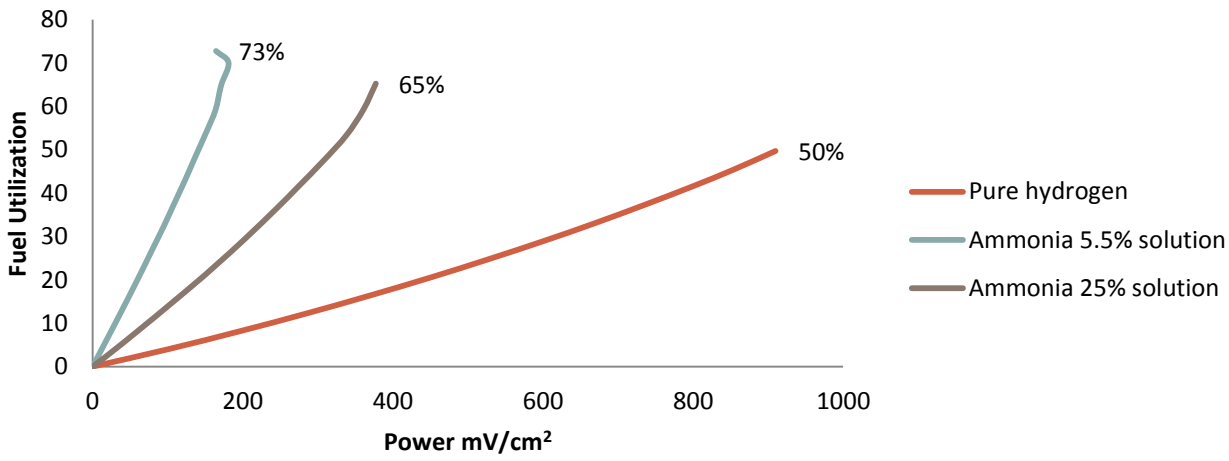

Figure 9.7 Fuel Utilization against power production

9.3 DISCUSSION

CALCULATING FUEL UTILIZATION AMMONIA

For calculating the fuel utilization, equation 8.18 and 8.19 have been used (section 8.1.3). First the calculation has been done for hydrogen, assuming the production of 2 electrons following reaction 8.1. Since direct internal reforming is asumed, i.e. ammonia is directly reformed by the cell due to the high temperature and the presence of catalysts, reaction 8.22 is assumed to take place with all incoming ammonia. Because a 100% efficient reforming is assumed, it is said that for 2 moles of ammonia results in 3 moles of hydrogen. As explained in 8.1.3, equations 8.19, 8.20 and 8.21 have been used to calculate the fuel utilization. Since the complete direct reforming of ammonia into hydrogen is assumed (in a ratio of 1:1.5), the moles of fuel required to obtain 1 ampere (S_{1A}) for ammonia have been required by dividing the S_{1A} for hydrogen by a factor 1.5. Since the off-gas was not measured, this complete reforming of ammonia to hydrogen could not be verified. If it is the case that the reforming is not optimal, the fuel utilization is currently under-estimated for ammonia.

LIMITED DRAWABLE CURRENT

A relatively low fuel utilization was measured for pure hydrogen (50%). The fuel utilization of hydrogen is limited by the power supply of the test set-up. The used power supply cannot produce more resistance, and therefore 12 ampere was the limit. This is not enough for determining the maximum fuel utilization of hydrogen. For both the ammonia I-V curve the maximum fuel utilization is reached. In this case of the ammonia solution, with a lower flow of fuel, the power supply is not the limited factor, but the cell resistance.

PRACTICAL PROBLEMS PROHIBITING TESTS WITH BIOGAS AS A FUEL

Originally the intention was to also obtain an I-V curve for biogas as a fuel, as produced by the AnMBR (described in chapter 2). As shown in figure 9.8, bags with biogas were brought along to Switzerland and a set-up existing out of a vacuum-pomp and a gas-flow meter was used. Unfortunately, the vacuum-pomp was leaking. Due to the small available volume of biogas

and the significant leakage, it was not possible to feed the fuel cell with a constant biogas flow and therefore not data could be obtained.

Figure 9.8 Set up used for tests with biogas as the fuel

9.4 CONCLUSION

Single cell SOFC experiments were carried out with the ammonia solution produced within this thesis research as a fuel, and results demonstrated that the SOFC can actually utilize this ammonia 5.5% solution to produce electrical power. At the anode site of the fuel cell, the ammonia was internally reformed into hydrogen and nitrogen, after which the hydrogen was electrochemically converted into electricity. Furthermore, tests were done with pure hydrogen as a reference, which proved that the fuel cell was functioning as expected and corresponding to the manufacturers' data. Experiments with a solution with a higher ammonia concentration have been carried out, showing that it is indeed possible to draw more current and produce more power with a higher percentage of ammonia in the fuel.

10 THE ENERGY BALANCE

10.1 INDICATION OF THE ENERGY BALANCE

In this chapter, an indication is given of the energy balance of the proposed combination of technologies, up-scaled to a flow comparable with the sewage treatment plant Harnaschpolder. The Harnaschpolder sewage treatment plant has been taken as a reference because it can be considered as a state of the art sewage treatment plant in the Netherlands (Delfluent, 2014).

The decision was made not to focus on costs, since it is difficult to make reasoned assumptions on the investment and operation costs due to the infancy of both the design and the experience in practice with the proposed technologies.

The proposed combination of technologies is still in its infancy, and therefore the following numbers should be considered only as an indication than as actual values. In the discussion an elaboration is given on the major uncertainties and made assumptions. Figure 10.1 shows the simplified flow chart of the proposed combination of technologies and table 10.1 shows the characteristics of the indicated flows in between the different units (based on a flow comparable with the wastewater treatment plant Harnaschpolder (Delfluent, 2014).

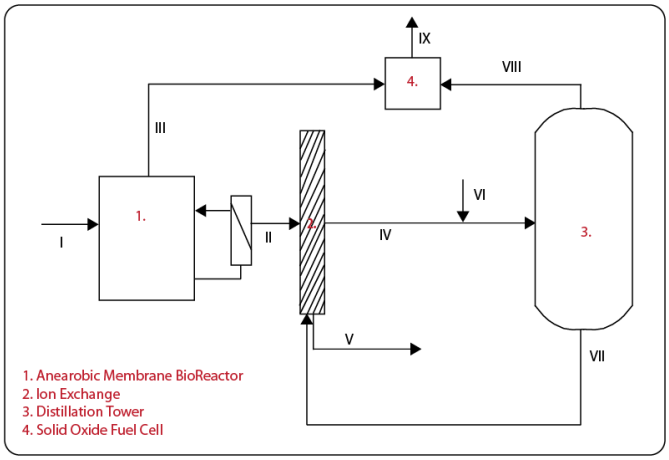

Figure 10.1 flow chart, indicating flows

Table 10.1 Composition of flows, indicated in figure 11.1

		I	II	III	IV	V	VI	VII	VIII	IX
Q	kg/h	8000	8000	-	107	8000	10	102	5	-
COD	kg/h	3200	480	-	-	760	-	-	-	-
TN-N	kg/h	560	544	-	538	24	-	290	245	?
NH_4-N	kg/h	240	536	-	538	-	-	290	-	-
NH_3	kg/h	-	-	-	-	-	-	-	245	?
CH_4	kg/h	-	-	681	-	-	-	-	-	-
NaOH	kg/h	-	-	-	-	-	2	-	-	-
H2	kg/h	-	-	-	-	-	-	-	-	?
CO2	kg/h	-	-	-	-	-	-	-	-	?

The following notes relate to table 10.1:

- The influent characteristics are based on the influent of the sewage treatment plant Harnaschpolder (Delfluent, 2014)
- The orders of magnitude of the flows, relative to each other, are based on the data obtained during the laboratory work carried out during this thesis research
- The composition of the off-gas from the SOFC (flow IX) is un-clear. Based on the completeness of the reactions taking place at the anode and cathode, it consists of hydrogen, ammonia, nitrogen, water vapor and oxygen depleted air. At this stage it is impossible to indicate the exact composition.
- The ammonium composition of flow IV is based on a different ion exchange operational regime as carried out in this thesis. Instead of regeneration after a day of loading, regeneration is done after the bed is saturated. In this way, even a higher concentration is possible (see appendix 5.2).

Table 10.2 lists the energy requirements and energy production of the up-scaled proposed combination of technologies. The values in table 10.2 are assumed in consultation with Ir. G. Smith (engineer at Pentair, personal communication, September 2014).

Table 10.2 Energy requirements versus energy production, for a combination of an AnMBR, an ion exchange column, a distillation tower and a SOFC

Energy Requirements		
anMBR	[kwh/m^3 of treated wastewater]	0,12
Distillation tower	[kwh/m^3 of treated wastewater]	0,09
Ion Exchange + Rest	[kwh/m^3 of treated wastewater]	0,12
Total	*[kwh/m^3 of treated wastewater]*	*0,33*
Energy production		
Biogas	[kwh/m^3 of treated wastewater]	0,83
NH_4	[kwh/m^3 of treated wastewater]	0,16
Total	*[kwh/m^3 of treated wastewater]*	*0,99*
Energy produced	[kwh/m^3 of treated wastewater]	**0,66**

Table 10.2 shows that a combination of an anMBR, an ion exchange column, a distillation tower and a SOFC can produce 0,66 kWh/m^3 of treated wastewater. For a wastewater treatment plant in the size of Harnaschpolder, this would mean a power production of 5280 kwh/day.

Table 10.2 is based on an influent COD concentration of 400 mg/L and an ion exchange brine with an ammonium concentration of 5 g NH_4/L (as described in table 10.1). The incoming COD concentration and the ion exchange brine ammonium concentration are quite influential on the power production of the combined anMBR, an ion exchange column, a distillation tower and a SOFC. Figure 10.2a shows the impact of the influent COD concentration of the sewage on the net electricity production. Figure 10.2a shows a significant influence of the influent COD of the sewage on the energy production. This impact can be explained by two phenomena: 1. A higher influent COD results in a higher biogas production. More biogas means more fuel and thus a higher electricity production. 2. More biogas results in the production of more steam in the fuel cell (see appendix 10.1). Since this steam flow is used for heating the ion exchange brine, a larger steam flow reduces the amount of energy that has to be added for heating the ion exchange brine in the distillation tower.

Figure 10.2b shows the influence of the ammonia concentration in the ion exchange brine on the energy production. The ammonia concentration in the brine depends on the operations and optimization of the ion exchange process. It is assumed that all the influent ammonium is converted into ammonia and present in the ion exchange brine. Therefore, a higher ammonia concentration corresponds to a smaller brine volume. A smaller brine volume results in a smaller energy requirement for vaporization in the distillation tower. Figure 10.2b also shows that for low ammonia concentrations in the brine, this concentration has an effect on the overall produced electricity, with higher concentrations the differences between concentrations become smaller. However, figure 10.2a shows that the influence of the influent COD concentration on the electricity production is larger than the influence of the ammonia concentration in the brine.

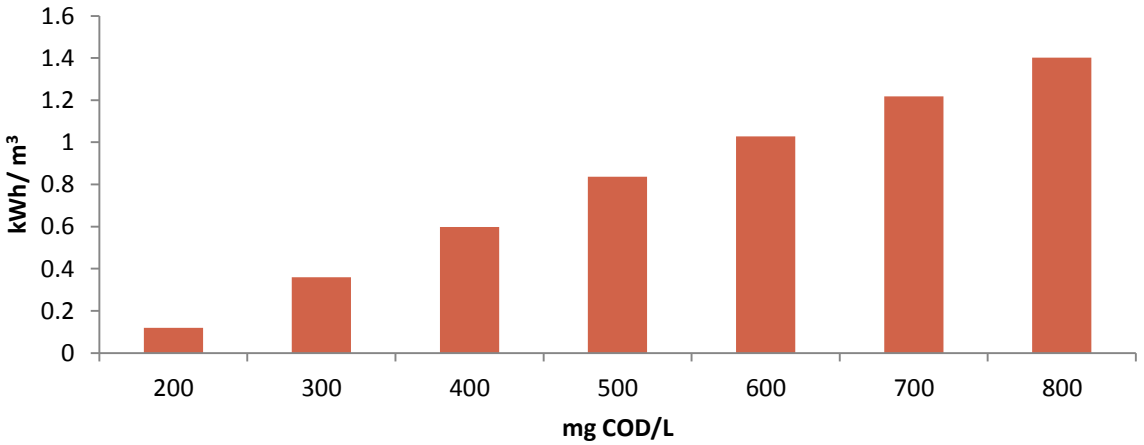

(a)

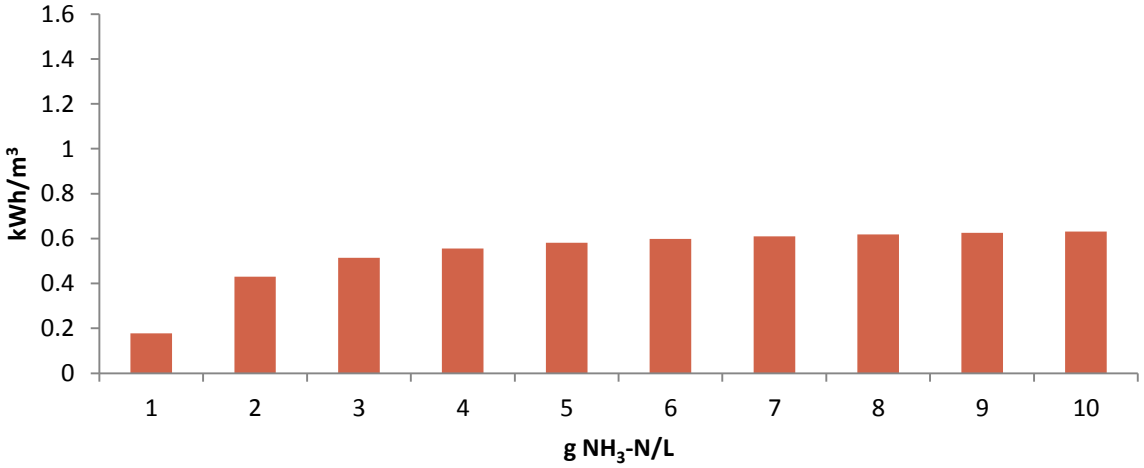

(b)

Figure 10.2 a. the energy production in kWh per m^3 of treated sewage, depending on the influent COD of the influent sewage (other characteristics fixed as in table 10.1, thus an ammonia concentration of 5 mg NH_3-N/L in the ion exchange brine), b. The energy production per m^3 of treated wastewater depending on the ammonia concentration in the ion exchange brine (other characteristics as in table 10.1, thus a COD concentration of 400 mg COD/L)

10.2 DISCUSSION

The following uncertainties are major contributors to the difficulty in scaling up the proposed design:

- During this thesis research, not all the used laboratory-scale technologies were optimized for the used scale and for example the distillation tower was clearly a sub-optimal size (combined with a general sub-optimal functioning, see 7.3.1). This hinders a reliable up-scaling of the data obtained with the laboratory work.
- As is the case for all single cell fuel cell set-ups, that require external heating, it is difficult to upscale due to the significant impact of an internal heating compared to an external heating mechanism.
- The research as described in this thesis has been carried out with independent laboratory scale set-ups. Since it was not possible to test an incorporated set-up, assumptions were necessary regarding the potential heat recovery.

Therefore the following assumptions were made to calculate the energy requirements, as shown in table 10.2:

- The energy requirements of the anMBR, the ion exchange column and the remaining energy requirements were roughly based on typical values in practice, in consultation with G. Smith (personal communication, September 2014).
- Total heat recovery was assumed for the heat required for the solid oxide fuel cell.
- The electricity production when ammonia is fed to a fuel cell is based on the total theoretical potential and the fuel utilization as measured and described in chapter 9.
- A fuel utilization of 70% has been assumed for the biogas and the produced ammonia gas.
- It is assumed that a mixture of ammonia and water vapor is produced in the distillation tower, consisting for 25 mole% of ammonia.
- The energy requirements of the distillation tower are based on an optimized design, using the produced steam in the fuel cell as the heating source. See Appendix 10.1 for an elaboration on this design and the calculations used to calculate the energy requirement.

10.3 CONCLUSION

The roughly estimated energy balance indicates that an electricity production of 0,66 kWh/m^3 of treated sewage can be achieved by a combination of anMBR, an ion exchange column, a distillation tower and SOFC. Moreover, it is shown that the influent COD of the sewage has a significant influence on the potentially produced electricity. A higher COD of the influent sewage results in a significantly larger potential electricity production. The ammonia concentration in the ion exchange brine also influences the potentially produced electricity, though to a lesser extend compared to the influent COD concentration of the sewage.

11 DISCUSSION AND RECOMMENDATIONS FOR FURTHER RESEARCH

This thesis research aimed at verifying the possibility of turning organically-bound nitrogen and ammonium present in sewage from a pollutant into a fuel. The organically bound nitrogen has been converted into ammonium and separated from suspended solids by the Anaerobic Membrane BioReactor (AnMBR), the ammonium has been isolated from the AnMBR effluent and concentrated through ion exchange, the concentrated ammonium solution resulting from ion exchange has been further concentrated and converted into ammonia via distillation and finally power has been produced by feeding this ammonia solution to a Solid Oxide Fuel Cell (SOFC). Moreover, the ion exchange effluent has an extremely low ammonium concentration (<2 mg NH_4-N/L and < 4 mg TN/L) and therefore easily meets the discharge standard of 10 mg TN/L. Figure 11.1 graphically shows the combined technologies.

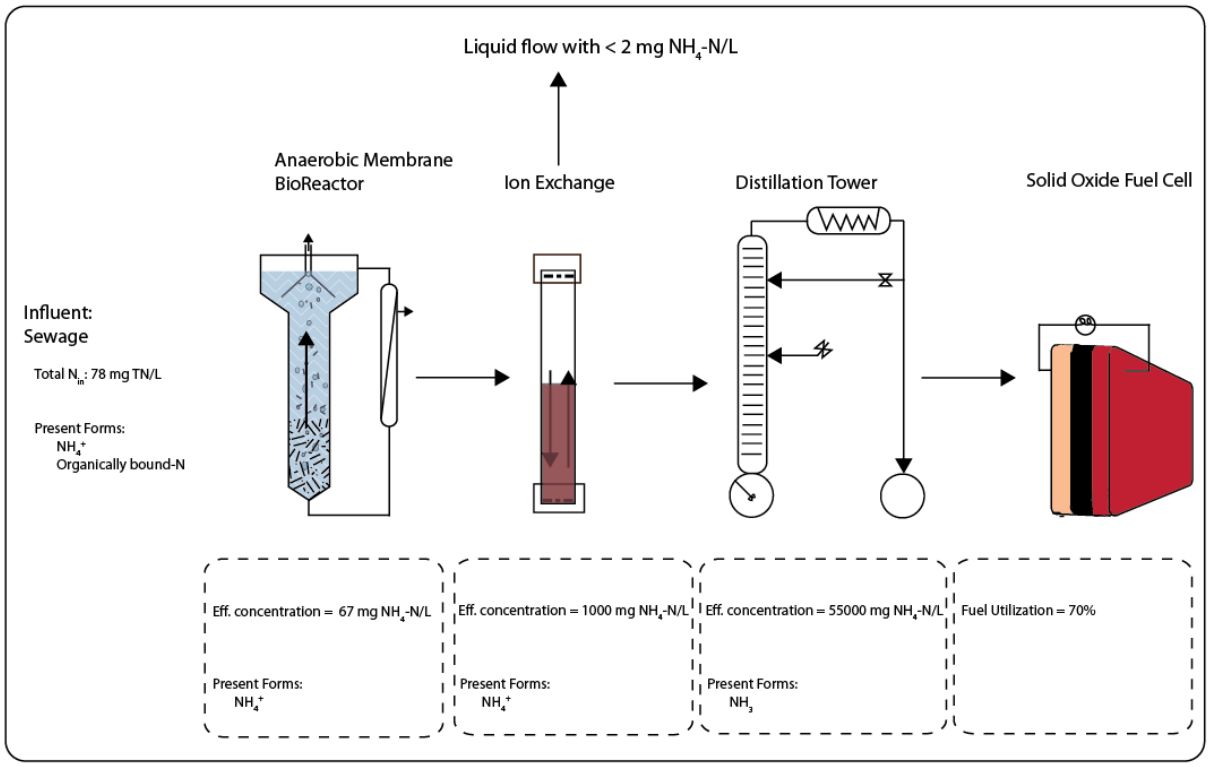

Figure 11.1 Overview combined technologies and results

The organically bound nitrogen and ammonium from sewage have successfully been converted and concentrated into a water solution sufficiently rich in ammonia for power production in a SOFC. As a proof of principle, the implemented laboratory set-up appeared successful. However, this is not to say that up-scaling is straightforward.

Figure 11.2 shows the nitrogen recovery over the various steps. For the SOFC the fuel utilization is shown, since nitrogen recovery is not applicable to a fuel cell. As shown in figure 11.2, a low nitrogen recovery was obtained with the distillation tower. This low nitrogen recovery resulted in the production of an ammonia-water mixture that just met the minimal ammonia concentration required for power production by a solid oxide fuel cell. However, as shown in chapter 9, the ammonia-water mixture as produced within this thesis research (thus with the minimal ammonia concentration) could indeed be utilized to produce power, but the SOFC behaved significantly better when fed with a water-ammonia mixture with a higher ammonia percentage.

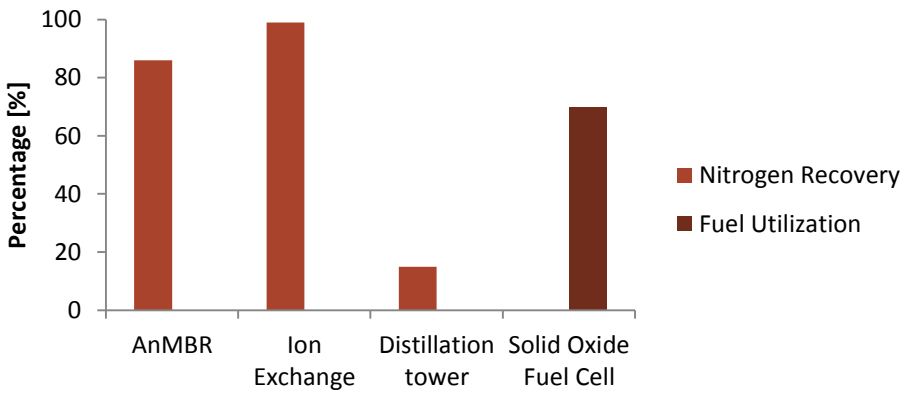

Figure 11.2 Nitrogen recovery/fuel utilization per proposed technology

However, the low nitrogen recovery can be attributed to the use of a non-optimal distillation tower design. A distillation tower is a widely applied conventional technology, and therefore it is reasonable to assume the possibility of optimizing its design considering the nitrogen recovery and the energy demand. This is done in chapter 10, and it was indicated that when an optimized and heat integrated distillation tower design is assumed, it is possible to achieve a net electricity production while also meeting the nitrogen discharge standards.

Yet, for an accurate assessment of the feasibility of the implementation of the combination of an AnMBR, an ion exchange column, a distillation tower and a SOFC, further research is required in the following fields:

1. The integration of the anMBR, an ion exchange column, a distillation tower and a SOFC

In chapter 10, an integrated combination of an AnMBR, an ion exchange column, a distillation tower and a SOFC is described, in which the gas produced by the SOFC is used to heat the ion exchange brine in the distillation tower and where the bottom liquid of the distillation tower is recycled as ion exchange regeneration solution (as described in appendix 10.1). The research described in this thesis was carried out using separate laboratory-scale set-ups and these proposed integrations have not been tested in practice. Further research is needed on the possibility and feasibility of these proposed integrations.

2. The combined feeding of ammonia and biogas to a SOFC

In chapter 10 it was assumed that ammonia and biogas can be combined and be fed to a fuel cell. Research indicates that this is possible, in fact that is how it was discovered that ammonia can function as a fuel on itself (Staniforth and Ormerod, 2003a). However, more research is needed on long term behavior of the solid oxide fuel cell and on the requirement for pre-treatment of the biogas.

3. Other types of wastewater as the influent

For this thesis research, the choice was made to work with sewage (municipal wastewater) as the influent. Since the objective of this thesis research was to proof the principle of power production using nitrogen from wastewater as a fuel, it made sense to use sewage. Sewage is namely, next to one of the most abundant types of wastewaters, also one of the most challenging types of waste water to work with, considering the combination of a relative low influent nitrogen and COD concentration due to dilution and a relative high suspended solids concentration. Since it was possible to use the nitrogen from sewage for electricity production, it is interesting to investigate the utilization of the nitrogen from other wastewater

types, since those might be (even) more feasible. Especially since in chapter 10 it was shown that the influent COD concentration has a significant impact on the net power production, it seems attractive to explore the removal of nitrogen from other (stronger) types of waste waters, while utilizing it for power production by means of a combination of an anMBR, an ion exchange column, a distillation tower and a SOFC.

4. The optimization of ion exchange operations

In this research, the choice was made to collect the first two liters of the ion exchange brine separately from the rest of the brine, while catching the total daily influent of ammonium (mg) to the ion exchange column within these two liters. In this way the ammonium was isolated from the rest of the AnMBR effluent and concentrated up to a concentration of 1 g NH_4-N/L. However, in appendix 5.2 it is shown that higher ammonium concentrations are achievable, when the ion exchange bed is not regenerated after being loaded with the daily AnMBR effluent (as done in this thesis), but when the ion exchange bed is regenerated once it is saturated with ammonium instead. In chapter 10 it was shown that an increase in the ammonium concentration in the brine of 1 g NH_4-N/L can already result in a significant increase in the net power production of the total installation. Therefore it is recommended to thoroughly investigate and optimize the ion exchange operational parameters, focusing on obtaining a higher ammonium concentration in the collectable brine.

5. The costs

In appendix 11.1, a rough calculation of the investment costs is given, if the combination of an AnMBR, an ion exchange column, a distillation tower and a SOFC would be implemented on a scale comparable with the Harnaschpolder sewage treatment plant (Delfluent, 2014). The calculated investment costs amount to € 396 per population equivalent (70% of this price can be attributed to the fuel cell). This value is only a rough estimation. However, it can be stated that the fuel cell would be the most expensive technology of the total installation. Literature suggests that the costs of fuel cells can be expected to decrease over time (Staniforth and Ormerod, 2003b). However, more research is required to give a more accurate estimation of the investment costs of the proposed combination of technologies.

6. Biogas stripping

Distillation is required for obtaining a mixture of water and ammonia sufficiently rich in ammonia in order to function as a fuel for a SOFC. However, if ammonia could be stripped (chapter 6) from the ion exchange brine by a stripping gas that could also be used as a fuel in a SOFC on itself, this minimum ammonia concentration in the fuel would no longer be relevant. Biogas has been studied intensively as a fuel for SOFCs, both on laboratory and pilot scale, and proved to be an attractive option (Staniforth and Kendall, 1998, Staniforth and Ormerod, 2003a, Staniforth and Ormerod, 2003b, Laycock et al, 2001, Papurello et al, 2014). It was demonstrated that biogas could provide power equivalent to hydrogen and in particular it proved possible to run SOFCs with a genuinely useful power output at significant lower levels of methane content than is possible with heat engines, which are conventionally used to utilize biogas (van Herle et al, 2004). The AnMBR incorporated in the setup described in this thesis, obviously produces biogas. If this biogas would be used as the stripping agent for stripping the ammonia from the ion exchange brine, this would result in the following two benefits:

I. If ammonia is directly stripped out of the ion exchange brine by biogas as the stripping agent, the distillation tower would be redundant. This would make the complete set-up more compact, robust and energy efficient.
II. Biogas utilization in a SOFC can in theory obtain higher efficiencies than possible in conventional combustion engines (Staniforth and Ormerod, 2003a). Thus, the use of biogas as a stripping agent could not only make

the transformation from organically bound nitrogen and ammonium from wastewater into a fuel more efficient, it could also improve the utilization of the biogas itself. Moreover, a SOFC directly converts the chemical energy of biogas into electricity, which is a wider applicable form of energy than gas. Furthermore, a local and direct utilization of the biogas in a SOFC reduces transport and storage costs.

Literature on ammonia stripping with biogas is limited. The found literature on ammonia stripping using biogas focusses on in-situ or side-stream ammonia removal through biogas stripping with a focus on lowering the ammonia concentration inside anaerobic bioreactors itself (Serna-Maza et al, 2014, Walker et al, 2011). Despite the difference in application between these studies and the proposed implementation of ammonia removal from the ion exchange brine by biogas, the studies of Serna-Maza et al (2014) and Walker et al (2011) demonstrate that biogas stripping of ammonia is effective and that regular stripping kinetics as discussed in chapter 6 apply. This increases the likelihood that ammonia stripping with biogas is feasible and emphasizes the need for research on a combination of anaerobic membrane bioreactors, ion exchange and biogas stripping followed by a solid oxide fuel cell. Appendix 11.2 shows a quick indicative calculation on the potential power production that could be achieved if a combination of an AnMBR, ion exchange column, biogas stripping and SOFC would be implemented at a scale comparable with Harnaschpolder (Defluent, 2014). Further research is required to enable a combined and integrated electricity production, through the removal of organically bound nitrogen, ammonium and organic matter out of sewage using biogas stripping. Within this research, a focus is required on assessing the need for pre-treatment of the biogas before the biogas can be used as a stripping agent.

12 CONCLUSION

This thesis is a proof of principle for electricity production using nitrogen from sewage as a fuel, while meeting the discharge regulations for the total nitrogen concentration.

It was shown that an AnMBR can convert 86% of the total nitrogen content of sewage into ammonium ions through the process of anaerobic digestion. During the anaerobic digestion, 82% of the COD content of the sewage was removed and biogas was produced. Ion exchange was used for the production of an effluent with a low ammonium concentration (< 4 mg TN/L) that amply meets the nitrogen discharge standards (10 mg TN/L). A fractionized collection of the ion exchange brine was applied, which resulted in a concentrated ammonium solution with a high nitrogen recovery. The ammonium ions have been converted into ammonia and further concentrated using a distillation tower. The produced gas mixture of ammonia and water vapor was fed as a fuel to a solid oxide fuel cell that generated electricity.

Considering the nitrogen recovery, the weakest link of the applied combination of technologies was the distillation tower. However, the used distillation tower was not functioning adequately. The low nitrogen recovery in the distillation tower resulted in the production a gas mixture of ammonia and water vapor that barely met the minimum ammonia concentration required for power production by a solid oxide fuel cell. Indeed power production proved to be possible utilizing this gas mixture of ammonia and water vapor as a fuel, however the SOFC behaved significantly better when fed with a gas mixture with a higher ammonia concentration.

Since a distillation tower is a widely applied and conventional technology, it is reasonable to assume the possibility of optimizing its design considering the nitrogen recovery and the energy demand. If an optimized and heat integrated distillation tower design is assumed, it is possible to achieve a net electricity production while also meeting the nitrogen discharge standards. If the proposed combination of an AnMBR, an ion exchange column, a distillation tower and a SOFC would be implemented on a scale comparable with the sewage treatment plant Harnaschpolder, an estimated power production of 0,66 kWh/ m^3 of treated wastewater could be achieved.

Yet, for an accurate assessment of the feasibility of the implementation of the combination of an AnMBR, an ion exchange column, a distillation tower and a SOFC, further research is required in the following fields:

1. The integration of the AnMBR, ion exchange, the distillation tower and the SOFC, focusing on heat recovery
2. The combined feeding of ammonia and biogas to a SOFC
3. Other types of waste water as the influent
4. The optimization of ion exchange operations
5. Biogas stripping

The results obtained in this thesis indicate the feasibility of electricity production using nitrogen from sewage as a fuel, while meeting the nitrogen discharge standards.

REFERENCES

American Public Health Association, (2005). Standard methods for the examination of water and wastewater. Washington, D.C.

An, Y., Yang, F., Bucciali, B., & Wong, F. (2009). Municipal wastewater treatment using a UASB coupled with cross-flow membrane filtration. Journal of environmental engineering, 135(2), 86-91.

Bolto, B. A., & Pawłowski, Ł. (1987). Wastewater treatment by ion-exchange. London, Spon.

Bolto, B. A., & Weiss, D. E. (1977). The Thermal Regeneration of Ion-Exchange Resins. Ion Exchange and Solvent Extraction, 7, 221-289.

Booker, N., Cooney, E., & Priestley, A. (1996). Ammonia removal from sewage using natural Australian zeolite. Water science and technology, 34(9), 17-24.

Budzianowski, W., & Koziol, A. (2005). Stripping of ammonia from aqueous solutions in the presence of carbon dioxide: effect of negative enhancement of mass transfer. Chemical Engineering Research and Design, 83(2), 196-204.

Chachuat, B., Mitsos, A., & Barton, P. (2010). Optimal start-up of microfabricated power generation processes employing fuel cells. Optimal Control Applications and Methods, 31(5), 471-495.

Chen, M., Wang, W., Feng, Y., Zhu, X., Zhou, H., Tan, Z., & Li, X. (2014). Impact resistance of different factors on ammonia removal by heterotrophic nitrification–aerobic denitrification bacterium Aeromonas. Bioresource technology, 167(0), 456-461. doi: http://dx.doi.org/10.1016/j.biortech.2014.06.001

Chmielewska-Horvathová, E. (1996). Advanced wastewater treatment using clinoptilolite. Environmental Protection Engineering, 22, 15-22.

Christensen, C. H., Johannessen, T., Sørensen, R. Z., & Nørskov, J. K. (2006). Towards an ammonia-mediated hydrogen economy? Catalysis Today, 111(1), 140-144.

Cook, D. M. (1975). The theory of the electromagnetic field: Courier Dover Publications.

Crittenden, J. C., Trussell, R. R., Hand, D. W., Howe, K. J., & Tchobanoglous, G. (2012). MWH's Water Treatment: Principles and Design. Wiley.

Dahdal, N., Grzetich, D., Jackson, S., & Chadha, S. (1999). Absorption and Sripping. Senior Design CHE 396. NDSS Consulting

Defluent. (2014). AWZI Harnaschpolder Retrieved 16-09-2014, from http://delfluent.nl/plant/awzi_harnaschpolder/

Dekker, N., & Rietveld, G. (2006). Highly efficient conversion of ammonia in electricity by solid oxide fuel cells. Journal of fuel cell science and technology, 3(4), 499-502.

Delft Technology of Technology (2005). Water Treatment: Micro and Ultrafiltration, course manual. Technical University Delft. Delft.

Eaton, A. D., Clesceri, L. S., & Greenberg, A. E. (2005). Standard methods for the examination of water and wastewater American Public Health Association. Washington, DC.

EPA. (2003). Drinking Water Advisory: Consumer Acceptability Advice and Health Effects Analysis on Sodium: United States Environmental Protection Agency.

Eurotherm (1997). Profibus-DP PID Controllers. In E. C. Limited (Ed.), (Vol. 2).

Feynman, R. P., Leighton, R. B., & Sands, M. (2013). The Feynman Lectures on Physics, Desktop Edition Volume I (Vol. 1): Basic Books.

Fournier, G., Cumming, I., & Hellgardt, K. (2006). High performance direct ammonia solid oxide fuel cell. Journal of Power Sources, 162(1), 198-206.

Frijns, J., Hofman, J., & Nederlof, M. (2013). The potential of (waste) water as energy carrier. Energy Conversion and Management, 65, 357-363.

Fuerte, A., Valenzuela, R., Escudero, M., & Daza, L. (2009). Ammonia as efficient fuel for SOFC. Journal of Power Sources, 192(1), 170-174.

Fuller, R. B. (1971). The View from the year 2000. Life Magazine.

Gambhir, R., & Banerjee, D. (1993). Foundations Of Physics (Vol. 2): New Age International.

Green, M., Mels, A., & Lahav, O. (1996). Biological-ion exchange process for ammonium removal from secondary effluent. Water science and technology, 34(1), 449-458.

Greiner, W., Neise, L., & Stöcker, H. (1999). Thermodynamics and statistical mechanics: Springer.

Halling-Sørensen, B., & Jorgensen, S. (1993). The removal of nitrogen compounds from wastewater: Elsevier.

Haralambous, A., Maliou, E., & Malamis, M. (1992). The use of zeolite for ammonium uptake. Water Science & Technology, 25(1), 139-145.

Hedström, A. (2001). Ion exchange of ammonium in zeolites: a literature review. Journal of environmental engineering, 127(8), 673-681.

Heidrich, E. S., Curtis, T. P., & Dolfing, J. (2010). Determination of the Internal Chemical Energy of Wastewater. Environmental Science & Technology, 45(2), 827-832. doi: 10.1021/es103058w

Henley, E. J., Seader, J. D., & Roper, D. K. (2011). Separation process principles: Wiley.

Hwang, Y. L., Keller, G. E., & Olson, J. D. (1992). Steam stripping for removal of organic pollutants from water. 1. Stripping effectiveness and stripper design. Industrial & Engineering Chemistry Research, 31(7), 1753-1759. doi: 10.1021/ie00007a021

Ihringer, R. (2011). 2R-Cell™: A universal cell for an easy and safe SOFC operation. Not published

Jaques, S., & Prahl, S. (1998). Fick's first law of diffusion Retrieved 12-2014, from http://omlc.ogi.edu/classroom/ece532/class5/ficks1.html

Jeager. (1996). Steam Stripper Retrieved 18-9-2014, from http://www.jaeger.com

Jha, V. K., & Hayashi, S. (2009). Modification on natural clinoptilolite zeolite for its NH< sub> 4</sub>< sup>+</sup> retention capacity. Journal of hazardous materials, 169(1), 29-35.

Jørgensen, S. E., Libor, O., Lea Graber, K., & Barkacs, K. (1976). Ammonia removal by use of clinoptilolite. Water Research, 10, 213-224.

Kalló, D. (1995). Wastewater purification in Hungary using natural zeolites. Natural zeolites, 93, 341-350.

Kister, H. Z. (1992). Distillation design (Vol. 223): McGraw-Hill New York.

Kocadagistan, E., & Topcu, N. (2007). Treatment investigation of the Erzurum City municipal wastewaters with anaerobic membrane bioreactors. Desalination, 216(1–3), 367-376. doi: http://dx.doi.org/10.1016/j.desal.2006.10.038

Koon, J. H., & Kaufman, W. J. (1975). Ammonia removal from municipal wastewaters by ion exchange. Journal (Water Pollution Control Federation), 448-465.

Kreuer, K.-D. (2013). Fuel Cells, Introduction. In K.-D. Kreuer (Ed.), Fuel Cells (pp. 1-7): Springer New York.

Langwaldt, J. (2008). Ammonium removal from water by eight natural zeolites: A comparative study. Separation Science and Technology, 43(8), 2166-2182.

Larminie, J., Dicks, A., & McDonald, M. S. (2003). Fuel cell systems explained (Vol. 2): Wiley New York.

Laycock, C. J., Staniforth, J. Z., & Ormerod, R. M. (2011). Biogas as a fuel for solid oxide fuel cells and synthesis gas production: effects of ceria-doping and hydrogen sulfide on the performance of nickel-based anode materials. Dalton Transactions, 40(20), 5494-5504.

Lettinga, G., Van Velsen, A., Hobma, S. W., De Zeeuw, W., & Klapwijk, A. (1980). Use of the upflow sludge blanket (USB) reactor concept for biological wastewater treatment, especially for anaerobic treatment. Biotechnology and bioengineering, 22(4), 699-734.

Leyva-Ramos, R., Monsivais-Rocha, J., Aragon-Piña, A., Berber-Mendoza, M., Guerrero-Coronado, R., Alonso-Davila, P., & Mendoza-Barron, J. (2010). Removal of ammonium from aqueous solution by ion exchange on natural and modified chabazite. Journal of environmental management, 91(12), 2662-2668.

Liao, P., Chen, A., & Lo, K. (1995). Removal of nitrogen from swine manure wastewaters by ammonia stripping. Bioresource technology, 54(1), 17-20.

Liberti, L. (1982). Ion exchange advanced treatment to remove nutrients from sewage. Studies in Environmental Science, 19, 225-238.

Liberti, L., Boari, G., Petruzzelli, D., & Passino, R. (1981). Nutrient removal and recovery from wastewater by ion exchange. Water Research, 15(3), 337-342.

Lin, H., Peng, W., Zhang, M., Chen, J., Hong, H., & Zhang, Y. (2013). A review on anaerobic membrane bioreactors: applications, membrane fouling and future perspectives. Desalination, 314, 169-188.

Liu, H., Ramnarayanan, R., & Logan, B. E. (2004). Production of electricity during wastewater treatment using a single chamber microbial fuel cell. Environmental Science & Technology, 38(7), 2281-2285.

Ma, Q., Peng, R., Tian, L., & Meng, G. (2006). Direct utilization of ammonia in intermediate-temperature solid oxide fuel cells. Electrochemistry communications, 8(11), 1791-1795.

Malovanyy, A., Sakalova, H., Yatchyshyn, Y., Plaza, E., & Malovanyy, M. (2013). Concentration of ammonium from municipal wastewater using ion exchange process. Desalination, 329, 93-102.

McLaren, J. R., & Farquhar, G. J. (1973). Factors affecting ammonia removal by clinoptilolite. Journal of the Environmental Engineering Division, 99(4), 429-446.

Meng, G., Jiang, C., Ma, J., Ma, Q., & Liu, X. (2007). Comparative study on the performance of a SDC-based SOFC fueled by ammonia and hydrogen. Journal of Power Sources, 173(1), 189-193.

Mercer, B., Ames, L., Touhill, C., Van Slyke, W., & Dean, R. (1970). Ammonia removal from secondary effluents by selective ion exchange. Journal (Water Pollution Control Federation), R95-R107.

Metcalf, I., & Eddy, H. (2003). Wastewater engineering; treatment and reuse. Fourth Edition, International Edition, McGraw-Hill, New York.

Minnis, P. (2009). Sources of Nutrients in Wastewater. Retrieved 8-2014 from http://www.ces.ncsu.edu/plymouth/septic3/MinnisNutrientsText.pdf

Mohr, P. J., Taylor, B. N., & Newell, D. B. (2008). CODATA recommended values of the fundamental physical constants: 2006a). Journal of Physical and Chemical Reference Data, 37(3), 1187-1284.

Moritz, P., & Hasse, H. (1999). Fluid dynamics in reactive distillation packing Katapak®-S. Chemical Engineering Science, 54(10), 1367-1374.

Nguyen, M., & Tanner, C. (1998). Ammonium removal from wastewaters using natural New Zealand zeolites. New Zealand Journal of Agricultural Research, 41(3), 427-446.

Ni, M., Leung, M. K., & Leung, D. Y. (2009). Ammonia-fed solid oxide fuel cells for power generation—A review. International Journal of Energy Research, 33(11), 943-959.

Nickels, L. (2007). Wastewater treatment: Energy-efficiency: the future of wastewater. Filtration & Separation, 44(7), 40-42.

Nzila, C. K. (2011). Potential of biogas production from biowaste in Kenya and its contribution to environmental sustainability. Ghent University, Belgium.

O'Hayre, R. P., Cha, S.-W., Colella, W., & Prinz, F. B. (2006). Fuel cell fundamentals: John Wiley and Sons

Olujic, Z., & Kramer, H. J. M. (2001). Introduction to process technology: Delft university of technology.

Ozgun, H., Dereli, R. K., Ersahin, M. E., Kinaci, C., Spanjers, H., & van Lier, J. B. (2013a). A review of anaerobic membrane bioreactors for municipal wastewater treatment: Integration options, limitations and expectations. Separation and Purification Technology, 118(0), 89-104.

Ozgun, H., Ersahin, M. E., Tao, Y., Spanjers, H., & van Lier, J. B. (2013b). Effect of upflow velocity on the effluent membrane fouling potential in membrane coupled upflow anaerobic sludge blanket reactors. Bioresource technology, 147, 285-292.

Papurello, D., Lanzini, A., Leone, P., Santarelli, M., & Silvestri, S. (2014). Biogas from the organic fraction of municipal solid waste: Dealing with contaminants for a solid oxide fuel cell energy generator. Waste Management

Price, R. M. (1997). Distillation, Retrieved 19-08-2014, from http://facstaff.cbu.edu/~rprice/lectures/distill.html#princip

Qianli, M. A., Ranran, P., Longzhang, T., & Guangyao, M. (2006). Direct utilization of ammonia in intermediate-temperature solid oxide fuel cells. Electrochemistry communications, 8(11), 1791-1795.

Rahmani, A. R., & Mahvi, A. H. (2006). Use of ion exchange for removal of ammonium: a biological regeneration of zeolite. Global NEST Journal, 8(2), 146-150.

Salazar-Peláez, M., Morgan-Sagastume, J., & Noyola, A. (2011). Influence of hydraulic retention time on UASB post-treatment with UF membranes. Water Science & Technology, 64(11), 2299-2305.

Sato, N., Okubo, T., Onodera, T., Ohashi, A., & Harada, H. (2006). Prospects for a self-sustainable sewage treatment system: A case study on full-scale UASB system in India's Yamuna River Basin. Journal of environmental management, 80(3), 198-207.

Schweitzer, P. A. (1979). Handbook of separation techniques for chemical engineers: McGraw-Hill New York.

Semmens, M. J., Wang, J. T., & Booth, A. C. (1977). Biological regeneration of ammonium-saturated clinoptilolite. II. Mechanism of regeneration and influence of salt concentration. Environmental Science & Technology, 11(3), 260-265.

Serna-Maza, A., Heaven, S., & Banks, C. J. (2014). Ammonia removal in food waste anaerobic digestion using a side-stream stripping process. Bioresource technology, 152(0), 307-315. doi: http://dx.doi.org/10.1016/j.biortech.2013.10.093

Staniforth, J., and Kendall, K. (1998). Biogas powering a small tubular solid oxide fuel cell. Journal of Power Sources, 71(1–2), 275-277. doi: http://dx.doi.org/10.1016/S0378-7753(97)02762-6

Staniforth, J., and Ormerod, R. M. (2003a). Clean destruction of waste ammonia with consummate production of electrical power within a solid oxide fuel cell system. Green Chemistry, 5(5), 606-609.

Staniforth, J., a nd Ormerod, R. M. (2003b). Running solid oxide fuel cells on biogas. Ionics, 9(5-6), 336-341. doi: 10.1007/bf02376583

Steele, B. C. H., & Heinzel, A. (2001). Materials for fuel-cell technologies. [10.1038/35104620]. Nature, 414(6861), 345-352.

STOWA (Stichting Toegepast Onderzoek Waterbeheer (1995). Behandeling van stikstofrijke retourstromen op rioolwaterzuiveringsinrichtingen- praktijkonderzoek aan lucht en stroomstrip installaties bij de RWZI in Utrecht. Utrecht; Zoetermeer: STOWA

Sulzer. (2013). Structured Packings for distillation, absorption and reactive distillation. In S. c. Sulzer Chemtech Ltd (Ed.). Switserland.

Torre Gutiérrez, L. d. l. (1999). Ammonium Removal from Municipal Wastewater by Ion Exchange. Msc, Technical University Delft, Delft.

Van Dijk, J., & Braakensiek, H. (1984). Phosphate removal by crystallization in a fluidized bed. Water Sci. Technol, 17, 133-142.

Van herle, J., Membrez, Y., & Bucheli, O. (2004). Biogas as a fuel source for SOFC co-generators. Journal of Power Sources, 127(1–2), 300-312. doi: http://dx.doi.org/10.1016/j.jpowsour.2003.09.027

van Lier, J. B. (2008a). High-rate anaerobic wastewater treatment: diversifying from end-of-the-pipe treatment to resource-oriented conversion techniques: IWA Publ.

Van Lier, J. B., Mahmoud, N., & Zeeman, G. (2008b). Anaerobic wastewater treatment. Biological Wastewater Treatment.

Verkerk, J. M. (2003). Ionenwisseling voor stikstofverwijdering uit afvalwater: STOWA, Stichting Toegepast Onderzoek Waterbeheer.

Verkerk, J. M., & van der Graaf, J. H. J. M. (1999). Ammonium removal by ion exchange: Interactions between regeneration and brine treatment. Delft: Dept. of Sanitary Engrg., Facu. of Civ. Engrg. and Geoscience, Delft University of Technology.

Walker, M., Iyer, K., Heaven, S., & Banks, C. J. (2011). Ammonia removal in anaerobic digestion by biogas stripping: An evaluation of process alternatives using a first order rate model based on experimental findings. Chemical Engineering Journal, 178(0), 138-145. doi: http://dx.doi.org/10.1016/j.cej.2011.10.027

Wang, J. (2011). Fundamentals of Classical Thermodynamics: Springer.

Wojcik, A., Middleton, H., and Damopoulos, I. (2003). Ammonia as a fuel in solid oxide fuel cells. Journal of Power Sources, 118(1), 342-348.

Xie, K., Ma, Q., Lin, B., Jiang, Y., Gao, J., Liu, X., & Meng, G. (2007). An ammonia fuelled SOFC with a BaCe0.9Nd0.1O3−δ thin electrolyte prepared with a suspension spray. Journal of Power Sources, 170(1), 38-41. doi: http://dx.doi.org/10.1016/j.jpowsour.2007.03.059

Zamfirescu, C., & Dincer, I. (2008). Using ammonia as a sustainable fuel. Journal of Power Sources, 185(1), 459-465.

Zhang, F., Ge, Z., Grimaud, J., Hurst, J., & He, Z. (2013). Long-term performance of liter-scale microbial fuel cells treating primary effluent installed in a municipal wastewater treatment facility. Environmental Science & Technology, 47(9), 4941-4948.

Appendix 3.1

TABLE OF CONTENTS

Appendix 3.1

APPENDIX 3.1 DATA FILE ULTRA FILTRATION UNIT

Norit X-Flow
leading in purification

CAPFIL ULTRAFILTRATION MEMBRANE

UFC M5 LE

BASIC CHARACTERISTICS

- Hydrophilic polyethersulfone membrane
- Capillary membrane available in 0.8 and 1.5 mm
- Structure asymmetric/microporous
- Developed for inside-out filtration
- Developed for use in large-scale processes for water purification
- High performance and a very good anti-fouling behaviour
- Membrane elements can be backflushed for efficient membrane cleaning

APPLICATIONS

- Pre-treatment RO and NF
- Surface water
- Drinking and process water production
- Recovery of sandfilter backwash water
- Waste water treatment

MEMBRANE COMPOSITION

- Hydrophilic membrane composed of a blend of polyvinylpyrrolidone and polyethersulfone (patented)
- M5: Contains glycerine for pore protection and bisulfite for prevention of microbiological growth

PERFORMANCE DATA

parameter	unit	UFC M5	remarks
Transmembrane pressure	kPa	-300....+300	
pH feed		2 - 12	
Chlorine exposure	ppm.h	250000	500 ppm max. at 0 - 40 °C
Temperature	°C	1 - 30	

Operation of membranes at any combination of maximum limits of pH, concentration, pressure or temperature, during cleaning or production, will severely influence the membrane lifetime.

X-FLOW

CAPFIL MEMBRANE PRODUCTS

X-Flow CAPFIL membranes are only available as complete membrane modules. A product code consists of a combination of the membrane type (Table 1) and the module type (Table 2).

Table 1		CAPFIL MEMBRANES (0.8, 1.5 mm)			
Duty		MF		UF	NF
Membrane type		MF02 M2	MF05 M2	UFC M5	NF50 M10
Available internal diameter	[mm]	1.5	1.5	0.8/1.5	1.5
Membrane material		hydrophilic PES/PVP blend (patented)			Comp.
Max. pore size	[µm]	0.2	0.5		
MWCO(*)	[kDa]			200	
Rejection:					
NaCl	[%]				35±5
Mg SO_4	[%]				94±2
Max. pressure	[kPa]	300	300	300	700
Max. temperature (**)	[°C]	80	80	80	40
pH feed		2-12	2-12	2-12	4-10
PES: polyethersulfone PVP: polyvinylpyrrolidone		Comp.: thin film polyamide/polyethersulfone composite			

(*) *On dextranes*
(**) *Maximum temperature of operation is determined by the module used. See module technical datasheet for more information.*
M2: moderate hydrophilic, for food and beverage applications.
M5: moderate hydrophilic and treated with glycerine for pore protection (for UF capillary only).
M10: polyamide coating.

NOTES:
1. For further information, see membrane and module technical datasheets.
2. Final maximum operating limits are determined by the lowest values of the membrane and module pressure and temperature specifications.
3. It is not advisable to operate a membrane module at any combination of the maximum limits of pH, concentration, pressure, or temperature, during cleaning or production; doing so will severely influence the membrane lifetime.
4. The product code is composed as follows (for example):
   - S-225 FSFC PVC module
   - 1.5 mm moderate hydrophilic ultrafiltration membrane gives:
   - Module type S-225 FSFC PVC 0.8 UFC M5

150704

CAPF-ALL-0429
(replaces: CAPF-ALL-0368)

Table 2	CAPFIL PRODUCTS (0.8, 1.5 mm)				
Module type	Length [m]	Diameter [inch]	Membrane ID [mm]	Membrane area [m^2]	Available housing materials
S-30 FSFC	1	4	0.8	6.2	PSU
S-30 FSFC	1	4	1.5	3.6	PSU
S-225 FSFC	1.5	8	0.8	35	PVC
S-225 FSFC	1.5	8	1.5	20	PVC
SXL-225 FSFC	1.5	8	0.8	40	PVC
Insert type	Length [m]	Diameter [inch]	Membrane ID [mm]	Membrane area [m^2]	Available housing materials
R-100(*)	1	6	1.5	9.3	Stainless steel
S-30 FSFC	1	4	0.8	6.2	PSU
S-30 FSFC	1	4	1.5	3.6	PSU
S-225 FSFC	1.5	8	0.8	35	PVC
S-225 FSFC	1.5	8	1.5	20	PVC
SXL-225 FSFC	1.5	8	0.8	40	PVC
PSU : polysulfone			Stainless steel : AISI 316		
PVC : polyvinyl chloride					

(*) R-100 is also available as refill

The maximum allowable temperature for a PVC module housing is 40°C, for a PSU one 60°C and for a stainless steel one 80 °C.

For more information please write or call to:

X-Flow B.V.
P.O.Box 739
7500 AS Enschede
The Netherlands

Phone: + 31 (0)53 4287350
Fax: + 31 (0)53 4287351
E-mail: info@xflow.nl
Web site: www.x-flow.com

CAPF ALL 0429

Appendix 3.2

APPENDIX 3.2 COD BALANCE

COD Balance

Theory

Total C

Partly reduced (CH4)

Partly oxidized (CO2)

Actual production lower then theoretical due to:

- Limited biodegradability
- Part of organic matter used for cell growth
- Possible presence of alternative electron acceptors
- High solubility of CO2/HCO3 in the water fraction (influences ratio CO2/CH4, not CH4 production)

COD influent = CODeffluent + CODsludge + CODgas+ CODretained?

COD influent:

COD solids

COD colloidal

COD soluble

COD effluent:

COD soluble organic

COD soluble inorganic (e.g. H2, S)

COD dissolved reduced gases

COD solids

COD gas

COD CH4

COD H2S

COD H2

COD sludge

COD entrapped solids

COD newly grown biomass

COD entrapped

Appendix 3.2

COD balance

COD influent		
Influent COD	530	mg/L
Influent COD/day	14840	mg/day
COD effluent		
effluent COD	60	mg/L
effluent COD/day	1680	mg/day
COD biogas		
gas production	1,86	L/day
biogas %	80	%
1 mol CH_4:	2	mol O_2
22.4 liter (STP) CH_4:	64	g O_2/ g COD
1 l CH_4:	2,86	g COD
1 g COD	0,35	L CH_4 (STP)
CH4 production	1,4904	L/d
g COD required	4258,29	mg COD/day
COD sludge yield		
sludge yield (in percentage of COD in)	10	%
sluge yield (COD/day)	1484	
Balance		
CODin - CODeff -CODgas - CODsludge	7417,71	mg COD
percentage of COD in	49,99	%
methane yield	0,11	(L CH_4/g COD removed)

Appendix 4.1

APPENDIX 4.1 TYPES OF ION EXCHANGERS AND THEIR PROPERTIES

Two types of ion exchangers can be found: zeolites and organic resins. Zeolites are either won out of natural resources (mines) or artifically produced. Resins are always artificially produced. Resins are made up of a polymeric network with sulphonic acid or carboxylic acid groups. On these groups are were the actual ion exchange would take place. The selectivity of these resins is based on the electrostatic attraction of ions. In the following paragraphs, the main properties of zeolites and orgnaic resins are discussed. Shortly, alternative ion exchangers are mentioned as well.

ZEOLITES

Both natural and synthetic zeolites are inorganic ion exchangers. The first type is find as a mineral in the earth's crust, the second type is produced artificially. The structure of the natural and the synthetic zeolites is basically the same (Verkerk, 2003)

A Zeolite is a mineral, built up from hydrated aluminosilicates. As can be seen in figure 1, the basic structure of zeolites is very regular and forms a aluminosiliciummatrix. The matrix is made up out of silicium- and aluminiumtetrahedrons. This means that every silicium- or aluminiumatom is surrounded by four oxygen-atoms, and that each oxygen-atom is being shared by two tetrahedra (Verkerk, 2003).

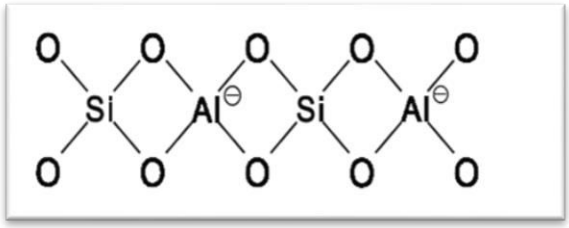

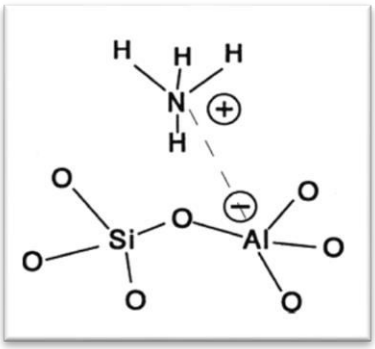

Figure 1.Basic chemical structure of zeolites Figure 1.2 adsorption of an ammonium ion to the zeolite matrix (Adapted from Teunissen, 1994)

Because some of the the silicium-atoms (Si_4^+) are replaced by aluminium-atoms (Al_3^+), negatively charged 'sites' can arise. This negatively charged sites have to be 'filled' by positively charged mono- or divalent cations or watermolecules. These cations and water molecules are lossely connected to the matrix, and can therefore take part in the ion exchange process (see figure 1.2). A divalent ion occupies the sites of two monovalent ions.

The silicium-aluminium molratio (Si/Al) of natural zeolites ranges between 1 and 6, while synthetic zeolites can have a ratio up to 100 (Verkerk, 2003). The smaller the ratio, the more 'sites' are available for ion exchange. This influences the ion exchange characteristics of the zeolite, like the ion exchange capacity and the selectivity. The total capacity increases with a lower Si/Al-ratio (Verkerk, 2003). At the same time, however, the sites will get to lie closer to each oter. As a result of the electrostatic forces, some of these 'sites' will loose there ability to be filled. The rate of this effect differs significantly per ion.

The most commonly encountered cations attached to zeolites are sodium, potassium and calcium. However, research over the past 30 years has shown that specific types of zeolites have a high cation-exchange capacity and selectivity for ammonium (Verkerk, 2003, Malovanyy et al ,2013, Nguyen and Tanner, 1998, Leyva-Ramos et al, 2010, Langwaldt, 2008). The selectivity of ion exchange with zeolites revolves around the concept of 'molecular sieving'. Zeolites have a very high pore volume and thus a large surface area. The small pores inside the zeolites essentially all have nearly uniform size. Because of the uniform dimensions of the pores, ions with more or less the same dimensions are able to penetrate the pores of the zeolite. Ammonium ions in water have a smaller diameter compared to most other ions, and are therefore able

to easily enter the matrix of the zeolites. This partly explains the selectivity of for example the zeolite Clinoptilolite for ammonium, considering that the pore diameter of clinoptilolite is 4 Ångströms (see table 1.1). (Verkerk, 2003). Table 1 is slightly misleading, since it is showing the size of the ions in water. In crystal structures, ions have a diameter around 1 Ångström. They are bigger in water, because they are surrounded by a shell of water molecules. This shell of water molecules makes it difficult for the ion to enter and needs to be divested first, which delays the exchange process. The ions with the thinnest shell enter the fastest. The thickness of the water shell is dependent on the valence of the ion. A larger loading will result in a thicker watershell. Since the low valence of amonium, ammonium has a relatively thin watershell, and has a comparative advance over other ions in the ion exchange process using a zeolite with a small pore size (Verkerk, 2003). Thus, ammonium has a twofold advantage in terms of selectivity of zeolites, it's small size and its low valence.

Table 1: effective ion-radius in water solutions (Dean, 1992 via Verkerk, 2003)

Radius in Angstroms (Å)	Cation
2,5	NH_4^+, Cs^+
3	K^+, Cl^-, NO_3^-,
3,5	OH^-
4	Na^+, HCO_3^-, SO_4^{3-}, PO_4^{3-}
4,5	$Pb2^+$, CO_3^{2-}
5	Sr^{2+}, Ba^{2+}, Ra^{2+}, Cd^{2+}, Hg^{2+}, S^{2-}
6	Li^+, Ca^{2+}, Cu^{2+}, Zn^{2+},Fe^{2+}, Ni^{2+}
8	Mg^{2+}
9	H^+, Al^{3+}, Fe^{3+}, Cr^{3+}
11	Th^{4+}, Ce^{4+}, Sn^{4+}

Another mechanism that can explain the preference of natural zeolites for monovalent ions, is the distance between the exchange sites in the crystal structure. Because the negatively charged sites are all monovalent, multi-valent ions can only exchange and 'occupy' several negetively charged sites as long as the electro-neutrality is guaranteed. This means that the negatively charged sites have to be located close to each other. On zeolites with a higher Si/Al-ratio, the anionic sites are generally located further apart compared to zeolites with a lower Si/Al-ratio (in literature this principel is refered to as 'anionic site seperation'). It must be noted that once the sites are located too close, the kations can reject each other, resulting in a loss of practical available sites.

Acids can affect the structure of natural zeolites via de-aluminizing. In an alkaline environment, the original zeolite matrix changes, and so do the ion exchange properties (Verkerk, 2003).

In general, zeolites are assumed to have a life spam of years, as long the pH remains in the range between 5 and 8,5.

ORGANIC RESINS

Organic resins consists of an irregular three-dimentionsal network of polymers which having functional groups, wherein the dissociated ions can attach to. Resins are made by the chemical industry and numerous types are available. Resins can be both cations and anion exchangers. Only organic resins are applicable for ammonium removal from wastewater, and thus 'resin' will always refer to an organic resin in this chapter.

Organic resins used for kation exchange can be divided into strong acid cations (SAC) and weak acid cations (WAC) (Verkerk, 2003). WAC's are made up of acryldivenylbenzeenpolymers, and SAC's consists of styrene-divenylbenzeepolymers. Attached to the polymer-matrixes are functional groups, with exchangeble cations. For SAC's these functional groups contain sulfonic acid-groups, with exchangeble H^+ or Na^+ attached to it (SO_3Na or SO_3H). For WAC's the funcional groups consists of carboxylic acid-groups that can be exchanged (COOH) (see figure 2). The term 'strong acid' means that the

functional group is always completely dissociated, independend of ionic form or pH. While for 'weak acids' the carboxylic-groups of the functional groups are only partly ionized. The forces between the ions are van der Waals-forces and the amount of functional groups determine the ion exchange capacity of the resin (Verkerk, 2003). WAC's have a larger capacity and have a higher selecitvity for NH_4^+-ions compared to SAC's. However, WAC's still prefer H^+ ions above NH_4^+-ions.

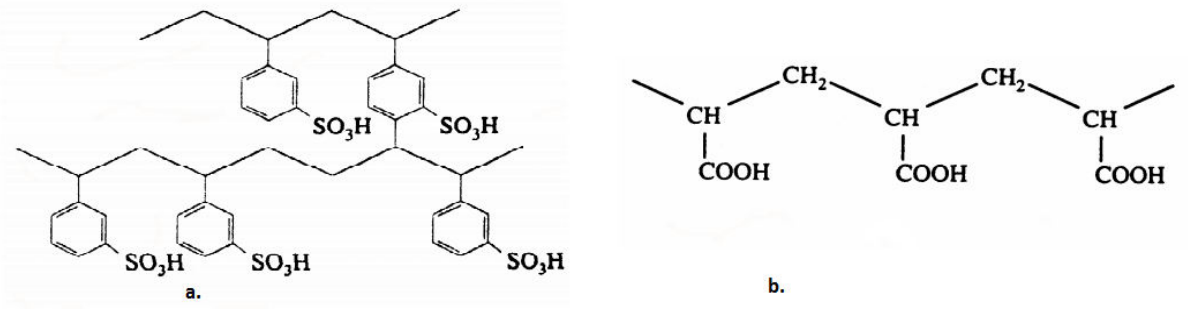

Figure 2: a: Strong acid cation structure and b: Weak acid cation structure (based Verkerk, 2003)

An important parameter of organic resins is the rate of cross-linking (the amount of crosslinks that connect the moleculair chains). The rate of ion exchange to and from resins is highly dependent on the mobility of the ions in solutiotion and mobility of the the exchangeable ions attached to the funcitonal groups. This mobility is dependent of the rate of cross linking of the resin.

A high degree of cross-linking will result in a lower ion exchange capacity. However, a high degree of cross-linking will also ensure the resin to swell less. The swelling of the resin is related to the uptake of water and the hydratation of ions in the resin-structure and the rate of crosslinking determines how much swelling occurs; this can be up to 35% for a WAC. For SACs, this percentage is lower (a maximum of 10%). For the design of an ion exchange installation, it is important to know the expected rate of swelling of the specific resin. When the resins are swollen, the access of the inside of the polymer can get blocked and the resin becomes more fragile.

A rasin can be both macro-porous or gel-type. A gel-type resin is not porous (it does not contain any cavities and channels), and the average distance between the polymers is about 4 nm (Verkerk, 2003). An estimation of the maximal rate of crosslinking is general around 12%. The gel-type is in this case refers to the structure of the resin and not to the consistency (gel-type resins are hard marble-like rounds with a diameter of around 1 mm) (Verkerk, 2003).

Macro-porous resins on the other hand, are designed with pores and channels in order to ease diffusion within the resin. The functional groups are easier to access and thus the exchange rate is higher. Macro-porous resins consist of many crosslinks, and are therefore mechanical stronger then gel-type resins (Verkerk, 2003). Since the macro-porous resins contain real pores, the number of functional groups per gram of resin is lower compared to those of gels. Therefore, macro-porous resins have a lower capacity (Verkerk, 2003). Due to the large pore size (5 nm), macro-porous resins are capable of exchanging large cations easily. The internal surface is calculateble, which is not possible for gel-type resins.

Another difference between macro-porous and gel-type resins is the life expectancy. In general, gel-type resins have a shorter lifespam (weeks) compared to the lifetime of macro-porous resins (years) (Verkerk, 2003). This is primarly caused by the sensitivity for 'cracking'. During the loading and discharging, the resins are exposed to local pressure differences (osmotic shocks). The resins expand in the loading phase and shrink in the regeneration phase, whereby connections break due to inhomogeneneous forces within the matrix (this is referred to as 'cracking'). This happens especially during the first few ion exchange cycli, afterwards it will stabilize. Macro-porous resins are less senstive to cracking than gel-type resins due to the higher rate of crosslinking (8% cracking compared to 78%) (Bolto et al, 1977).

Appendix 4.1

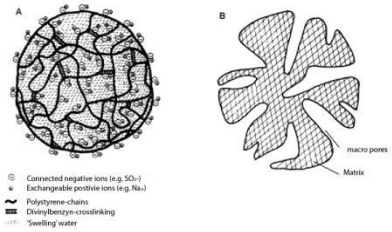

Figure 3 Resin structures. A) gel-type resins, B) macro-porous resins (based on Smolders, 1992)

As opposed to zeolites, molecular sieving of ions hardly plays a role for ion exchange with resins. The pores and openings of the resins are not uniform in size and thus the valence of the ion plays the most significant role for the selectivity of the resins. The selectivity of resins is based on electrostatic attraction of positive ions. The greater the valence, the stronger the appeal (Verkerk, 2003). in a lesser extend, the size of the ions determines the selectivity; the smaller the ion, the more easily it penetrates the network. The preference for smaller ions can also be explained by the internal pressure, smaller ions move more easily thourgh the matrix and cuase less pressure-differences (osmotic pressure differences) (Verkerk, 2003).

Organic resins are bacly resistant to nuclear ionizing radiation and strong oxidizing solutions. When organic resins are brought in contact with concentrated nitric acid, a risk on explosion occurs (Verkerk, 2003). WAC's can only be used at a pH largen than 4.

ALTERNATIVE ION EXCHANGERS

In principle, after chemical treatment al kinds of natural materials that react with sulfuric acid (without dissolving) can obtain ion exchanging properties. However, the chemical stability and exchange capacity are in general inferior in comparision with the meantioned organic resins and zeolites.

The following materials can be treated to have ion exchange capacities:

- Different (stone) coals and clays
- Ground olive stones, coconut shells, nut shells, coffee, teer, paper and cotton (Verkerk, 2003)
- Residual waste products, like combustion snails

There exists also liquid ion exchangers, these are hydrophobic and can be easily mixed with water, without dissolving. However, the phase seperation is difficult and loss of material is the direct result (Verkerk, 2003).

THE INFLUENCE ON WASTE WATER ON ION EXCHANGE PROPERTIES

The characteristics of in exchangers can be influenced by the surrounding conditions. In order to choose the most suitable type of ion exchanger for seperating and concentrating the ammonium in the AnMBR effluent and for concentrating this ammonium, it is important to know how the ion exchanger will behave if it is brought in contact with pre-treated wastewater.

Important mechanical properties of ion exchangers are mechnical robustness and resilience against wear and fouling (pollution with organic compounds, which influences the life spam of the ion exchanger). The ion exchanger can suffer from wear due to abrasion of the grains against each other, which will especially happen in systems with a fluidized or moving bed, or in systems where the ion exchanger is pumped around. Granules can also be crushed by valves. The wearing of the ion exchanger can cause an increased turbidity in the effluent and ofcourse a loss of material. The hydraulic properties of an ion exchange bed are similar to those of rapid filtration. When a small grain diameter is used, the resistance over the bed can increase, ultimately resulting in the crushin of grains. The flow rate needs to be adapted to the maximal head loss over the bed (Verkerk, 2003).

The rate of wearing is not equal for all types of ione exchangers. In literature wearing is barely mentioned, however, according to Verkerk (2003) wearing is neglectable for natural zeolites. According to Verkerk (2003), resins do not suffer significantly from wear as well, although they can crumble due to internal forces (as described in 1.2.2).

Appendix 4.1

Organic material in the feed can pollute the ion exchanger, this mechanism is called fouling. Humic acids, fatty acids and oil-like compounds can be adsorbed to the ion exchanger and can be difficult to remove during backwashing. These organic compounds are anionic, and in general they are more harmfull by anion exchange compared to kantion exchange (ammonium exchange is kation exchange). Fouling can cause a delayed rate of exchange, a decreased ion exchange capacity, clotting of the bed, canal formation and leakage (Verkerk, 2003). Zeolites affected by fouling can be 'burned clean' at high temperatures. Polluted resins can be thoroughly cleaned with chemicals (like a strong base). The risk on fouling depends highly on the influent and there is no significant difference between resins and zeolites found in literature.

Appendix 4.2

APPENDIX 4.2 CHARACTERISTICS OF THE ION EXCHANGERS

Characteristics of the ion exchangers (as supplied by the supplier)			
	Chabazite	Clinoptilolite	Clinoptilolite (thermally pre-treated)
Brand name	Bowie Chabazite	Natural Zeolite	Ash Meadows Clinoptilolite
Supplier	St. Cloud	Zeolite Products (NL)	St.Cloud
Country of Origin	USA	Indonesia	USA
Color	Light Brown	Green	Dark Brown
Chemical name	Anhydrous Sodium Aluminosilicate	Hydrated Calcium Aluminosilicate	Hydrous Sodium Aluminosilicate
Type	Natural Herschelite-Sodium Chabazite	Natural Clinoptilolite	Natural Clinoptilolite with thermal pre-treatment
Composition	(Ca Na K)Al4 Si8 O24 .13H2O	(Ca,K2,Na2,Mg)4Al8Si40O96 .24H2O	-
Si/Al ratio	approx 4:1	4,8-4,5	-
Selectivity	$Tl^+ > CS^+ > K^+ > AG^+ > RB^+ > NH_4^+ > PB^{2+} > Na^+ = BA^{2+} > SR^{2+} > CA^{2+} > LI^+$	$Cs^+ > NH_4^+ > Pb2^+ > K^+ > Na^+ > Ca^{2+} > Mg^{2+} > Ba^{2+} > Cu^{2+,} Zn^{2+}$	-
Form	Granules	Granules	Granules
Effective diameter pores (nm)	0,43	0,4	0,4
Total capacity (meq/g)	2,5	1,2	1,85
Total capacity (mg NH4+-N/g)	35	16,8	25,9
Operational Capacity (breakthrough of 1 mg NH4/L) (mg NH4/ g zeolite)	4 (STOWA, 2001)	6 (Nguyen and Tanner, 1998)	not known
Packing Density (kg/m3) (approx)	550	934	1603
mesh size (mm)	1 x 0,5	0,3 - 1	1 x 0,5
Uniformity coefficient			
Stability (ph range)	3-5	6 - 7	3-5

Appendix 4.3

APPENDIX 4.3 LOADING PARAMETERS ION EXCHANGE

This appendix describes the loading parameters which are not described in chapter 4.2.2.1

LOADING PARAMETER 2: FLOW RATE THROUGH THE COLUMN

Table 1 shows some flow rates (in BV/h) found in literature, plus the details of the specific study. The main conclusion that can be drawn reads that it is difficult to compare studies due to different researched parameters. It would be usefull to compare studies with corresponding influent ammonium concentrations, for differences is flow rate, operational capacities and treated bed volumes before (a corresponding) break through is reached. Since a significant part of the mentioned data is not available, this is unfortunately not possible.

However, a few primary conclusions can be drawn based on table 1. Firstly, a higher flow rate leads to a significant decrease in bed volumes before break through is achieved i.e. ammonium leakage occurs earlier. This is quite logical since the exchange front is more disperse, so leakage is more likely to happen compared to a very sharp exchange profile related to a small flow velocity. Also, a higher influent flow rate results in a larger absolute ammonium influent, also resulting in a faster satisfaction of the zeolite bed and a consequentual faster occuring break through of amonnium.

Table 1: found flow rates in literature, with other study details

Source	**Ammonium Concentration Influent**	**ion exchanger**	**flow rate**	**Operational Capacity**	**Break through**	**Treated BVs before breakthrough**
	[mg NH_4-N/L]	[-]	[BV/h]	[mg/g]	[mg NH_4-N/L]	[-]
Verkerk (2003)	50	Chabazite	5 10	9,7 9,1	1	70 55
McLaren et al (1973)	70	Clinoptilolite	6 13	- -	2	84 70
Green et al (1996)	40	ChabazIte	10 20	- -	2	76 49
Jorgensen et al (1976)	25 38	Clinoptilolite	6 6	0,56 1,26	- -	- -
Booker et al (1996)	50	Clinoptilolite	7 15	- -	2	75 23
Liberti et al (1982)	40	Clinoptilolite	15	-	-	-
Liberti et al (1981)	28	Clinoptilolite	24	-	-	-
Koon et al (1975)	20	Clinoptilolite	10 - 15	-	-	-

Appendix 4.3

LOADING PARAMETER 3: THE REQUIRED EFFLUENT CONCENTRATION OF AMMONIUM (THE BREAK-THROUGH POINT)

The loading process can be shown by a breakthrough curve (figure 1). The break-through curve shows the ammonium concentration in the effluent of the ion exchange bed, against bed volumes that have passed the ion exchange bed (considering ion exchange, usually time is shown in terms of 'bed volumes that passed the ion exchange volume' instead of 'minutes'. This makes it possible to compare ion exchange beds that have been operated under different flow velocities).

The breakthrough point is a fixed (chosen) point, defining the allowable concentration of ammonium in the effluent. A posible break-through point is 0, meaning that no outflow of ammonium is tolerated. In figure 1, this would mean a required regeneration after 40 bedvolumes of loading (after 40 bed volumes have passed the ion exchange bed, leakage starts to occur). The breakthrough point can also be set on C/C_0 =0,1. In figure 1 this would mean a required regerenation after 80 bedvolumes (to be able to compare different ion exchange set-ups, often volume is referred to as the bed volume of the specific exchanger. So when a zeolite bed of 500 ml is used, 80 bedvolumes would refer to 40 liter of influent). The breakthrough capacity, is the capacity at the moment that the set break-through point is reached in the effluent. The break-through capacity is lower then the total capacity of the ion exchanger (Verkerk, 2003).

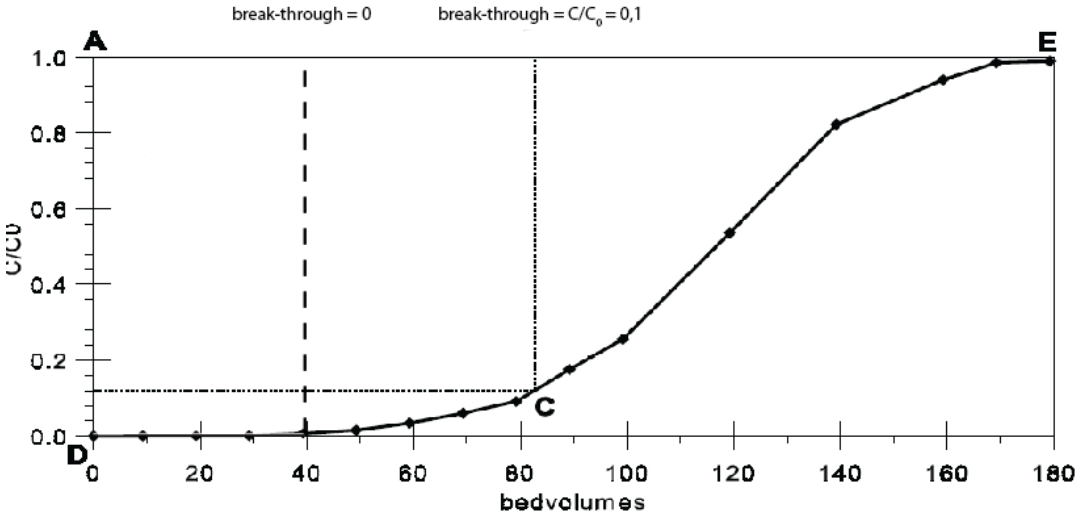

Figure 1: schematical display of a breakthrough curve (based on Verkerk, 2003). For the break-through point C/C0= 0,1, the break-through capacity is shown by ABCD, while the total capacity is shown by AECD.

LOADING PARAMETER 4: THE SIZE OF THE ION EXCHANGE GRAINS

As described in the chapter on ion exchane kinetics, a smaller grainsize corresponds to a larger rate of ion exchange, but also an increase in head loss over the bed. Jorgensens et al (1976) did an empirical study on the effect of the grain size, and came up with the following graph in order to prove the kinetics. It can be seen that a smaller grain size does not only result in a quicker exchange rate, but also a higher exchange capacity. This is also proven by Booker et al (1996).

However, a smaller grain size will also result in a higher head loss over the bed. This increased pressure can lead to prematurely interruption of the loading process (Verkerk, 2003). Moreover, the grains can break due to forces exerted when they collide.

Appendix 4.3

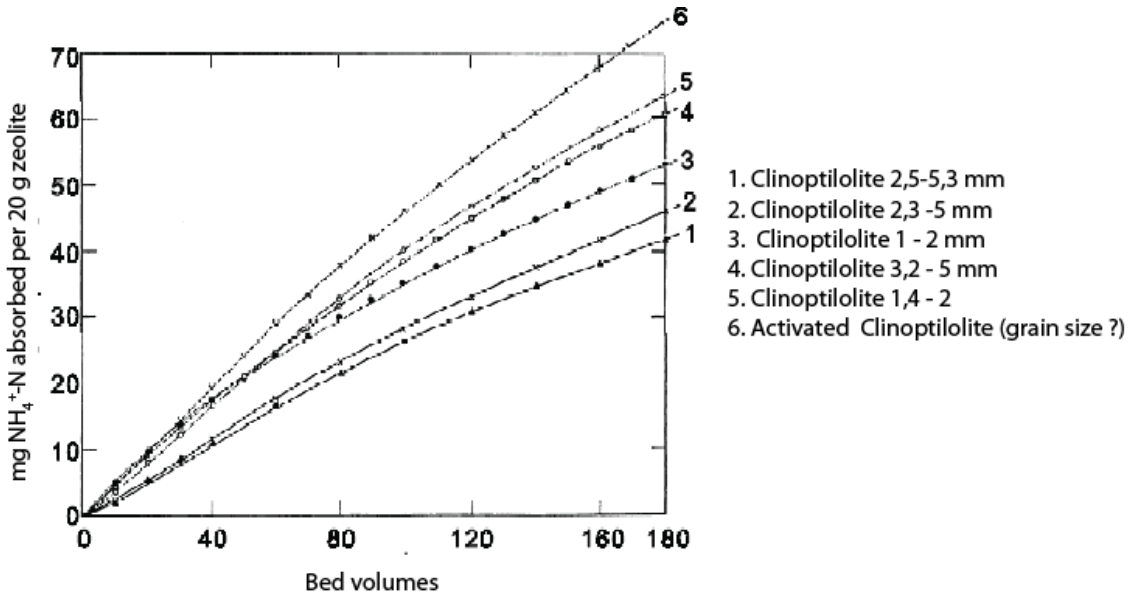

Figure 2: the influence of a smaller grain size on the exchange rate and capacity (Jorgensens et al, 1976).

Natural zeolites are available in a range of grain sizes (1 – 3 mm is regular). Resins have a fixed grain size; ca 0,5 mm. Synthetic zeolites can occur as powders, but can also be pressed into grains (1 – 1,5 mm). (Verkerk, 2003)

LOADING PARAMETER 5: FEED CHARACTERISTICS (PRESENCE OF COMPETING IONS)

The ammonium concentration of the feed has a significant influence on the exchange capacity on ion exchangers, larger than the flow rate and the temperature (Verkerk, 2003). According to McLaren et al, 1973, increasing the ammonium concentration of the feed from 17 to 70 mg NH_4-N/L, leads to doubling of the operational capacity. However, a high ammonium feed concentration results in a more frequent required regeneration. According to Verkerk (2003), this will make the use of ion exchange for solutions with high ammonium concentrations (> 70 mg NH_4-N/L) undesirable.

The ammonium concentration of Dutch municipal waste water is approximately 50 mg NH_4-N/L. Compared to other countries this is a high value (Verkerk, 2003). The relatively high consumption of meat and dairy products might be an influencing factor.

Municipal waste water contains all sorts of organic and inorganic compounds. Table 2 gives an overview of typical compositions of untreated municipal wastewater.

Table 2: Typical compositions of untreated municipal waste water

(Adapted from Metcalf and Eddy, 2004)

Contaminants		Unit	Weak	Medium	Strong
Total Solids (TS)		[mg / L]	350	720	1200
Total Dissolved Solids (TDS)		[mg / L]	250	500	850
	Fixed	[mg / L]	145	300	525
	Volatile	[mg / L]	105	200	325
Suspended Solids (SS)		[mg / L]	100	220	350
	Fixed	[mg / L]	20	55	75

Appendix 4.3

	Volatile	[mg / L]	80	165	275
Settleable solids		[mg / L]	5	110	20
BOD5 (20 degrees)		[mg / L]	110	220	400
Total Organic Carbon (TOC)		[mg / L]	80	160	290
Chemical Oxygen Demand (COD)		[mg / L]	250	500	1000
Nitrogen (Total N)		[mg / L]	20	40	85
	Organic N	[mg / L]	8	15	35
	Free Ammonia	[mg / L]	12	25	50
	Nitrites	[mg / L]	0	0	0
	Nitrates	[mg / L]	0	0	0
Phsopheros (Total P)		[mg / L]	4	8	15
	Organic P	[mg / L]	1	3	5
	Inorganic P	[mg / L]	3	5	10
Chlorides		[mg / L]	30	50	100
Sulfate		[mg / L]	20	30	50
Alkalinity (as CaCO3)		[mg / L]	50	100	200
Grease		[mg / L]	50	100	150
Total Coliform		CFU 100/ml	10^6-10^7	10^7-10^8	10^8-10^9
Volatile Organic Compounds (VOC)		[mg / L]	<100	100-400	>400

Factors that are negatively influencing the ion exchange process are turbidity, presence of suspended solids, strong acids and competing anions.

The installation described by this thesis, municipal waste water is fed to an anaerobic digester firstly and afterwards led over an UF membrane**,** before coming in contact with the ion exchanger. Therefore, problems with turbidity or high suspended solids are not at issue.

Compounds that are considered as a problem for the ion exchange process are competing cations. Cations are, like ammonium, not held by the membrane and thus will they be present in the feed for the ion exchange. The main present compounds are Calcium (Ca_2^+), Sodium (Na^+),Magnesium (Mg_2^+) and Potassium (K^+).

It is difficult to get an idea of the average cation composition of pre-treated municipal wastewater, since it differs so much per situation and pre-treatment and it is not often analyzed. Just for the sake of an impression, de la Torre (1999) examined the composition of pre-treated wastewater in Berker, the Netherlands (the pre-treatment consisted of sedimentation, nitrification-denitrification and post-sedimentation). The conclusion that can be drawn is that significant cation competition can be expected once ammonium is removed from wastewater. The composition showed in table 3 is comparable to the expected composition of the used AnMBR effluent.

Table 3: Cation composition pre-treated municipal wastewater (de la Torre, 1999)

Cation	[mg/L]
Potassium (K+)	19
Sodium (Na+)	74
Calcium (Ca2+)	106
Magnesium (Mg2+)	14

The presence of competing cations can be expressed as the cation strength. The cation strength basically refers to the sum of the present cation concentrations multiplied by their valences. Koon et al (1975) showed the decrease in ion exchange capacity due to an increasing cation strength of the influent. The ion exchange capacity of the zeolite Clinoptilolite for ammonium was tested for multiple influents with different cation strength, but corresponding ammonium concentrations. The capacity for ammonium exchange decreased significantly due to a higher cation strength. This negative reaction can be explained by the selectivity of zeolites for ammonium. In principle most used ion exchangers for ammonium removal have an affinity for absorbing ammonium (a high selectivity for ammonium). Figure X shows the selectivity-coefficient (expressed as α) for ammonium compared with concentrations of sodium, calcium and magnesium for Clinoptolite. The graph shows that Clinoptilolite is selective for ammonium (α>1) with respect to all other cations, except for potassium.

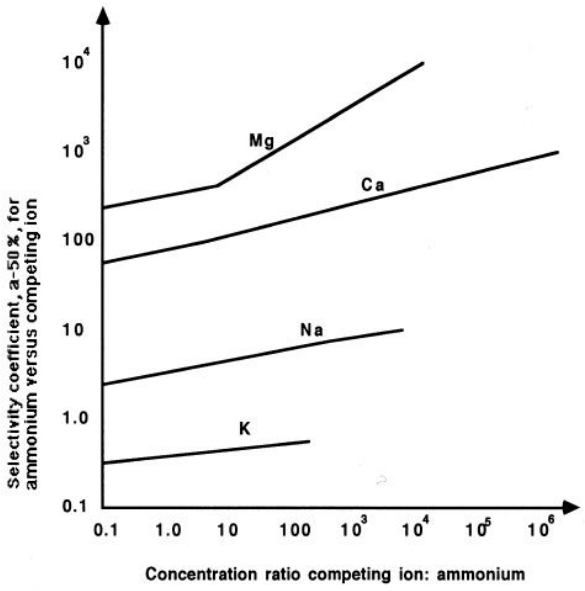

Figure 3: Selectivity coefficient for ammonium in competition with potassium, natrium, calcium and magnesium (Verkerk, 2003)

However, a larger availability of other competings cations will undermine this selectivity, since more exchange-spots will be taken by other cations. This is reversely showed in figure 3, a higher ammonium concentration results in a higher selectivity for ammonium. This negative relation between ion exchange capacity and cation strength of the influent is shown only for the total capacity, but also applies to the operational capacity (Verkerk, 2003). The selectivity for ammonium differs significantly between types of ion exchangers and thus also the sensitivity for competition with other cations is very dependent on the used type of ion exchanger.

Appendix 4.3

LOADING PARAMETER 6: THE DEPTH OF THE ION EXCHANGE BED

A larger depth of the ion exchange bed (thus a larger absolute volume of ion exchanger) results in an increasing total exchange capacity. The minimal required bedvolume can be calculated using the measured/obtained operational capacity of the ion exchanger and the to-be-removed volume of ammonium.

When an ion exchanger with a strong selecitvity for ammonium is used, the ion exchange front will have a sharp profile. However, in the case of ion exchangers with a low selectivity for ammonium, the ion exchange front will be more dispersed. When using an ion exchanger with a low selecitivity for ammonium, it is advisable to rather over-design the required ion exchanger volume to avoid breakthrough (Verkerk, 2003).

A deeper bed results in a larger head loss. High resistance leads to low productivity or high flow velocities and un-uniform flow patterns. In practice, the ion exchange bed heights vary between 0,8 and 6 meter for zeolites and between 1 to 3 meter for resins (Schweitzer, 1997). At laboratorium scale, generally bed heights of 20 to 30 cm are used (with a column diamater around ø 2,5 to 3, 5 cm). Attention must be paid to not choose a too small column diameter, to prevent wall effects. Wall effects have a significant influence once the diameter of the column is less than 30 times the grain size of the ion exchanger (Verkerk, 2003).

LOADING PARAMETER 7: PH

The ionic form of (mainly resins) is depending on the pH, as well as the configuration of the kations. With a low pH, a competition occurs between ammonium and hydrogen ions. At a high pH, the ammonium will transform into ammonia. It is not possible to remove nitrogen in the from of ammonia using ion exchange. Koon et al (1975) did column tests for similar cation composition of the influent and differing pH. Between a pH of 4 and 8 the highest ammonium exchange capacities were measured, with an optimum of 6. The ion exchange capacity decreased significantly with a pH of 6.

A pH outside the 4 – 8 range will damage the cristal matrix of zeolites irreversibly. Resins are not damaged by high or low pH values.

LOADING PARAMETER 8: TEMPERATURE

In theory, the temperature of the influent affects the ion exchange equilibrium and the exchange kinetics. According to McLaren et al (1973), a low temperature will result in a higher exchange capacity when the selectivity for ammonium is large. For exchangers with a low selectivity, this is not observed. McLaren et al (1973) state that this can be explained by the thermodynamic equilibrium-temperature relation. This relation gives the dependency between the equilibrium constants and the change in Gibbs energy. In this relation, the equilibrium constant is inversily proportional to the temperature. Thus, a lower temperature should lead to a higher exchange capacity. The same study shows that an increase in temperature does not lead to a capacity increase for low ammonium concentrations (14 mg NH_4-N/L), but leads to an increase (!) in capacity for high ammonium concentrations (70 mg NH_4-N/L). This is explained using the exchange kinetics. The kinetic exchange rate is proportional to the temperature, if pore diffusion is the rate limiting step in the exchange process. The increase of the exchange capacity due to the change in the equilibrium is then nullified by the decrease in diffusion-speed caused by the lower temperature. However, in general it can be stated that the temperature effects can be neglected for temperatures between 2 and 23 º C, since the impacts of the ammonium concentration and the flow velocities are significantly stronger (Verkerk, 2003)

LOADING PARAMETER 8: PRE-TREATMENT OF THE ION EXCHANGER

Ion exchangers can be thermically pre-treated and/or be rinsed with a salt of acid solution (Verkerk, 2003). According to Semmens (1988) pre-treatment is important and increases the capacity of the ion exchanger. Haralambous (1992) agrees that pre-treatment can increase the exchange capacity, but states that after a few cycli the ion exchanger will be conditionized comparably. Jorgensen et al (1976) reaches the same conclusions and describes that the ion exchange capacity will stabilize after 5 cycli (this research was done using Clinoptilolite). Different types of pre-treatment were investigated by Korobchanskii (1987) (as explained in Verkerk (2003). Heating decreased the capacity with 4%, pre-treatment with a 3,6 g/L HCL solution (0,1 M HCL) increases the capacity with 2% and a pre-treatment with a combination of acid and salt (3,6 g/L HCL and 60 g/L NaCl) increased the capacity with 4%. In Verkerk's study (2003), a 24 hour pre-treatment period with the regeneration solution was applied (100 g NaCl/L). The effect of this pre-treatment has not been studied.

Appendix 4.3

APPENDIX 4.4 CALCULATION OF REQUIRED ZEOLITE BED VOLUME

For the calculation of the required zeolite bed volume, the following starting points were taken into account:

- The objective of the complete installation is to abstract as much ammonium as possible from the waste water, to be able to use it as a fuel.
- The function of the ion exchange installation is to absorb as much as possible ammonium from the MBR effluent (in order not to 'lose' it, both because we want to use it as a fuel and also because we don't want to discharge ammonium rich effluent) and to concentrate the ammonium. It is required to recover the ammonium in a higher concentration, in order to facilitate the transformation from ammonium to an ammonia rich gas.
- According to the previous two points, at this moment the focus is not on optimizing (minimizing) the size of the ion exchange installation. However, the installation needs to be practically implementable and connectable to the AnMBR installation in the water laboratory of the TU Delft.

The most important factor for the calculation of a required bed volume is the ion exchange capacity of the used zeolite. In chapter 5.1 is concluded that Chabazite is the most suitable zeolite for this installation. Table 1 shows data on the ion exchange capacity of Chabazite. As shown

Table 1: Chabazite ion exchange capacity

Total ion exchange capacity [mg/g]	35	Supplied by supplier
Measured operational ion exchange capacity [mg/g]	1,4	Measured during batch test. During the experiments, problems with mixing have occured
Operational capacity found in literature [mg/g]	4-15	(STOWA, 2001, de la Torre, 1999, Rahmani and Mahvi, 2006, Verkerk and van der Graaf, 1999, Nguyen and Tanner, 1998)

The differences in table 1, and especially between the given total ion exchange capacity and the measured operational capacity, are quite significant. As explained in chapter 4, this is to be expected. However, the measured operational capacity is also low compared to other operational capacities as found in literature[1]. It can be read in chapter X that during the batch tests, problems occurred with the mixing (due to the scraping effect of the magnetic mixer, the zeolites were difficult recoverable after the batch test, impeding the calculation of the actual operational capacity). Therefore it is chosen to assume an operation capacity value from literature.

The operational capacity is however very depending on waste water input, loading times, loading velocity and frequency of regeneration. In order to be safe, and taking into account the previously described starting points, the choice has been made to assume an operational capacity of 7 mg NH_4-N/g Chabazite. This assumption is made based on a relatively low loading time, a frequent regeneration and a high assumption of the ammonium concentration of the AnMBR effluent. (making it an even safer choice).

Table 2 shows the used values and the calculated required ion exchange bed volume.

Table2: Ion Exchange bed volume calculation

Effluent AnMBR	[l/day]	30

[1] It must be noted that literature on chabazite is relatively scarce compared to other types of natural zeolites.

Appendix 4.4

NH_4-N concentration AnMBR effluent	[NH_4-N/L]	**67**
Total available NH_4	[NH_4-N/L]	2010
Operational capacity chabazite	[mg NH_4-N/L /g chabazite]	**7**
chabazite required	[g]	287,1429
packing density	[kg/m3]	550
Required volume of Chabazite	[ml]	522
Decided bed volume	[ml]	600

Thus, table 2 shows that the calculated required bed volume of zeolite is 522 ml. In order to make sure that the ion exchange installation will manage to absorb all ammonium of the AnMBR effluent (zero-breakthrough), the choice has been made for a bed volume of 600 ml.

Appendix 5.1

APPENDIX 5.1 ADDITIONAL COLLUMN TESTS - SEA WATER

USING SEA WATER AS THE REGENERATION AGENT

Based on literature, the choice has been made to use a NaCl solution as the regeneration agent during the regime tests. Out of personal interest, potential savings of chemical usage and potential economic advantages, the use of sea water as a regeneration agent has also been tested.

MATERIALS AND METHODS

Table 1 shows the operational parameters used. One IE cycle is executed using the column set-up as described 5.2 , and samples have been taken in order to compose the regeneration curve and to assess the obtainable ammonium concentration in the regeneration effluent using PCC. The ammonium concentration of the samples has been measured using standard methods (2005, APHA).

Table 1: Sea water regeneration test

Height column [m]	1
Bed Volume [ml]	600
V_L [BV/h] , [l/h]	15 , 7.5
V_R [BV/h] , [l/h]	15 , 7.5
Ion exchange feed [-]	AnMBR effluent
C_R	Sea Water

Figure 1 collecting sea water at Scheveningen (10 degrees!)

Appendix 5.1

RESULTS

Figure 1 shows the regeneration curve as obtained from one IE cycle while sea water is used as an regeneration agent. As a reference, the data obtained from the first cycle of regime B has been plotted in the same graph.

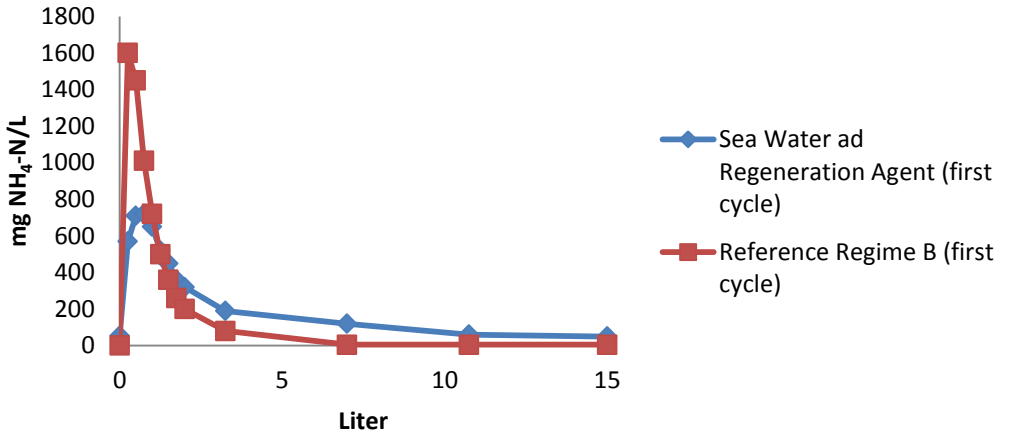

Figure 2 Regeneration curve sea water

Figure 2 shows that the regeneration curve of sea water follows the 'peak-pattern'. As expected, regeneration with sea water is less complete compared to the regeneration with a 150 g NaCl/L solution and thus the peak is less steep and less high. This was predictable due to the lower NaCl concentration of sea water (30 g NaCl/L) (EPA, 2003). Also the presence of other competing cations like magnesium, calcium and potassium are likely to have a negative effect on the regeneration capacity of sea water, due to the competition over the absorbable spots on the Chabazite. Chabazite has a stronger selectivity for potassium then for both sodium and ammonium, resulting in a permanent loss of exchangeable spots on the Chabazite for sodium and ammonium. The peak in the regeneration curve of the sea water is not only smaller, it is also broader compared to the first cycle of regime B. The peak is not located within the first 2 liter of regeneration effluent, but rather in the first 3. Therefore, PCC has been applied by separately collecting the first 3 liter. It must be noted that only one IE cycle is executed with sea water as a regeneration agent. Figure 3 shows the measured ammonium concentration using PCC for sea water and 150 g NaCl as the regeneration agent.

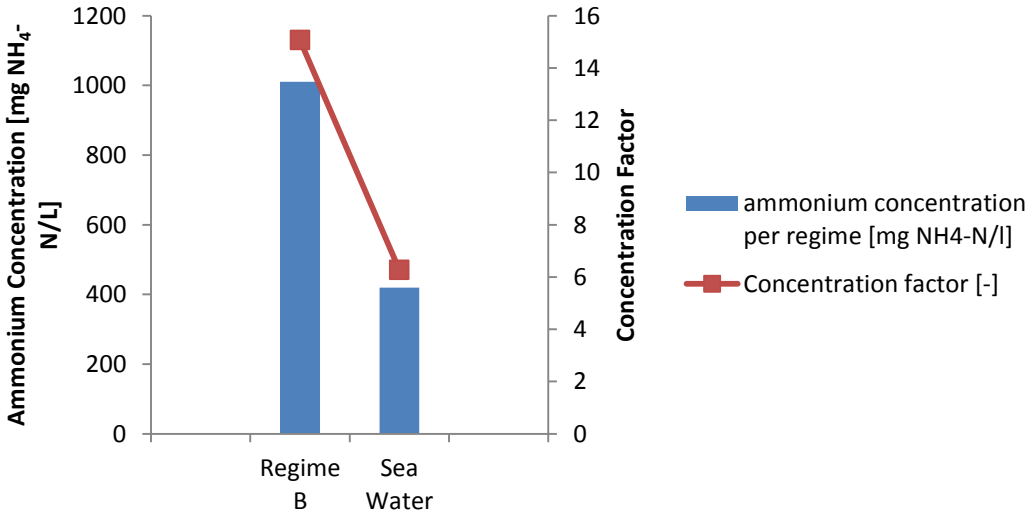

Figure 3 Measured ammonium concentrations using PCC, plus the achieved concentration factors

Appendix 5.1

Table 2: Percentage of retrieved ammonium using PCC

Sea Water	Regime B
62	100

Table 2 shows the percentage of retrieved ammonium, thus the percentage of the total input ammonium (that is fed on a daily basis to the IE set up via the AnMBR effluent) that is concentrated in the first separately collected 3 liter, while applying PCC. As expected, the concentration factor of sea water as the regeneration agent is low.

However, it is useful to have a quantitative approximation of what happens when sea water is used. Regeneration of the Chabazite actually does take place, Although the obtained data show a not optimal regeneration.

Appendix 5.2

APPENDIX 5.2 ADDITIONAL COLUMN TESTS- SATURATED BED

In the previous paragraphs, the operational conditions for concentrating the ammonium from the AnMBR effluent have been assessed, using PCC. The starting point of that assessment is a feed flow of 30 liter of AnMBR effluent per day, and a required daily production of a concentrated ammonium solution.

At the moment of execution of this research, the way in which the concentrated ammonium will be transformed into an ammonia rich gas was not yet known. Consequently, the minimal ammonium concentration required for this transformation was not known as well. Considering the possibility that the required ammonium concentration might be higher than was achieved during the regime column tests, another way of operation has been assessed. The objective of this tests is to analyse if it is possible to obtain higher ammonium concentrations using PCC, if not the daily effluent production of the AnMBR is used, but when the ion exchange bed is saturated with ammonium instead. In practice this refers to only one ion exchange cycle in a longer period, instead of one ion exchange cycle per day. Thus, it would not be possible to produce an ammonia rich gas every day.

MATERIALS AND METHODS

In order to assess the maximum obtainable ammonium concentration using PCC, the IE set-up as described in chapter 5 is operated following the parameters shown in table 3. In order to make sure the IE bed is saturated with ammonium, the IE bed is fed with a solution of 1000 mg NH_4-N/L for 24 hours.

Table1: saturated bed test

Height column [m]	1
Bed Volume [ml]	600
V_L [BV/h] , [l/h]	15 , 7.5
V_R [BV/h] , [l/h]	15 , 7.5
Ion exchange feed [-]	AnMBR effluent + 1000 mg NH_4-N/L (24 hours)
C_R	150 g NaCl/L

During the regeneration, samples have been taken in order to compose the regeneration curve and PCC has been performed. The ammonium concentration has been measured according to the standard methods (APHA, 2005). To test if the ion exchange bed was saturated before the regeneration, the ammonium concentration of the ion exchange effluent was measured after 24 hours. Since the ammonium concentration of the feed and the effluent matched (complete break through), it can be said that the ion exchange bed was indeed saturated.

RESULTS

Figure 1 shows the measured regeneration curve, of the first cycle with a saturated ion exchange bed. For the sake of context, the data of the first cycle of regime B with the daily production of AnMBR effluent is also shown in the same graph. The data of regime B is chosen as a reference, since this regime resulted in the highest ammonium concentrations using

peak concentration collection.

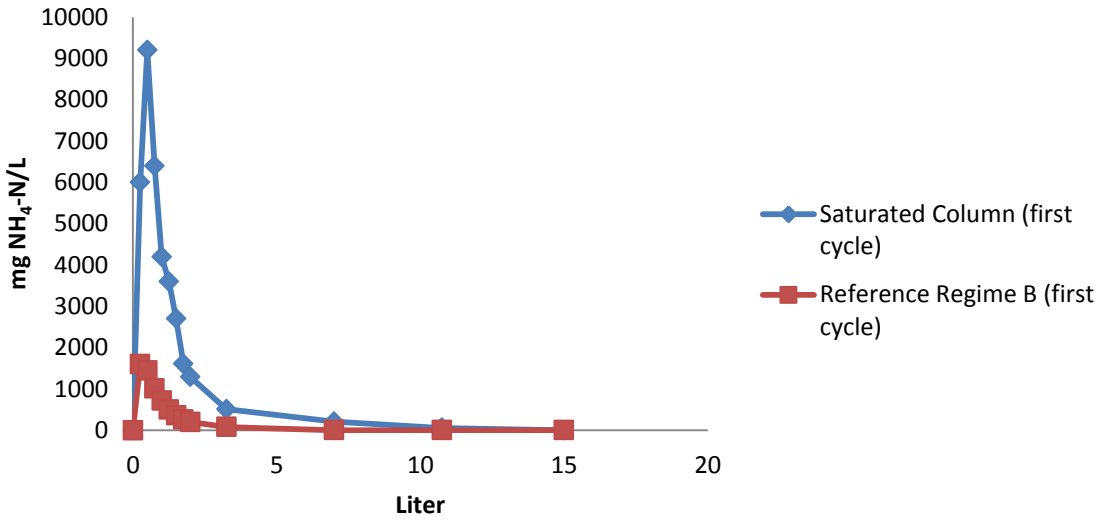

Figure 1 Regeneration curve saturated bed

Figure 1 show that the saturated bed results in a significantly higher, broader and steeper peak in the regeneration curve. It can be seen that the peak is more or less situated within the first 3 liter, thus PCC has been implemented by collecting separately these first 3 liter.

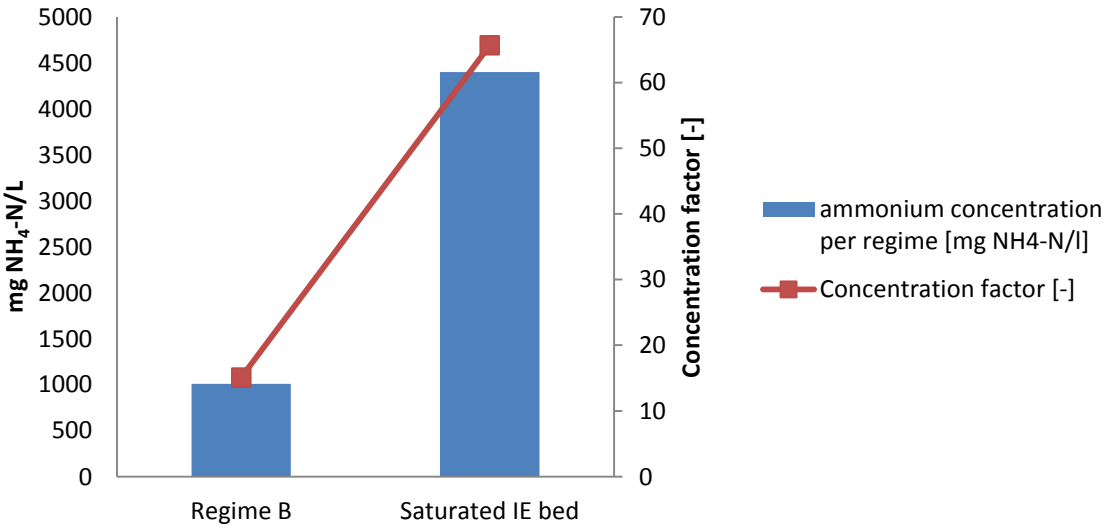

Figure 2 Measured ammonium concentrations using PCC and the achieved concentration factors Saturated Bed

Figure 2 shows the obtained ammonium concentration using PCC. For a saturated bed, applying PCC by taking away the first 3 liter of regeneration solution, results in an ammonium concentration of 4400 mg NH_4-N/L.

To create an saturated bed in the ion exchange set-up of this thesis (without adding additional ammonium), the IE installation has to be fed for 39 days with the AnMBR effluent. This is calculated an ion exchange bed volume of 500 ml, a packing density of the Chabazite of 550 kg/m^3 and a total capacity of Chabazite of 35 mg NH_4-N/g Chabazite. Thus, if the IE set up would be fed with AnMBR effluent for 5 days, and then regenerated, while separately collecting the first 6 bed volumes, a concentration factor of 66 could be achievable.

Appendix 5.2

Since the focus of this research is on producing an ammonia-rich gas on a daily basis, initially this was not the way to go. However, it is interesting to know that such high concentration factors are possible. It can actually be said that the size of the IE bed and the time available for loading determines the possible concentration factor.

CONCLUSIONS OF THE ADDITIONAL COLUMN TESTS

Two additional column tests have been done, besides the regime tests. Firstly, sea water has been tested as a regeneration agent. Secondly, the regeneration of a IE bed that is saturated with ammonium has been analysed.

The conclusion of the sea water test reads as follows: Sea water can be used for the regeneration of an IE bed, consisting out of ammonium exchanging Chabazite. However, the regeneration capacity of sea water is less than a pure NaCl concentration in the range of 100- 150 g NaCl. This is logical, considering the lower NaCl concentration and the presence of competing cations.

The tests with the saturated bed showed that if the ammonium concentrations that are achieved with the regime tests are not high enough for the follow up step, e.g. for creating an ammonia-rich gas, it can be interesting to look at a saturated bed operation of the IE installation. Because, it is indeed possible to obtain very high ammonium concentrations (by applying PCC) when the IE bed is saturated, compared to a bed that is only fed with the daily AnMBR effluent. However, Only one IE cycle was tested. Therefore, more tests are required for detailed information on how the IE installation works when it is only regenerated after the ion exchange bed is saturated.

Appendix 5.3

APPENDIX 5.3 DATA REGIME TESTS

Table 1. Synthetic AnMBR effluent ammonium concentrations and the IE effluent concentration for each measured cycle

		synthetic AnMBR influent	IE Effluent
		mg NH_4-N/L	mg NH_4-N/L
Regime A	Cycle 1	68	<2
	Cycle 3	65	<2
	Cycle 5	71	<2
Regime B	Cycle 1	64	<2
	Cycle 2	65	<2
	Cycle 3	63	<2
	Cycle 4	64	<2
	Cycle 5	70	<2
	Cycle 6	71	<2
Regime C	Cycle 1	65	<2
	Cycle 3	65	<2
	Cycle 5	69	<2
Regime D	Cycle 1	64	<2
	Cycle 3	66	<2
	Cycle 5	69	<2
	Average	67	<2

Appendix 5.3

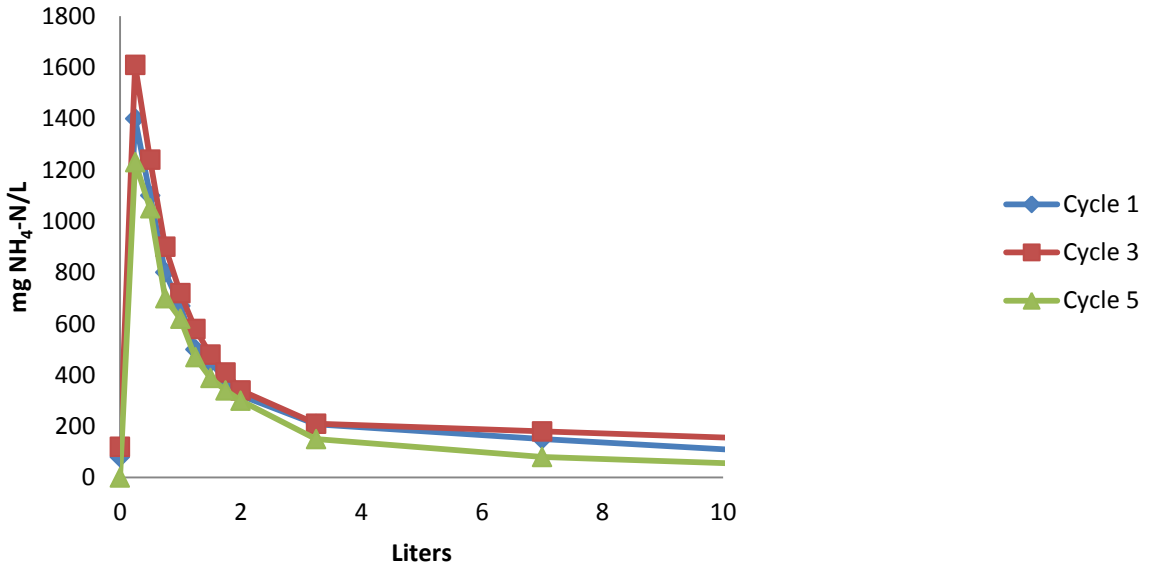

Figure 1 Regeneration curves regime A

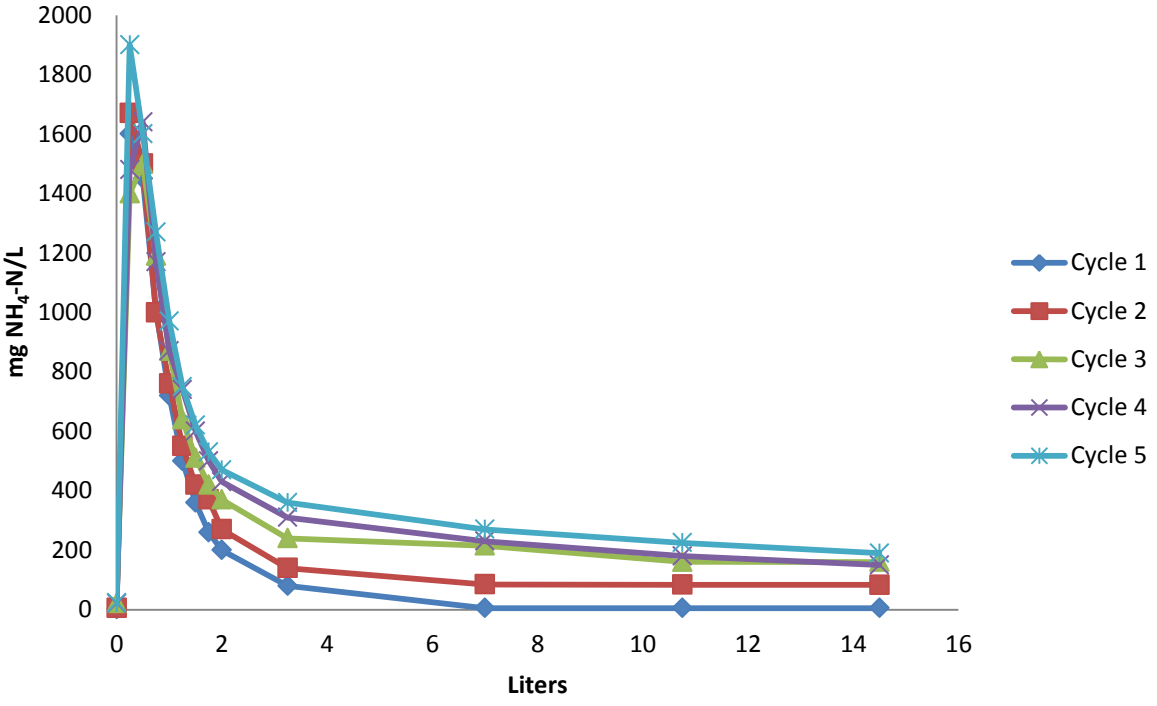

Figure 2 Regeneration curves regime B

Appendix 5.3

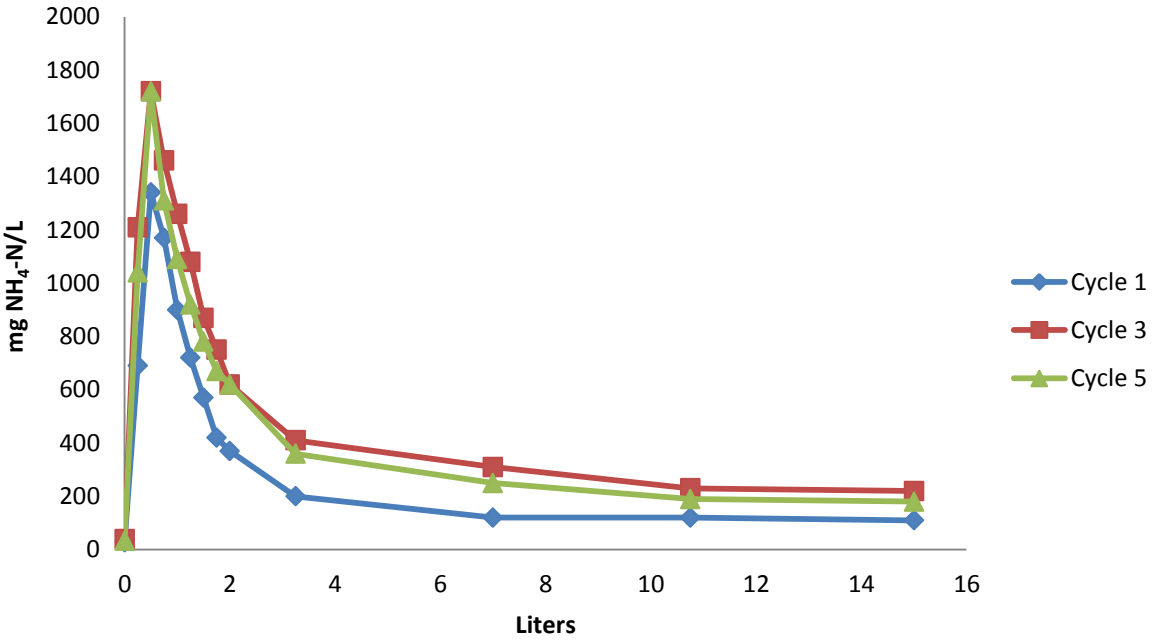

Figure 3 Regeneration curves regime C

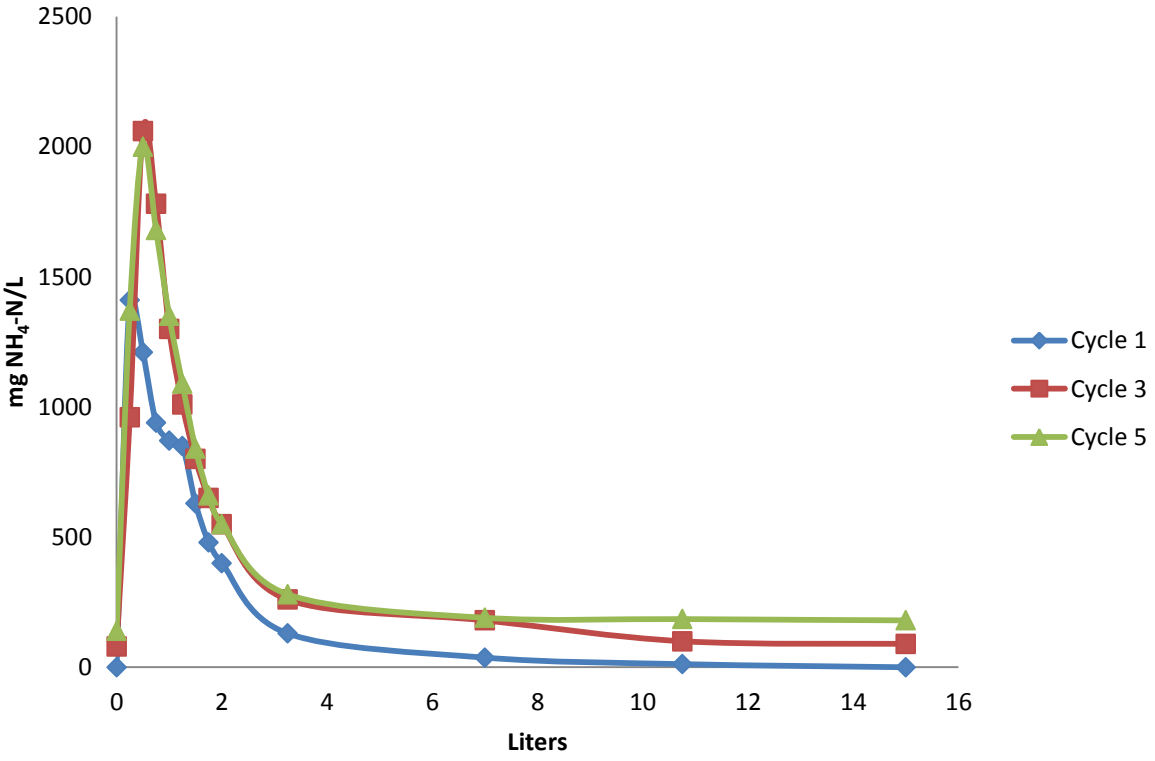

Figure 4 Regeneration curves regime D

Appendix 5.4

APPENDIX 5.4 DATA LONG TERM OPERATIONS

Table 1. Synthetic AnMBR effluent ammonium concentrations and the IE effluent concentration for each measured cycle

	synthetic AnMBR influent	IE Effluent
	mg NH_4-N/L	NH_4-N/L
Cycle 1	68	<2
Cycle 2	65	<2
Cycle 3	69	<2
Cycle 4	-	-
Cycle 5	-	-
Cycle 6	-	-
Cycle 7	65	<2
Cycle 8	-	-
Cycle 9	-	-
Cycle 10	-	-
Cycle 11	64	<2
Cycle 12	-	-
Cycle 13	-	-
Cycle 14	-	-
Cycle 15	70	<2
Average	67	<2

Appendix 5.4

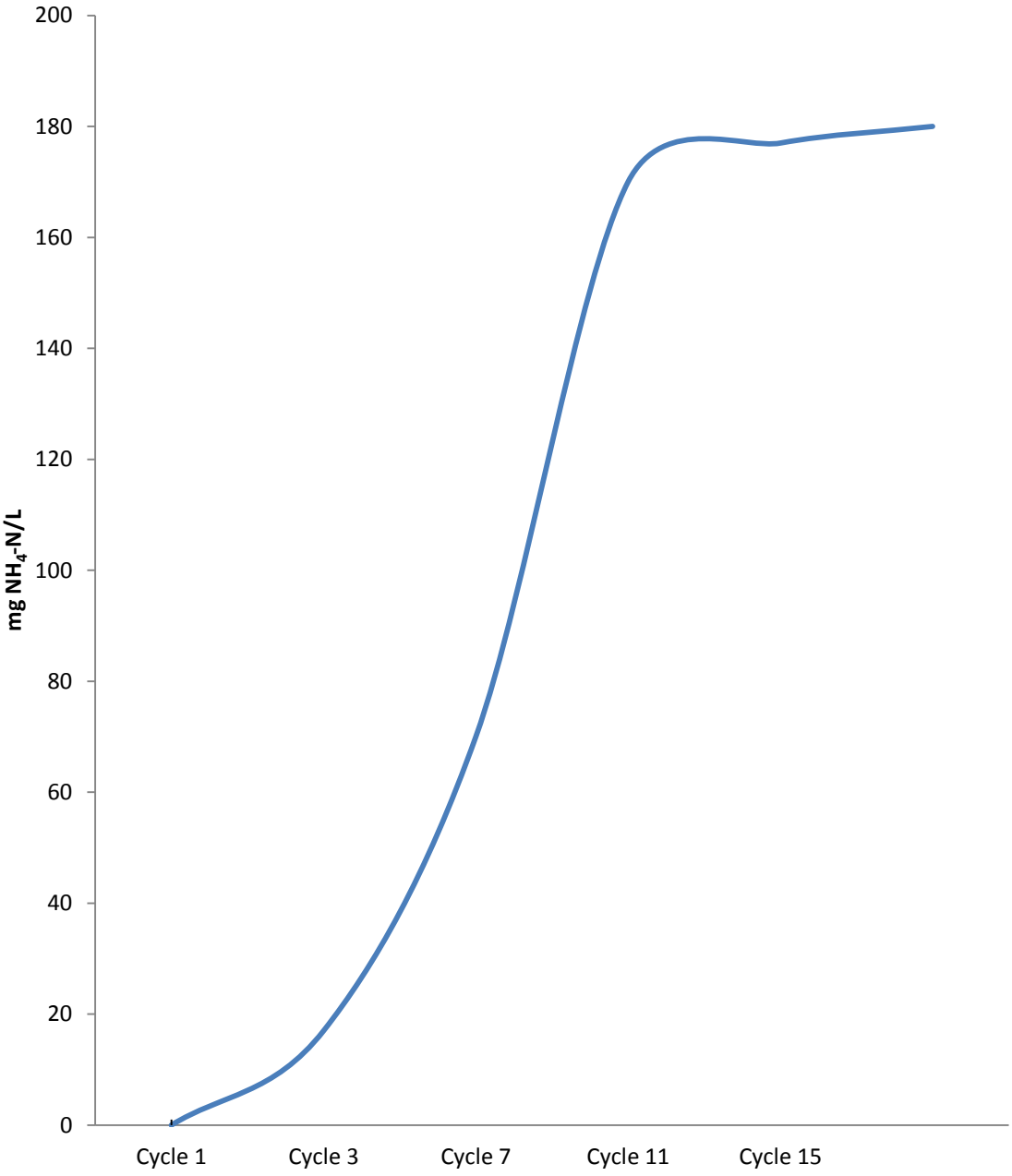

Figure 1 Accumulated mg NH_4-N/L in regeneration concentration measured after complete cycle

Appendix 7.1

APPENDIX 7.1 CALCULATION OF HETP PACKING DISTILLATION TOWER

In figure 1 the HETP value is given, for different F-factors. Figure 1 is supplied by the supplier of the column material. Type DX is used in the used column. The F factor can be calculated as follows:

$$F = w_g \cdot \sqrt{\rho_g} \qquad \text{[equation 1]}$$

Where: F = packing specific factor [m/s $\sqrt{(\mathrm{kg}/m^3)} = \sqrt{Pa}$]
W_G = superficial gas velocity
ρ_G = gas density

Table 1 shows the values used for calculating the F factor of the used packing in the distillation tower. It can be seen that the HETP is in the range between 0,04 -0,05.

Table 1: calculation F factor

ΔH mixture	2500	kJ/kg
Total Mixture	14	L
Total power	2900	W
Steam production	1,16	g/s
1,16 gram equals	0,0014968	m^3/s
ρ_G (steam, 1,7 bar, 100 °C)	0,755	kg/m^3
r	0,025	m^3
A	0,0019635	m^2
Wg	0,7623015	m/s
SQRT(Ro)	0,8689074	$\sqrt{\rho_G}$
F	**0,6623694**	$\sqrt{Pa}$

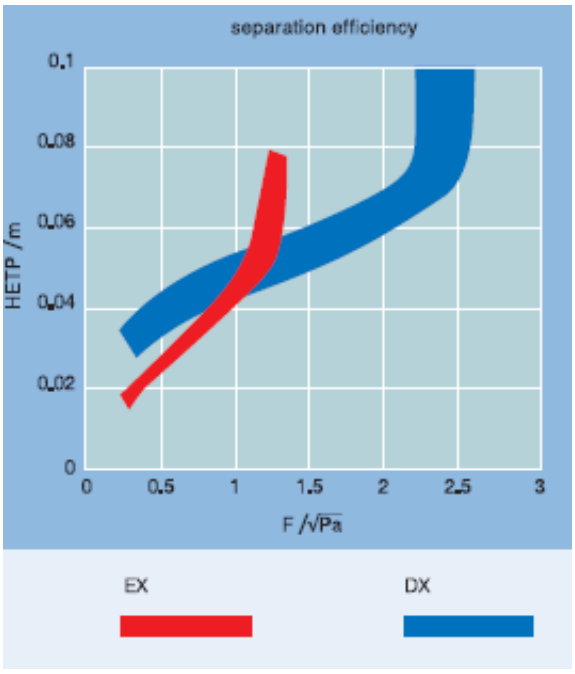

Figure 1 HETP for two types of packing, expressed per F-factor

Appendix 7.2

APPENDIX 7.2 CALCULATION OF THEORETICAL REQUIRED STAGES FOR THE DISTILLATION PROCESS

Figure 1 shows the equilibrium mass fraction of ammonia in a mixture of water and ammonia, against the temperature. The blue line indicates the mass fraction of ammonia in a saturated liquid and the green line shows the ammonia fraction in a saturated vapour. The other way round, the blue line also shows the boiling point of a water-ammonia mixture, when the mass faction of ammonia is known. This graph is obtained from ASPEN, and the required equilibrium steps are modelled using Fluidprop, in order to calculate the required equilibrium steps for creating a solution sufficiently rich in ammonia.

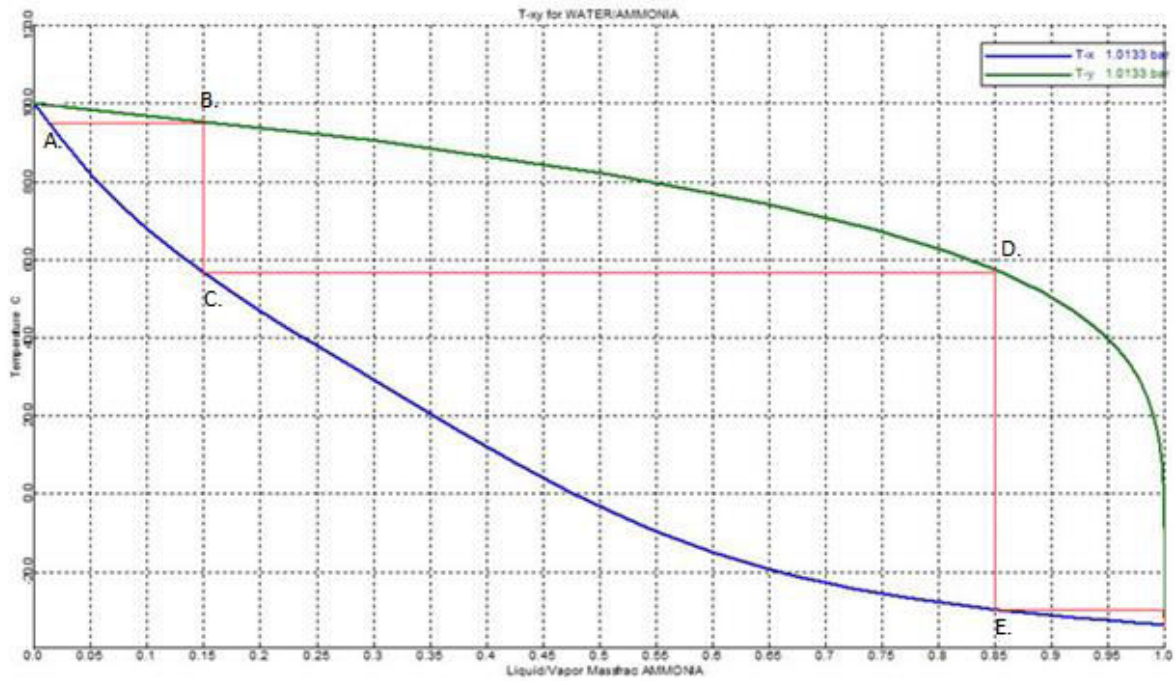

Figure 1 Equilibrium ammonia mass fraction in ammonia-water mixture (modelled in ASPEN)

The red line gives an indication of the theoretical minimal amount of equilibrium stages, required to increase the ammonia mass fraction of the mixture from 0.001 mole %(1 g NH_4-N/L) to an almost pure ammonia gas. The red line starts at x = 0.001 and y = 99.28 °C, since this is the boiling point of a mixture with an ammonia mass fraction of 0.001 and the rest water (point A. in the graph). At the onset of boiling, the equilibrium composition of the vapour above the boiling mixture, is indicated with point B. A significant increase in the mass fraction of ammonia is shown in the created vapour. Thus, ammonia tends to vaporize easier than water. If the vapour of composition B. is condensed completely (assuming that all vaporized ammonia is condensing back into solution), a liquid mixture is obtained with an ammonia mass fraction shown by point C. If the mixture, indicated with point C, is heated up to boiling point again, a gas with composition D. is created. If this gas is condensed again, a liquid with an ammonia fraction shown by E. is formed and so on.

In figure 2, the same figure is shown, but now is the increase in mass fraction per equilibrium step indicated. It can be seen that in three equilibrium steps, almost a pure ammonia gas is obtainable.

Appendix 7.2

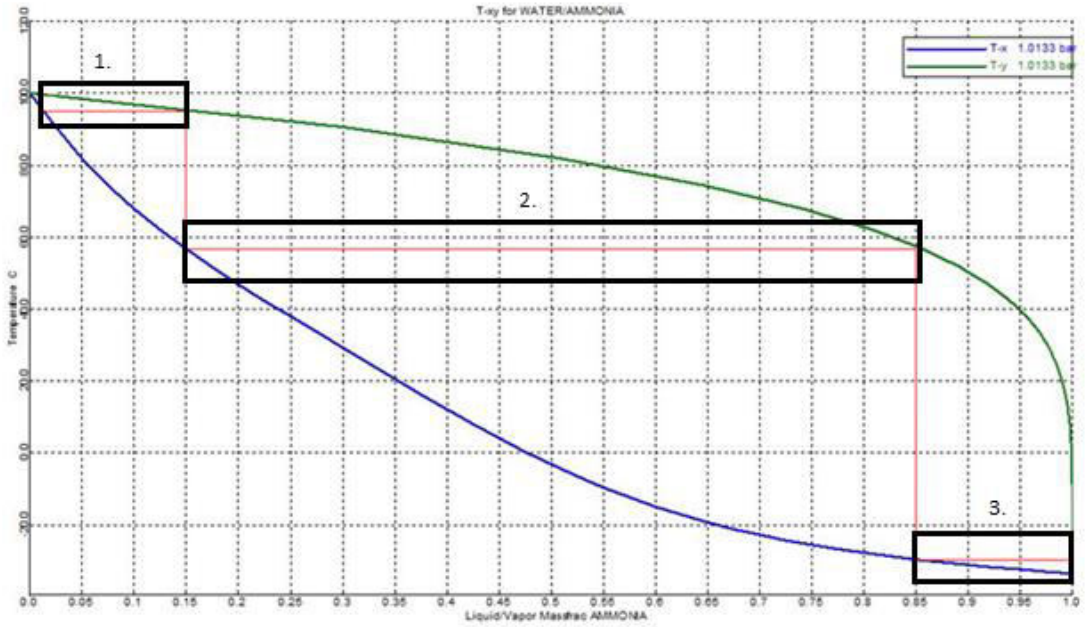

Table 1: ammonia mass fraction in water-ammonia mixture for each equilibrium step (as modelled using fluidprop)

Equilibrium step	ammonia mass fraction in water-ammonia mixture	Operating temperature (°C)
0 (initial value)	0.001	99.26
1	0.163	95.03
2	0.860	56.77
3	1.000	-30.30

As can be derived from figure 2, in theory only 3 equilibrium steps would be required to obtain a pure ammonia gas (86 mole%). However, in the distillation set up as used in the context of this thesis, a continuous process of vaporization and condensation takes place due to the reflux, and it is not possible to control the operating temperatures as shown in table 1.

Table 2: ammonia mass fraction in water-ammonia mixture for each equilibrium step (as modelled using fluidprop)

Equilibrium step	ammonia mass fraction in water-ammonia mixture	Operating temperature (°C)
0 (initial value)	0.001	99.2
1	0.004	99.5
2	0.023	99
3	0.060	98

Table 2 should be considered as an indication, since approximate operating temperatures are used to model the ammonia mass fraction, if the temperature is not controlled at exactly the boiling temperature of the liquid phase. It can be seen that this result in a significant lower ammonia mass fraction. In theory three stages are required to obtain a mixture that can be used as a fuel for a fuel cell. However, the described theory applies to batch equilibrium steps, while in practice a distillation tower was used. (gas flowing in upward direction →) (liquid flowing in downward direction ←).

APPENDIX 9.1 SOFC TEST SET UP INFORMATION SUPPLIED BY FIAXELL

Fiaxell
SOFC Technologies™

Components for
Solid Oxide Fuel Cell development

Integrated steamer for hydrolysis and gas processing

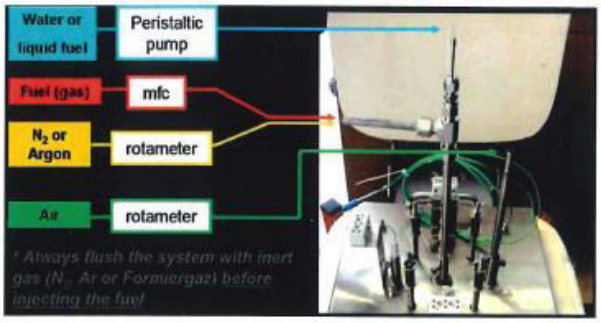

Thanks to the ceramic cartridge in the steamer, **a very constant steam flux** flows on the cell, which is necessary for hydrolysis tests (ask for our video demonstration).

Liquid fuel mixed with water can also be injected with the steamer.

The easy interchangeable ceramic cartridge can also be impregnated with catalyst of choice and **in-situ gas processing**, as **steam reforming** (see www.fiaxell.com) or **partial oxidation** will take place before to reach the SOFC cell.

Fuel utilisation and electrical efficency

Different fuel flow rates are injected for electrical efficiency study. Without any sealing, **till 85 % of fuel utilisation** and **electrical efficiency close to 50 %** have been achieved.

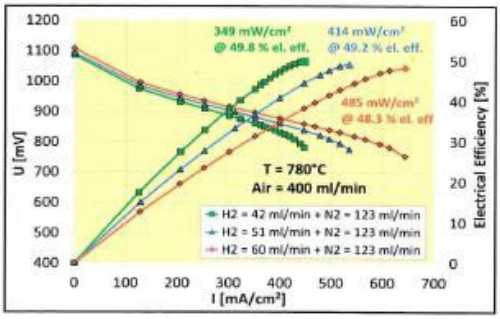

Test conditions: Open Flanges™ Set-Up with a 2R-Cell (cathode SA: 10.2 cm²)

Similar to a glass sealed setup

The graph shows that between 5 and 75 % of fuel utilisation the same electrical performances are observed for both tests, glass sealed and open flanges.

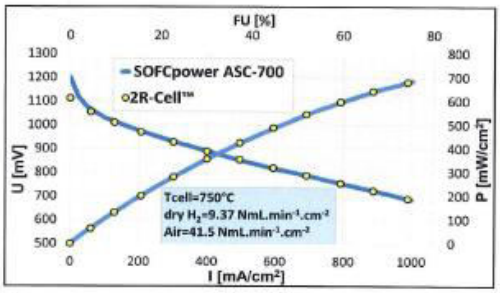

Test conditions: Open Flanges™ Set-Up with a 2R-Cell™ and a glass sealed rig at CEA Grenoble with a SOFCPower ASC-700 (SA cathodes: resp. 10.2 and 9.08 cm²) (from B. Morel et al., proceedings of 5th FDFC 2013, Karlsruhe).

Some of our customers and references:

Prof. H. Middleton, University of Adger-UIA (Norway); CSIR-Central Glass & Ceramic Research Institute, Kolkata (India); University of KwaZulu Natal (South Africa); *Prof. G. Taillades*, University of Montpellier (France), *Prof. O. Joubert*, IMN Nantes (France); *Prof. G. Caboche*, ICB Dijon (France). *Dr. J. Dally*, Eifer (Germany), *Prof. Anthony Chesnaud*, Paristech (FR), *Prof. Laurent Dessemond*, LEPMI, Grenoble (FR), *Dr. Per Martin Rørvik*, Sintef, (Norway)

www.fiaxell.com
Switzerland
PSE-A Science Park
info@fiaxell.com
CH - 1015 Lausanne
tel: +41 21 693 86 13

Fiaxell
SOFC Technologies™

Components for
Solid Oxide Fuel Cell development

Open Flanges Set-up™

One single set-up for all cell tests

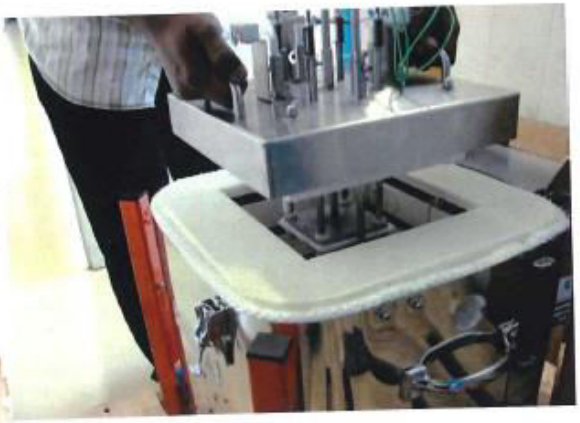

End of broken cells and secure testing: the cell is squeezed by a soft alumina felt that prevents any damages, the excess fuel burns continuously in the alumina felt at the cell edges

Results reproducibility: less than 2.5 % of discrepancy is measured between two same cells differing by their size of diameter 25 and 60 mm (see fiaxell.com)

Technical training: the set-up comes with a video manual with detailed instructions. A two days training is also offered in our lab.

Located in the Science Park of EPFL in Lausanne, Fiaxell is looking forward to your visit for a test demonstration

Flexible cell dimensions: cells of Ø 20 to Ø 80 mm (or square till 70x70 mm) can be successively installed

Quick start of experiment: less than 20 minutes to remount a new cell with different dimension, thanks to the simple design without sealing

Other SOFC components: the open flanges test rig is also useful for conductivity measurements (electrolyte, electrode material, interconnect etc.) and sealing tests

Open Flanges head with fuel diffuser and double thermocouple holder for optimal cell temperature control

Constant pressure load: 4 external springs ensure a constant and controlled pressure on the cell during the whole test

Heating: the Set-Up comes with a robust Kittec German furnace that can be used for the sintering of all SOFC components (electrodes, cell, powders etc.) till 1320°C

Corrosion resistant & robust: flanges and tubes (air and fuel) made in Inconel 600 & 601. The set-up is built up to last for years

www.fiaxell.com
Switzerland

PSE-A Science Park
info@fiaxell.com

CH - 1015 Lausanne
tel: +41 21 693 86 13

Fiaxell
SOFC Technologies™

Components for Solid Oxide Fuel Cell development

Power density

- LSC-GDC cathode and a GDC buffer layer
- Electrical performances are measured at 700, 730, 750 and 780 (°C)
- Current density of **1 A/cm²** achieved at **0.8 V and 780 °C**

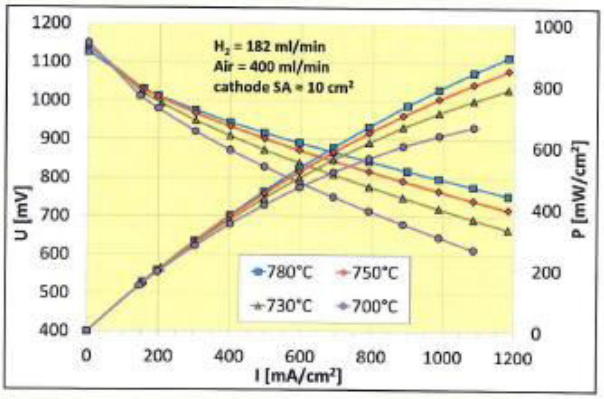

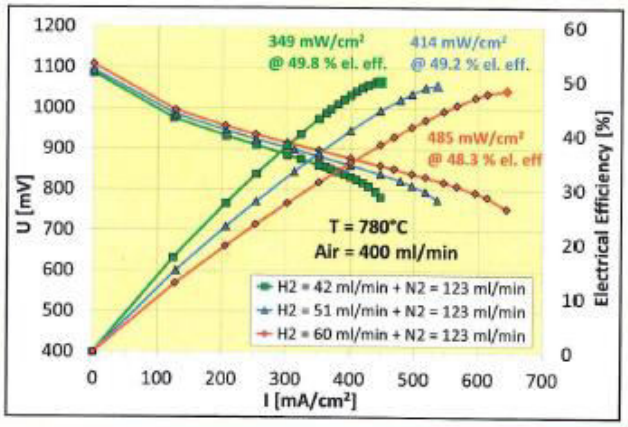

Efficiency

- Electrical efficiency at 42, 51 and 60 ml/min of dry H_2
- **Close to 50 % efficiency** obtained in the Open Flanges Set-Up™ (without any sealing)
- Maximum of **485 mW/cm²** with an efficiency greater than **48%**

Benefits

- **Redox 2R-Cell™** are made with very standard raw materials: NiO, 8YSZ, 3PSZ
- **Customizable**: compatible with other electrolyte materials such as ceria, BIT or BCY (protonic conductor)
- **Robust for electrolysis** test mode
- Removal of carbon and sulfur deposition simply by stack re-oxidation

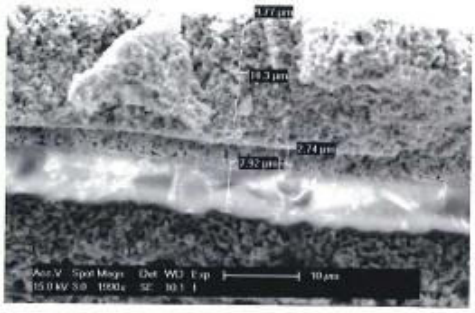

SEM cross section of 2R-Cell™. From bottom to top: AFL, electrolyte, GDC, LSC-GDC, LSC composite cathode

www.fiaxell.com
Switzerland

PSE-A Science Park
info@fiaxell.com

CH - 1015 Lausanne
tel: +41 21 693 86 13

Appendix 9.2

APPENDIX 9.2 CALCULATION OCV FOR HYDROGEN SOFC EXPERIMENT

$$E = \frac{-\Delta G_f}{n\,F} + \frac{RT}{nF} ln \left[\frac{P_{H_2} . P_{O_2}^{\frac{1}{2}}}{P_{H_2O}} \right] \quad [1]$$

So,

$$E = E^0 + \frac{RT}{nF} ln \left[\frac{P_{H_2} . P_{O_2}^{\frac{1}{2}}}{P_{H_2O}} \right] \quad [2]$$

Where E = EMF or open circuit voltage [Volt]

E^0 = EMF at standard temperature and pressure, and with pure reactants [Volt]

ΔG_f = Gibbs free energy of formation [Joules]

n = The amount of electrons that travel around the circuit per mole of fuel [-]

F = Faraday constant ($9{,}64853399 * 10^4$) (Mohr et al, 2008) [C mol^{-1}]

R = The universal gas constant (8,3144621) [J· $(mol \cdot K)^{-1}$]

T = Temperature [Kelvin]

P_x = Partial pressure of gas X [bar]

Table 1: calculation of Open Circuit Value hydrogen

dG	-192,46	Kj (Larminie and Dicks, 2003)
F	96485,34	c/mole
E0	0,99	Volt
R	8,31	J· $(mol \cdot K)^{-1}$
T	1053	Kelvin
Po	1	bar
P	1,02	bar
PH2	1,02	bar
PO2 (in air	0,21318	bar
PO2 (in SOFC)	0,2174436	bar
H2O in air	0,001	Bar (assumed high air humidity)
PH2O	0,0306	bar
E	**1,27**	**Volt**

Appendix 10.1

APPENDIX 10.1 OPTIMIZED DISTILLATION TOWER DESIGN – ENERGY REQUIREMENTS CALCULATION

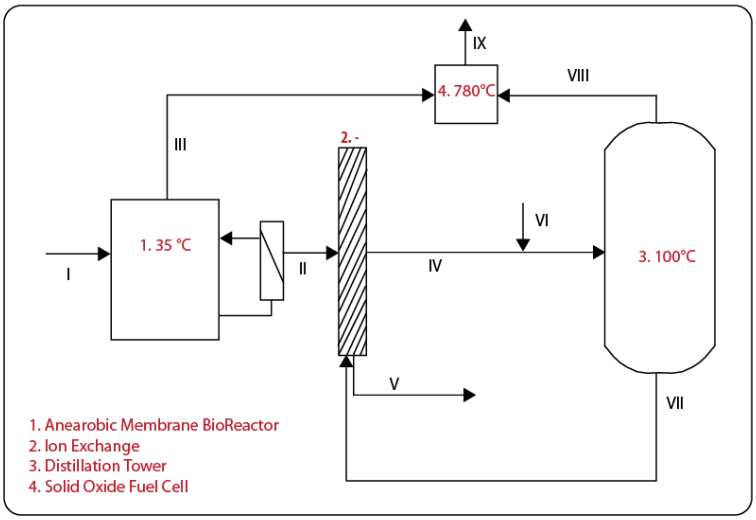

Figure 1: Flow chart including applied temperatures

Figure 1 shows the flow chart of the combination of anMBR, an ion exchange column, a distillation tower and a SOFC. The applied temperatures are indicated. It can be seen that there is a significant potential for heat recovery within the installation itself.

Based on STOWA (1995), an optimized design has been made of a distillation tower with heat integration by G. Smith (personal communication, October 2014). The flow chart is shown in figure 2. Figure 2 shows a design for a distillation tower with an integrated heat exchanger, which pre-heats the incoming brine by the bottom product and a compressor that compresses the steam produced by the fuel cell an efficient reuse of the energy in this stream is possible. The flows are indicated with numbers and table 1 shows the characteristics of the indicated flows. Table 2 shows the characteristics of the AnMBR effluent, the produced gas and the ion exchange brine(which corresponds with flow #1 in figure 2).

Then, the volume of produced gas (consisting out of water vapor and carbon dioxide) in a fuel cell was calculated, based on an assumed fuel utilization in the SOFC of flow #7 and #16. According to figure 1, this gas flow is led over a compressor, which increases the pressure of the gas flow. A higher pressure results in a higher condensation temperature. Thus, the water vapour condensates at a temperature larger than 100 °C so it can be used to heat the brine that is collected in the bottom of the distillation tower.

Subsequently, the amount of energy that is released when this gas flow (#8) is cooled and condensed was calculated using the evaporative heat of water, the specific heat of water vapor, and the specific heat of carbon dioxide.

In the design (figure 1) also a heat exchanger is added between the returning brine and the incoming brine.

Eventually, the released energy was subtracted from the required heat for vaporizing (minus the energy available via the heat exchanger) and it was calculated that with the used COD and ammonia concentration, an external steam flow (flow #14) was needed to fill the gap between the required energy for vaporizing the brine and the energy released by the gas produced by the fuel cell.

The overall required energy for the distillation tower consists then out of the required energy for the external steam flow and the energy required by the compressor.

Appendix 10.1

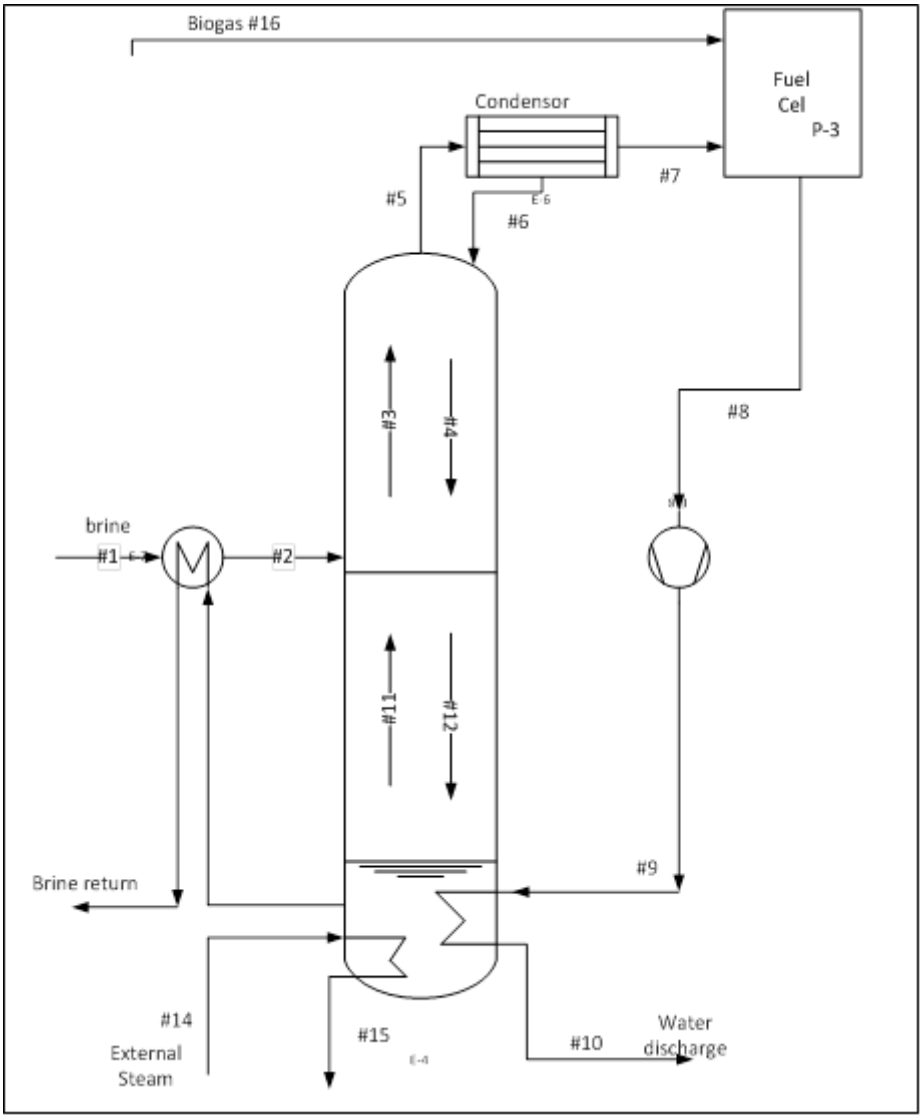

Figure 2: Optimized distillation tower design including heat recovery

The following assumptions have been made:

- A random reflux has been chosen. The reflux has to be optimized in a final design, based on the available reactor volume.
- A ammonia percentage in the effluent of the distillation tower of 25% has been assumed the possibility of this value is shown by (ref stowa report)
- A complete (100%) fuel utilization has been assumed
- A 100% removal of ammonia from the brine has been assumed

Appendix 10.1

Table 1. Composition and characteristics of flows indicated in figure 1(G. Smith, personal communication, September 2014)

Component	#1	#2	#3	#4	#5	#6	#7	#8	#9	#10	#11	#12	#13	#14	#15	#16
CH_4 [kg/h]	0	0	0	0	0	0	0	0	0	0	0	0	0	0	0	400
CO_2 [kg/h]	0	0	0	0	0	0	0	1300	1300	1300	0	0	0	0	0	200
NH_3 [kg/h]	0	0	?	?	?	?	544	0	0	0	0	0	0	0	0	0
NH_3 (aq) [kg/h]	544	544	?	?	?	?	0	0	0	0	?	?	0	0	0	0
H_20 (g) [kg/h]	0	0	?	?	?	?	1632	3396	3396	0	?	?	0	5833	0	0
H_2O [kg/h]	544000	544000	?	?	?	?	0	0	0	3396	?	?	542368	0	5833	0
total gas flow [L/h]	0	0	4352	0	4352	0	2176	4696	4696	1300	0	9633	0	5833	0	600
total liquid flow [L/h]	544000	544000	0	2176	0	2176	0	0	0	3396	546176	0	542368	0	5833	0
Temp [K]	293	368	373	373	?	?	?	473	555	393	373	373	373	298	-	-
P [bar]	1	1	1	1	1	1	1	1	2	1	1	1	1	1	1	1

Table 2. Influent characteristics

Characteristics overall influent (AnMBR influent)		
Q	8000	m^3/h
COD	200	mg/l
N	68	mg/l as NH_3
Q	8000000	kg/h
COD	1600	kg/h
N	544	kg/h
AnMBR Effluent		
methane	400	kg/h
CO_2	200	kg/h
Ion Exchange Brine		
water	544000	kg/h
NH_3	544	kg/h

Appendix 11.1

APPENDIX 11.1 COSTS INDICATION

Table 1 gives the estimated investment costs, of the proposed installation for a scale comparable with Harnaschpolder (Defluent, 2014). It must be noted that these values are indicative guesses, and particularly the costs of the solid oxide fuel cell is difficult to predict.

It can be seen that the total investment costs consist for 70% out of the fuel cells. Literature suggests a cost reduction of fuel cells in the future (Staniforth and Ormerod, 2003a, Steele and Heizel, 2001).

Table 1: Investment costs (G. Smith, personal communication, September 2014)

AnMBR (without membrane)	€ 45.000.000,00
Membrane AnMBR	€ 150.000.000,00
Ion exchanger	€ 10.000.000,00
Distillation tower	€ 10.000.000,00
Solid oxide fuel cell	€ 288.000.000,00
Total	€ 503.000.000,00
investment costs [€/ie]	€ 396,27

Appendix 11.2

APPENDIX 11.2 INDICATIVE POWER PRODUCTION ASSUMING BIOGAS STRIPPING

In chapter 11, further research in a similar, but different combination of technologies is proposed. The proposed combination consists out of an AnMBR, ion Exchange, biogas stripping and a solid oxide fuel cell. There is yet no proof of principle for this combination of technologies, but considering the potential advantages (compact installation, smart combination of resources and lower energy requirements) more research is required. As an indication, preliminary assumptions have been made on the potential electricity production of this combination of technologies. Figure 1 shows a schematic representation of the proposed flow chart.

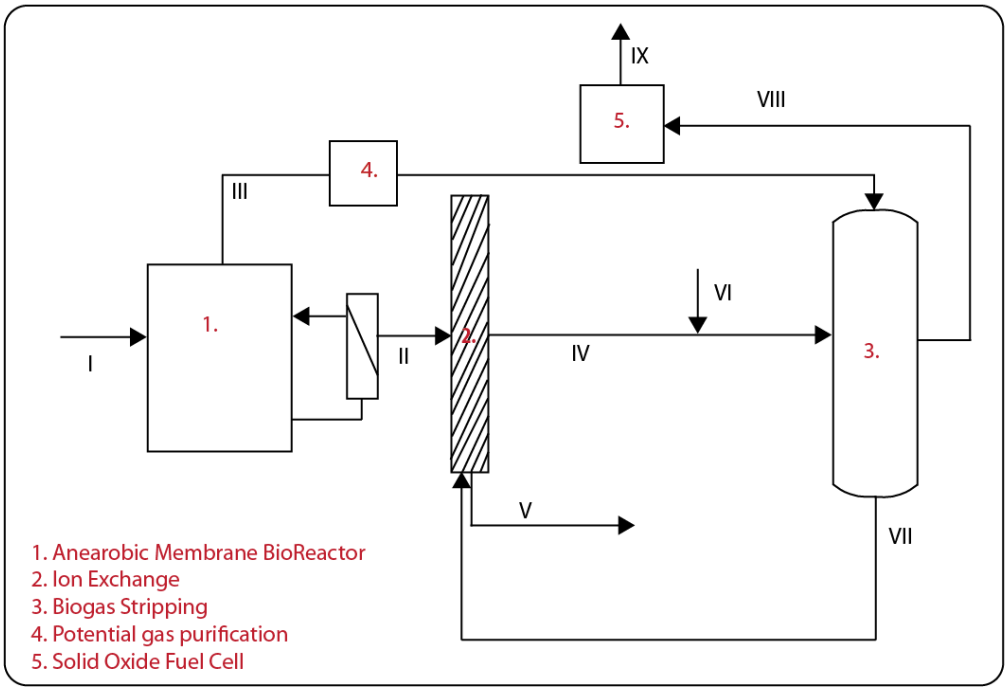

Figure 1 Flow chart of proposed combination of AnMBR, Ion Exchange, Biogas stripping and a fuel cell.

Table 1 shows the (assumed) energy requirements and energy production, when this combination would be up-scaled to a flow comparable with the wastewater treatment plant Harnaschpolder (Delfluent, 2014).

Table 1.Energy requirements versus energy production, for a combination of MBR, IE, Distillation tower and SOFC

Energy Requirements		
anMBR	[kwh/m^3 of treated wastewater]	0,12
Ion Exchange + Gas stripping + Rest	[kwh/m^3 of treated wastewater]	0,2
Total	[kwh/m^3 of treated wastewater]	0,32
Energy production		
Biogas	[kwh/m^3 of treated wastewater]	0,83
NH4	[kwh/m^3 of treated wastewater]	0,16
Total	[kwh/m^3 of treated wastewater]	0,99
Overall Electricity production	**[kwh/m^3 of treated wastewater]**	**0,75**

Appendix 11.2

Table 1 shows that the combination of AnMBR, Ion Exchange, biogas stripping and a fuel cell is actually electricity producing. For the described flow, a daily electricity production of 6008 kWh/day could be achieved, based on table 1. It must be noted that this value is based on assumptions as described for table 10.1, plus assumptions made on the energy requirements of the biogas stripping process (G. Smith, personal communication, September 2014).

However, It is not yet known if biogas treatment is required prior to biogas stripping. Gas treatment might be required for removing CO_2 and other gasses that are potentially harmful for a solid oxide fuel cell, from the produced biogas. This gas treatment might require energy as well, which has been neglected so far.